

UNIVERSITÀ DEGLI STUDI DI NAPOLI
“FEDERICO II”



Scuola Politecnica e delle Scienze di Base
Area Didattica di Scienze Matematiche Fisiche e Naturali

Dipartimento di Fisica “Ettore Pancini”

Laurea Magistrale in Fisica

Multipartite Entanglement Measures in
Quantum Spin Networks

Relatori:
Dr. Goffredo Chirco

Candidato:
Simone Cepollaro
Matr. N94000625

Anno Accademico 2021/2022

Contents

1	Introduction	5
2	Quantum geometry states	9
2.1	Canonical quantization of General Relativity	9
2.1.1	Hamiltonian formalism of General Relativity	11
2.1.2	Manifestly covariant formulations and vanishing Hamiltonian	14
2.2	Tetrad formalism and Ashtekar variables	15
2.2.1	Kinematic and physical Hilbert space	16
2.2.2	Tetrad formalism and spin connection	18
2.2.3	Hamiltonian analysis	20
2.2.4	Canonical quantization	21
2.2.5	Holonomy-flux algebra	22
2.3	Spin Network states	24
2.3.1	Cylindrical functions	24
2.3.2	Gauge-invariant Hilbert space	27
2.3.3	A Spin Network basis for Quantum Geometry States . . .	34
2.3.4	Spin Networks Dual to Simplicial Complexes	35
2.3.5	Quantum triangle in 3d gravity	35
2.3.6	Classical tetrahedra	36
2.4	Summary	38
3	Entanglement Entropy for Spin Network states	41
3.1	Density operator	42
3.1.1	Composite system	43
3.1.2	Separable and entangled states	44
3.2	Von Neumann Entropy	46
3.3	Rényi Entropy	48
3.3.1	Why Rényi Entropy?	50
3.4	Entanglement of Spin Network States	50
3.4.1	Entangled Wilson lines	51
3.4.2	Entangling tetrahedra via links	53
3.4.3	Entangling tetrahedra via intertwiners	55
3.5	Discussion on Entropy-Area scaling	56
3.6	Summary	58

4	Holographic properties of Random Spin Networks	61
4.1	GFT as Quantum Gravity model	62
4.1.1	Tensor networks	63
4.1.2	Adjacency matrix, bulk and boundary degrees of freedom	65
4.1.3	Bulk and boundary subspaces	66
4.1.4	Holographic map: from bulk to boundary	67
4.2	Rényi entropy from Ising free energy	69
4.3	Effects of bulk contribution and Ryu-Takayanagi formula	72
4.3.1	Homogeneous Spin Network	72
4.3.2	Vanishing bulk entropy	73
4.3.3	Bulk entropy effects	75
4.4	Summary	77
5	Negativity measures for Random Spin Networks	79
5.1	Rényi Negativity on random induced mixed states	79
5.1.1	Negativity	79
5.1.2	Rényi Negativity	80
5.1.3	Haar Random State	81
5.2	Diagrammatic approach	83
5.3	Permutation approach	90
5.3.1	Permutation Group	90
5.3.2	Geodesic on permutation group	91
5.4	Generalized Ising model for Rényi k-th Negativity	94
5.4.1	Ising action of a homogeneous spin network	100
6	Discussion	121

Chapter 1

Introduction

In recent years, the role of entanglement and information theory in shedding light on holography and space-time emergence has become more and more central in all the main approaches to quantum gravity, starting from the context of AdS/CFT, in string theory [1], up to the main non-perturbative quantum gravity approaches. In fact, a first key result showing a deep relation between entanglement and geometry was provided by the Ryu-Takayanagi holographic area/entropy formula [2], as a direct consequence of the holographic gauge/gravity duality setting. In this case, the entanglement entropy of a boundary CFT vacuum state was derived to be proportional to the area of a minimal surface in the dual AdS bulk. Via *holographic duality*, this result suggested the possibility to reconstruct information on geometrical data of a certain region of a AdS bulk via the quantum correlations of the CFT state at the boundary of such region. Many generalizations have followed since then. [3, 4, 5]

The radical idea of a correspondence between geometry and entanglement echoed in the framework of non-perturbative and background independent models of quantum gravity, such as Loop Quantum Gravity (LQG) [6] and its covariant generalizations [7], where continuum space-time geometry is replaced by pre-geometric structures, described by spin-networks labelled by algebraic and combinatorial variables. Spin network states provide a consistent model of quantum geometry that fits well the study of the nature of gravity in the quantum regime. Tools of quantum information and entanglement theory have been more and more used in this setting recently to describe the quantum skeleton of space-time as a set of fundamental microscopical entities held together by entanglement [8, 9, 10, 11]. In this sense, entanglement of spin networks is expected to play a key role in understanding how a continuum geometric description of space-time emerges from the quantum gravity regime [12, 13, 14]

The Thesis investigates the conjectured entanglement-geometry correspondence in non-perturbative quantum gravity [15, 10, 16], by studying for the first time measures of Rényi negativity [4, 17] in quantum states of 3d geometry described by quantum spin-networks [5] in the formalism of *Group Field Theory* [11], and investigating their holographic properties.

In Group Field Theory, space-time and geometry are emergent from a quantum many-body description of quantum space in terms of collections of interacting entangled simplicies, intended as quanta of space, dual to quantum spin network states.

In this formalism, generalised quantum spin network states can be described in terms of symmetric *tensor networks*. This allows to import techniques of quantum many-body physics in non-perturbative quantum gravity.

In this setting, our analysis focuses on the holographic properties of the typical Rényi negativity derived for **mixed** *random* spin-networks with boundaries, defined as open networks of entangled random simplices. The random character of the networks is motivated by attempt to mimic the complexity of the quantum geometry states as a signature of the (unknown) quantum gravitational dynamics.

Negativity [5, 18] is a measure of entanglement well defined for both pure and mixed states, this allows a generalisation of the study of quantum correlations in quantum geometry for system which are generally multi-partite.

Given a multi-partite system, negativity quantifies the entanglement of a state according to the amount of negative eigenvalues of the associated partial transposed density matrix. Indeed a necessary condition [19, 20] for a state to be unentangled is to have vanishing negativity. As for VN entropy, we can define also Rényi negativity of order k . In particular, we focus on logarithmic negativity [21] that is a monotone entanglement measure that provides many simplification in the calculations. In our approach, log-negativity will thus be obtained as the limit k to 1 of a k -th typical Rényi negativity.

The setting we consider is the following: we deal with an open random spin network state describing 3d quantum geometry with a boundary. We are interested in studying the holographic and geometric character of the entanglement among the subregions of the associated boundary state. In order to generalise the work in [16], we consider then a multi-partition of the boundary in three subregions A, B, C, and define a reduced boundary mixed state AB by tracing out the C system, intended as a generic environment. Thereby we look at the correlation among A and B with a measure of negativity.

To compute the typical k -th Rényi negativity we use two different approaches used in random tensor network literature: a diagrammatic approach [17] and a permutation approach [5]. In our analysis, both approaches require to be generalised in order to account for the symmetries and new degrees of freedom of the random spin networks, such as the intertwiners numbers associated to each vertex of the graph.

The diagrams method has been used in details for the calculations of *typical value* of 2nd and 3rd order Rényi negativity given by the ensemble averaging of the trace of the partial transposed density matrix to the power of the considered order.

In the calculation, tensor traces, adjacency matrix contractions and averaging can be graphically represented via diagrams and a list of short rules [4] allows us to write the result in term of the dimension of the Hilbert spaces of each subsystem.

The analysis of the results obtained via the diagrammatic approach for a set of simple spin network states, shows a clear internal symmetry emerging related to the Permutation group: one readily realise that the k -th order of negativity is the sum of a finite number of terms that is equal to the cardinality of the group S_k , given by $k!$ elements. This leads to reformulate the diagrammatic calculations of the k -th momenta of the mixed boundary in the Rényi formula in terms of a partition function of a generalised Ising model, with Ising spin variables replaced by elements of the permutation group attached to each vertex, interacting and spreading in the graph.

In this setting, we compute the typical log-negativity associated to a bipartition of a mixed spin network state. We recover the expected Ryu-Takanayagi area scaling law for the mutual information associated with the log-negativity at all orders, where again the minimal areas are associated to domain walls of the statistical model living on the spi-network graph.

Finally, we study the effect of bulk correlations by introducing link-wise maximal entangled correlators among intertwiners of the bulk network. We see that by adding non-local correlations to the bulk corresponds to a tendency of the domain walls to increase, with a sensible deformation of the area law.

The work is organized in six Chapters. Chapter two introduces to the notion of quantum geometry starting from the canonical quantization approach of the Einstein-Hilbert action, along with the original viewpoint of LQG, leading to the definition of quantum spin network states. Chapter three recall the notion of entanglement and its measurements in terms of Von Neumann entropy and Rényi generalisation. At this stage the main entanglement structures of spin networks are discussed. Chapter four introduces the notion *random* spin networks, recently proposed in [16], and it reviews the statistical derivation of Rényi entropy for such states with an emphasis on its holographic behaviour. Chapters two to four provide the conceptual and technical preliminary toolbox for the central part of the thesis consisting in the derivation of the typical negativity for a set of random spin network states in Chapter five. A summary of the results and a discussion follows in Chapter six.

Chapter 2

Quantum geometry states

As a first step of our work, in this Chapter we introduce the non-perturbative description of quantum geometry states given by quantum spin networks, as a result of the canonical quantization program for classical space-time first derived in Loop Quantum Gravity [7].

Starting from Einstein-Hilbert action and introducing ADM formalism, General Relativity is described as a dynamical theory with diffeomorphism invariance and on-shell conditions expressed through constraint on the metric space, described by a Lagrangian. Following Dirac quantization procedure one can consistently define a “kinematic” Hilbert space of the theory. The description of gravity in quantum language however further requires to reformulate the theory with a new set of variables in the Lagrangian, i.e. tetrad and Ashtekar connections. The latter are $\mathfrak{su}(2)$ -valued one forms of connection. A new Gauss constraint emerges, eventually leading to a description of gravity as a local $SU(2)$ Yang-Mills theory, which is now suitable for quantization.

Following the procedure of local gauge theory, connection and tetrads are smeared on paths and surfaces, leading to the holonomy-flux algebra in terms of which we perform canonical quantization [6]. Quantum states of 3d geometry are realised as wave functionals of holonomies evaluated on a finite set of holonomy-paths forming *closed graph* and expressed in terms of quantum spin network states. Some basic examples of spin networks are provided at this stage (i.e. Wilson line, trivalent node, tetra-valent node) [22] with an emphasis on the role of the gauge constraint in the construction of the Hilbert space and their geometrical interpretation [23, 24, 25].

2.1 Canonical quantization of General Relativity

The Hamiltonian formulation of GR [6] is the starting point of the canonical approach to the quantization of geometry. It is well known that it is possible to derive Einstein’s equation in vacuum by varying Einstein-Hilbert action whit

respect to the metric tensor:

$$S_{EH} = \frac{1}{16\pi G} \int d^4x \sqrt{-g} R^{\mu\nu} g_{\mu\nu} \quad (2.1)$$

$$\frac{\delta S_{EH}}{\delta g_{\mu\nu}} = 0 \implies R_{\mu\nu} - \frac{1}{2} R g_{\mu\nu} = 0 \quad (2.2)$$

where g is the determinant of the metric, $R_{\mu\nu}$ is Ricci's tensor and R is the scalar curvature.

In order to obtain a canonical formulation for Einstein's equation we need to identify a couple of conjugated variables and perform a Legendre transformation, namely to pass from a Lagrangian to a Hamiltonian formulation. The action describing the dynamics of a classical system can be written in terms of the Lagrangian $\mathcal{L}(q^i, \dot{q}^i) \in \mathcal{F}(TQ)$ that is a function on the tangent bundle of the configuration space Q .

$$S = \int dt \mathcal{L}(q^i, \dot{q}^i) \quad (2.3)$$

Thus we can define the conjugated canonical momentum as $p_i = \frac{\partial \mathcal{L}}{\partial \dot{q}^i}$ and map TQ into T^*Q as follows :

$$S = \int dt (p_i \dot{q}^i - \mathcal{H}(q^i, p^i)) \quad (2.4)$$

where $\mathcal{H} \in T^*Q$ is the Hamiltonian of the system. T^*Q is the phase space which dimension is $\dim(T^*Q) = 2\dim(Q)$ and it is endowed with the symplectic form

$$\omega = \frac{1}{2} \omega_{ij} dx^i \wedge dx^j \quad (2.5)$$

Being ω non degenerate by definition there exists its inverse matrix Λ such that

$$\omega_{ij}^{-1} = \Lambda^{ij} \implies \Lambda = \frac{1}{2} \Lambda^{ij} \frac{\partial}{\partial x^i} \wedge \frac{\partial}{\partial x^j} \quad (2.6)$$

$$\frac{\partial}{\partial x^i} = \begin{cases} \frac{\partial}{\partial x^i} & \text{for } i = 1 \dots n = \dim(Q) \\ \frac{\partial}{\partial p^i} & \text{for } i = n + 1 \dots 2n \end{cases} \quad (2.7)$$

Λ is called Poisson structure (or bivector) and it induces a skew-symmetric binary differential operation on $F(T^*Q)$ called Poisson bracket:

$$\{\cdot, \cdot\} : (f, g) \in F(T^*Q) \times F(T^*Q) \longrightarrow \{f, g\} = \frac{\partial f}{\partial x^i} \frac{\partial g}{\partial x^j} - \frac{\partial f}{\partial x^j} \frac{\partial g}{\partial x^i} \quad (2.8)$$

Since \mathcal{H} is defined as $\mathcal{H}(q, p) = p_i \dot{q}^i - \mathcal{L}(q^i, \dot{q}^i)$, it is possible to derive the equations of motion through the Poisson brackets:

$$\dot{\vec{q}} = \{\vec{q}, H\} \quad (2.9)$$

$$\dot{\vec{p}} = \{\vec{p}, H\} \quad (2.10)$$

According to this description, in order to perform canonical quantization, we need to find a couple of conjugated variables in terms of which we can rewrite the Einstein-Hilbert action.

2.1.1 Hamiltonian formalism of General Relativity

Let assume space-time manifold \mathcal{M} naturally split into $\mathcal{M} \cong \mathbb{R} \times \Sigma$ where Σ is a three-dimensional spatial manifold. Thus we can identify this split as a foliation of \mathcal{M} into a one-parameter family of spatial hypersurfaces obtained by embedding Σ into \mathcal{M} as follows :

$$\Sigma_t = X_t(\Sigma) \quad (2.11)$$

This allows us to identify also the parameter $t \in \mathbb{R}$ as a time parameter. Nevertheless a crucial point of this analysis is the fact that t has not the physical meaning of a time parameter as previously said: Einstein-Hilbert action is invariant under diffeomorphism, thus given $\phi \in Diff(\mathcal{M})$, the quantity $X' = X \circ \phi$ represent a new foliation with a different parameter t' . But we can also express diffeomorphisms as composition of multiple foliations i.e. $\phi = X \circ X'$. Thus, we can chose to work with a foliation Σ_t keeping in mind that physical quantities shall not depend on t .

Now we have to focus on the foliation X_t to understand its meaning in general relativistic sense. We shall focus on the approach proposed by Arnowitt, Deser and Misner in 1960 [26, 27]. They found a change of variables that simplifies the complexity of such canonical formulation, first attempted by Dirac in 1958 [28]. Through the following change of variables, we can provide a clear geometrical interpretation of kinematic between different foliations.

Given coordinates (t, x) on X_t , we can define the *time flow vector*:

$$\tau^\mu = \frac{\partial X^\mu(t)}{\partial t} = (1, 0, 0, 0) \quad s. t. \quad g_{\mu\nu} \tau^\mu \tau^\nu = g_{00} \quad (2.12)$$

Time flow vector is not to be confused with the *unit normal vector* n^μ . Such vector is also a time-like one:

$$g_{\mu\nu} n^\mu n^\nu = -1 \quad (2.13)$$

but they are not parallel in general.

Thus we can decompose τ in normal and tangential component with respect to n . We obtain:

$$\tau^\mu(x) = N(x)n^\mu + N^\mu(x) \quad (2.14)$$

where $N(x)$ is called *Lapse function* and N^μ has only spatial coordinates, say $N^\mu = (0, N^a)$. We refer to N^a as the *Shift vector*. It is useful for our aim to parametrize also n^μ in terms of Lapse and Shift to better understand their geometrical meanings.

$$n^\mu = \left(\frac{1}{N}, -\frac{N^a}{N} \right) \quad (2.15)$$

Now it's easy to graphically represent the role of Lapse and Shift during the evolution from different foliations X_t and $X_{t+\delta t}$:

In order to express Einstein-Hilbert action in terms of Lapse and Shift, the next

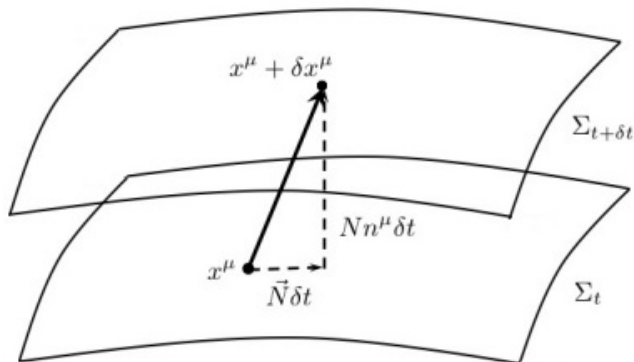


Figure 2.1: The point $y^\mu = x^\mu + \delta x^\mu$ lies on the surface labelled by time parameter $t + \delta t$. It's not hard to understand that the Lapse function is the proper time elapsed between the t surface and the $t + \delta t$ surface for a static observer on the surface. The Shift vector instead measures the shift of spatial coordinates between the two surfaces for an observer not moving on the initial surface.

step is to restrict our analysis only to the three-dimensional metric induced on the foliation by the space time metric¹:

$$g_{ab} = q_{ab} \text{ for } a, b = 1, 2, 3 \quad (2.16)$$

Furthermore, by considering (2.12) and (2.13), we can easily express N and N^a in terms of space-time metric components. In fact:

$$g_{\mu\nu} \tau^\mu \tau^\nu = g_{00} = -N^2 + g_{ab} N^a N^b \quad (2.17)$$

$$\begin{aligned} \tau_\mu N^\mu &= g_{0b} N^b = g_{\mu\nu} \tau^\mu N^\nu = g_{\mu\nu} (N^\mu + N^\mu) N^\nu = g_{ab} N^a N^b \\ &\Rightarrow g_{0b} = g_{ab} N^a = N_b \end{aligned} \quad (2.18)$$

The line element reads

$$ds^2 = -(N^2 - N_a N^a) dt^2 + 2N_a dx^a dt + q_{ab} dx^a dx^b \quad (2.19)$$

In addition to the useful geometric interpretation of these two fields, the main reason why this change of variables is clever will be soon evident: we are going to discover immediately that the Lagrangian does not depend on the time derivatives \dot{N} and \dot{N}^a [7]. This fact simplifies considerably the following canonical analysis leading us to an Hamiltonian proportional to Lagrange multipliers that vanishes on the constraint surfaces.

¹Actually the spatial component of the space-time metric $g_{\mu\nu}$ is different from the induced intrinsic metric on X_t . In fact we should rigorously define $q_{\mu\nu} = g_{\mu\nu} - n_\mu n_\nu$. However, any contraction between spatial tensors on X_t with n^μ clearly vanishes. This allows us to inherit calculus on X_t from the one on \mathcal{M} .

Now we can calculate the Lie derivative of the intrinsic metric with respect to the normal unit vector n , thus obtaining the extrinsic curvature of Σ_t :

$$\mathcal{L}_n q_{\mu\nu} = 2K_{\mu\nu} \quad (2.20)$$

This tensor encodes the differences between the Riemann tensors in \mathcal{M} and Σ_t , called respectively R and \mathcal{R} . In fact:

$$\mathcal{R}_{\nu\alpha\beta}^\mu = q_{\mu'}^\mu q_{\nu'}^{\nu'} q_{\alpha'}^{\alpha'} q_{\beta'}^{\beta'} R_{\nu'\alpha'\beta'}^{\mu'} - K_{\nu\alpha} K_{\beta}^\mu - K_{\nu\beta} K_{\alpha}^\mu \quad (2.21)$$

Now we are ready to exhibit formally the action in terms of curvature K and Riemann tensor \mathcal{R} evaluated on Σ :

$$S_{EH} = \frac{1}{16\pi G} \int dt \int_{\Sigma} d^3x \sqrt{q} N [\mathcal{R} - K^2 - Tr(KK)] \quad (2.22)$$

As anticipated we have found an action that involves no time derivatives of Lapse and Shift field. So N and N^a play the role of Lagrange multipliers with vanishing conjugated momenta :

$$\frac{\delta \mathcal{L}}{\delta \dot{N}} = 0 \quad \frac{\delta \mathcal{L}}{\delta \dot{N}^a} = 0 \quad (2.23)$$

The unique dynamical variables are the spatial component of the induced metric q_{ab} , whose conjugated momenta can be easily computed:

$$\pi_{ab} = \frac{\delta \mathcal{L}}{\delta \dot{q}_{ab}} = \sqrt{q} (K^{ab} - K q^{ab}) \quad (2.24)$$

Finally computing Legendre transform we obtain the Hamiltonian for gravitational field:

$$S(q^{ab}, \pi_{ab}, N, N^a) = \frac{1}{16\pi G} \int dt \int d^3x (\pi_{ab} \dot{q}_{ab} - N^a H_a - NH) \quad (2.25)$$

We are using short notation for H and H_a , defined as follows:

$$H = \frac{1}{\sqrt{q}} G_{abcd} \pi^{ab} \pi^{cd} - \sqrt{q} \mathcal{R} \quad G_{abcd} = q_{ac} q_{bd} + q_{ad} q_{bc} - q_{ab} q_{cd} \quad (2.26)$$

$$H_a = -2\sqrt{q} \nabla_b \left(\frac{\pi_a^b}{\sqrt{q}} \right)$$

The phase space of GR is thus parametrized by the canonical couple (q^{ab}, π_{ab}) with canonical Poisson bracket:

$$\{\pi_{ab}(t, x), q^{cd}(t, x')\} = \delta_{(a}^c \delta_{b)}^d \delta(x - x') \quad (2.27)$$

By varying the action with respect to Lagrange multiplier we trivially obtain:

$$H_a = 0 \quad H = 0 \quad (2.28)$$

called respectively **space-diffeomorphism constraint** and **scalar Hamiltonian constraint**. The Hamiltonian of the system is given by:

$$\mathcal{H} = \int d^3x (N^a H_a + NH) \quad (2.29)$$

where we have set $16\pi G = 1$.

Since Hamiltonian is proportional to Lagrange multipliers, it vanishes on-shell, i.e. when the constraints equations are satisfied. Hence we understand that there is no dynamics (or no physical evolution) with respect to the time parameter t , and this result is joyfully coherent with the previous discussion on the diffeomorphism invariance of the foliation induced by the topology of \mathcal{M} .

2.1.2 Manifestly covariant formulations and vanishing Hamiltonian

So far we have found a result (apparently) surprising since Hamiltonian vanishes and clearly there is no dependence on the parameter we have been using. Such fact obviously matches the requirement that t has no physical meaning because of diffeomorphism-invariance of General Relativity. Moreover the fact that \mathcal{H} vanishes does not mean that such formulation for the theory has no information on dynamics. To highlight the presence of this information it is possible to exhibit the result for a single particle equation in manifestly covariant formulation. The most basic action for such system is:

$$S = \int_{-\infty}^{+\infty} d\tau (\dot{x}^\mu k_\mu - N [k_\mu k_\nu \eta^{\mu\nu} - m_k^2]) \quad (2.30)$$

Where τ is an auxiliary parameter, x^μ are fields on the worldline, $\dot{x}^\mu = \frac{\partial x^\mu}{\partial \tau}$ and N is a Lagrange multiplier whose role is to impose the on-shell condition on momenta. Indeed:

$$\frac{\partial \mathcal{L}}{\partial N} = 0 \implies k_\mu k_\nu \eta^{\mu\nu} - m_k^2 = 0 \quad (2.31)$$

To obtain \mathcal{H} we compute Legendre map and we obtain:

$$\mathcal{H} = \dot{x}^\mu k_\mu - \mathcal{L} = N [k_\mu k_\nu \eta^{\mu\nu} - m_k^2] \quad (2.32)$$

Even in this case, we obtain an Hamiltonian which is proportional to constraints that vanishes for onshell (or physical) states, $\mathcal{H} = 0$. Nevertheless this only means that physics does not depend of the arbitrary parameter used to formulate the theory, and this is definitely a good result. Also evaluating Hamilton equation for x^μ :

$$\begin{aligned} \dot{x}^\mu &= \frac{\partial \mathcal{H}}{\partial k_\mu} = 2N (k_\nu \eta^{\mu\nu}) \\ x^\mu &= \bar{x}^\mu + 2N (k_\nu \eta^{\mu\nu}) \tau \end{aligned} \quad (2.33)$$

We understand that both time and spatial coordinates depends on N and τ . Thus we call *partial observables* the quantity $x^0(\tau)$ and $x^k(\tau)$ for reasons that will be clear soon: in fact if we invert $x^0(\tau)$ in $\tau(x^0)$ and combine $x^k(\tau(x^0))$ we get the equations of motion for special relativistic free particle:

$$x^k = \bar{x}^k + \frac{k^k}{k^0}(x^0 - \bar{x}^0) \quad (2.34)$$

We use the adjective *partial* to stress the fact that these observables evaluate the evolution of physical quantities with respect to the arbitrary parameter used to formulate theory, so they can be predicted from the knowledge of the initial state of the system but there is no way to *measure* their values as it is intended in quantum language. Nevertheless we have just shown that combining partial observables we can build up physical observables, that therefore can be defined as *relations* between partial observables.

Beside the physical interpretation of the equations derived, the crucial point of this analysis is that we manage to describe the dynamics even for a system with vanishing Hamiltonian.

2.2 Tetrad formalism and Ashtekar variables

Before continuing the path of canonical quantization, we shall recall briefly the main step we have already performed:

- We began with the search of a canonical formulation of EH action, focusing mainly of the role of diffeomorphism invariance of space time.
- We performed the ADM change of variables, that brought us to Lapse and Shift fields as the main protagonist of the evolution between leaves obtained by the foliation of space-time.
- Explicitly writing Lagrangian in such terms, we have easily computed the Hamiltonian related to gravitational field and we obtained a pure constraint Hamiltonian, proportional to Lapse and Shift, encoding diffeomorphism invariance and scalar Hamiltonian constraints as:

$$H_a = 0 \quad H = 0 \quad (2.35)$$

At this stage, we shall then perform a quantisation procedure à la Dirac, in the sense that we want to define the dynamical physical states as the ones that get annihilated by the constraints. To obtain such states in a coherent way we need to define:

- A map from the phase space onto an Hilbert space.

- A way to promote unambiguously commutation rules of Poisson brackets in terms of Lie Bracket:

$$\{\cdot\cdot\} \rightarrow \frac{1}{i\hbar} [\cdot, \cdot] \quad (2.36)$$

- A way to promote constraints to operator H^μ acting on some (*kinematic*) Hilbert space that will be defined afterwards.

After this steps we can finally impose constraints in quantum language by requiring, as anticipated, the condition:

$$H^\mu |\psi_{phys}\rangle = 0; \quad \forall |\psi_{phys}\rangle \in \mathcal{H}_{phys} \quad (2.37)$$

The meaning of this requirement is that we are restricting the previous Hilbert space to a new one, that we use to call *physical Hilbert space*.

In the following, it will be briefly shown how lots of difficulties emerge in this approach. We mainly focus on a rigorous definition of the kinematic and physical Hilbert space and the lack of possibility to define a scalar product structure that takes into account of diffeomorphism invariance of metrics tensor. This limit will bring us to introduce the tetrad formalism and a different point of view on a discretized geometry of space-time.

2.2.1 Kinematic and physical Hilbert space

Dirac's procedure has the advantage to apply to any constrained system. We would like to use this tool for gravity in ADM formulation.

What we are looking for is a set of functionals that realizes the quantum version of Poisson's algebra. Given q_{ab} and π^{ab} , we know that metrics' component and conjugated momenta realize a classical symplectic algebra. We can imagine to promote such quantities to operators with commutation rules:

$$\begin{aligned} [\hat{q}_{ab}(x), \hat{\pi}^{cd}(y)] &= i\hbar \delta_{(ab)}^{cd} \delta^{(3)}(x-y) \\ [\hat{q}_{ab}(x), \hat{q}_{cd}(y)] &= 0 \\ [\hat{\pi}^{ab}(x), \hat{\pi}^{cd}(y)] &= 0 \end{aligned} \quad (2.38)$$

We can decide to proceed similarly to the case of a scalar field, so considering a Schrödinger representation of these operators, such that they act by multiplication or derivative on the wave functional evaluated on the 3-metric:

$$\hat{q}_{ab}(x)\psi[q_{ab}] = q_{ab}(x)\psi[q_{ab}]; \quad \hat{\pi}^{ab}(x)\psi[q_{ab}] = -i\hbar \frac{\delta\psi[q_{ab}]}{\delta q_{ab}(x)} \quad (2.39)$$

At this level, to build this pre-geometric or kinematic Hilbert space, we only need to define a scalar product between wave functional. Although this is a well known, useful and practical procedure for scalar field, if we apply it to the gravitational context, a lot of difficulties and obstacles emerge:

- If we define the scalar product

$$\langle \psi | \psi' \rangle = \int dg \psi[\bar{g}] \psi'[g] \quad (2.40)$$

the absence of a Lebesgue measure on the space of metrics modulo diffeomorphism prevents us from defining the element dg in a clear mathematical way.

- If we do not define dg it is simply impossible to verify if \hat{q}_{ab} or $\hat{\pi}^{cd}$ are actually hermitian operators. We can't either prove that \hat{q}_{ab} has a positive definite spectrum, as required for a space-like metric.

Anyway, this problem has been vastly ignored in literature, and such analysis continued simply assuming that a well defined H_{Kin} could exist. The next step is to promote the vectorial and scalar constraints to operator and to impose the classical invariance in quantum terms, that is to narrow further the Hilbert space to constrained states:

$$H_{kin} \xrightarrow{\hat{H}^a} H_{Diff} \xrightarrow{\hat{H}} H_{Phys} \quad (2.41)$$

If we first consider the vectorial constraint in terms of Schrödinger representation, smearing the integral of \mathcal{H} over a surface Σ :

$$\hat{H}^a \psi[q_{ab}] = 2i\hbar \int_{\Sigma} d^3x \nabla_b N_a \frac{\delta \psi}{\delta q_{ab}} = 0 \quad (2.42)$$

This integral can be solved by integration by parts and leads to the condition:

$$\psi[q_{ab}] = \psi[q_{ab} + 2\nabla_{(a} N_{b)}] \quad (2.43)$$

This is the result of vector constraint and surprisingly it realizes, in a well defined way, diffeomorphism invariance of metric at quantum level. Although this result might seem encouraging, the main problem of this approach still exists, according to the fact that H_{Diff} clearly inherit from H_{Kin} the lack of Lebesgue measure, preventing us from define scalar product once again.

Moreover, if we use the same procedure to solve the scalar constraints H , we can write:

$$\hat{H} \psi[q_{ab}] = \left[-\frac{\hbar^2}{2} G^{abcd} + : \frac{1}{\sqrt{g}} \frac{\delta^2}{\delta q_{ab}(x) \delta q_{cd}(x)} : - \sqrt{g} R(g) \right] \psi[q_{ab}] \quad (2.44)$$

The $:\cdot\cdot:$ symbols stands for normal ordering product. The expression (2.44) is also know as Wheeler-DeWitt equation. Even if we assume to be able to perform a good normal ordering prescription, and so to regularize the product of operator in the same point, differently from the previous case, we have no characterization of solutions. Beside the lack of scalar product, it is not even remotely possible to understand the form of the physical states of this theory.

So far we developed an uncomplete theory, that clearly exhibit the anomalous behaviour of gravitational field at quantum level.

Instead of changing the quantization paradigm, we will now to try describe gravity using different variables. Indeed it's not surprising that not all choices of classical variables suit well during quantization.

We will use a different description for gravity that leads us to the tetrad formalism and still another formulation of EH action in terms of a two-form of curvature associated to an $\mathfrak{so}(1,3)$ -valued connection one-form. A new Gauss constraint will emerge, in a form that is very similar to a $SU(2)$ Yang-Mills theory. We will focus on the description of the theory in terms of Electric fields (Densitized triad) and Ashtekar-Barbero connections. The latter will be one of the main protagonist in the description of loop, thus finally writing the generic form of a LQG state.

2.2.2 Tetrad formalism and spin connection

A tetrad [6] is a quadruple of 1-form $e^I(x) = e^I_\mu(x)dx^\mu$ such that $\mu = 0, 1, 2, 3$ and $I = 0, 1, 2, 3$ is an internal index. We define tetrads starting by a general relativistic metric:

$$g_{\mu\nu}(x) = e^I_\mu(x)e^J_\nu(x)\eta_{IJ} \quad (2.45)$$

where η is the flat Minkowski metric. Tetrads represent an isomorphic map between general reference frame to an inertial map. Indeed we notice that they capture the information on the space-time coordinate x , expliciting the fact that space-time locally appears like a Minkowskian flat manifold.

The definition in (2.45) is manifestly Lorentz invariant:

$$e^I_\mu(x) \rightarrow \tilde{e}^I_\mu(x) = \Lambda^I_J(x)e^J_\mu(x) \quad (2.46)$$

Moreover contracting tetrads with tensors of any rank we obtain object that transforms under Lorentz group. Namely tetrads realize an isomorphism between the tangent bundle $T\mathcal{M}$ and a Lorentz principal bundle $\mathcal{F}(\mathcal{M}, SO(3,1))$. On the latter we can define the $\mathfrak{so}(3,1)$ valued connection 1-form ω_μ^{IJ} and a derivative of the fiber:

$$D_\mu v^I(x) = \partial_\mu v^I(x) + \omega_{\mu,J}^I(x)v^J(x) \quad (2.47)$$

We can also define covariant derivative, for object with both indices:

$$D_\mu e^I_\nu(x) = \partial_\mu e^I_\nu(x) + \omega_{\mu,J}^I(x)e^J_\nu(x) - \Gamma_{\mu\nu}^\rho(x)e^I_\rho(x) \quad (2.48)$$

We require the following condition:

- $\Gamma(x)$ is the Levi-Civita connection, so its metric compatible in the sense that $\nabla_\rho g_{\mu\nu} = 0$
- ω is tetrad compatible, in the sense that $D_\mu e^I_\nu = 0$. We call this object **spin connection**.

If we write explicitly this request and combine the 2 resulting equation we obtain that spin connection and tetrads are related by the following relations:

$$\begin{aligned} \omega_{\mu J}^I &= e_{\nu}^I \nabla_{\mu} e_{\nu}^J \\ d_{\omega} e^I &= de^I + \omega_J^I e^J = (\partial_{\mu} e_{\nu}^I + \omega_{\mu J}^I e_{\nu}^J) dx^{\mu} \wedge dx^{\nu} = 0 \end{aligned} \quad (2.49)$$

where we are using the following notation: d is the exterior derivative, \wedge is the wedge product between forms and d_{ω} is the covariant exterior derivative.

Given the spin connection, we can define the curvature associated to it:

$$F^{IJ} = d_{\omega} \omega = d\omega^{IJ} + \omega_K^I \omega^{KJ} \quad (2.50)$$

We can explicitly write its components:

$$F_{\mu\nu}^{IJ} = \partial_{\mu} \omega_{\nu}^{IJ} - \partial_{\nu} \omega_{\mu}^{IJ} + \omega_{K\mu}^I \omega_{\nu}^{KJ} - \omega_{K\nu}^J \omega_{\mu}^{KI} \quad (2.51)$$

Now if we use the relation between spin connection and Levi-Civita one from (2.49) in (2.51) we get the *Cartan second structure equation* :

$$F_{\mu\nu}^{IJ}(w(e)) = e^{I\rho} e^{J\sigma} R_{\mu\nu\rho\sigma} \quad (2.52)$$

Now we can write EH action in terms of F :

$$\begin{aligned} S_{EH} &= \int d^4x \sqrt{-g} g^{\mu\nu} R_{\mu\nu} = \\ &= \int d^4x e e^{\mu}_I e^{I\nu} R_{\mu\nu\rho\sigma} e^{\rho}_J e^{J\sigma} = \int d^4x e e^{\mu}_I e^{\rho}_J F_{\mu\nu}^{IJ}(w(e)) = \\ &= \int d^4x \frac{1}{4} \epsilon_{IJKL} \epsilon^{\mu\nu\rho\sigma} e^{\rho}_K e^{\sigma}_L F_{\mu\nu}^{IJ} = \\ &= \frac{1}{2} \epsilon_{IJKL} \int e^I \wedge e^J \wedge F^{KL}(w(e)) \end{aligned} \quad (2.53)$$

This result shows explicitly that gravity is a local gauge theory, its local group being the Lorentz group and Riemann tensor is defined as the field-strength of the spin connection.

We can also consider the connection as an independent variable such that we can write the renowned **Palatini action**:

$$S(e, \omega) = \frac{1}{2} \epsilon_{IJKL} \int e^I \wedge e^J \wedge F^{KL}(\omega) \quad (2.54)$$

Even if it depends on an extra field, this action gives the same equation of motion. In fact, varying with respect to ω we only impose the form for spin connection. We notice that the previous formulation of GR required that tetrads were not degenerate, i.e. invertible. The last equation instead does not require this condition since the inverses of tetrad do not appear. Moreover if we require connection being an independent variables, we can add another terms

to the Lagrangian that has mass dimension 4 and perfectly suits with all the symmetries:

$$S(e, \omega) = \left(\frac{1}{2} \epsilon_{IJKL} + \frac{1}{\gamma} \delta_{IJKL} \right) \int e^I \wedge e^j \wedge F^{KL}(\omega) \quad (2.55)$$

γ is a parameter ², while (2.55) is called *Holst action*.

2.2.3 Hamiltonian analysis

To obtain the Hamiltonian formulation of the theory we can proceed as previously done for the ADM formalism. We first suppose $M = \mathbb{R} \times \Sigma$, so the space-time foliates into a family of one-parameter hypersurfaces. Then we introduce the Lapse and Shift field (N, N^a) to encode information on observer on different sheets of space-time. We can express tetrad in terms of Lapse and Shift as follows:

$$e_0^I = e_\mu^I \tau^\mu = N n^I + N^a e_a^I, \quad \delta_{ij} e_a^i e_b^j = g_{ab} \quad (2.56)$$

The terms e_a^i are the spatial component of tetrads and are called *triad*.

Now we want to identify a pair of canonically conjugated variables. We will meet two different issues: the first one is that by using tetrad formalism we introduce a new symmetry in the theory, i.e. the local Lorentz invariance. The second one is the fact that we are treating tetrads and connections as independent variables, so the new variables will be function of both e and ω (besides their derivatives). To simplify the task we can work in "time gauge" $e_\mu^I n^\mu = \delta_0^I$ and introduce the following change of variables:

$$\begin{aligned} E_i^a &= \frac{1}{2} \epsilon_{ijk}^a e_b^j e_c^k && \text{(Densitized triads or Electric fields)} \\ A_a^i &= \gamma \omega_a^{0i} + \frac{1}{2} \epsilon_{jk}^i \omega_a^{jk} && \text{(Ashtekar-Barbero connection)} \end{aligned} \quad (2.57)$$

With an easy calculation it is possible to prove this variables to be conjugated. This allows us to write the action in terms of Lapse, Shift, densitized triads and Ashtekar connection:

$$S(A, E, N, N^a) = \frac{1}{\gamma} \int dt \int_\Sigma d^3x (\dot{A}_a^i E_i^a - A_0^i G_i - NH - N^a H_a) \quad (2.58)$$

where:

$$\begin{aligned} G_i &= D_a E_i^a = \partial_a E_i^a + \epsilon_{ijk} A_a^j E^{ka} \\ H_a &= \frac{1}{\gamma} F_{ab}^j E_j^b - \frac{1 + \gamma^2}{\gamma} K_a^i G_i \\ H &= [F_{ab}^j - (\gamma^2 + 1) \epsilon_{jmn} K_a^m K_b^n] \frac{\epsilon^{jkl} E_k^a E_l^b}{\det(E)} + \frac{1 + \gamma^2}{\gamma} G^i \partial_a \frac{E_i^a}{\det(E)} \\ F_{ab}^j &= \partial_a A_b^j - \partial_b A_a^j + \epsilon_{kl}^j A_a^k A_b^l \end{aligned} \quad (2.59)$$

²In quantum theory, this parameter plays a key role, and there it's called Immirzi parameter. If it's chosen to be real or imaginary, there are big consequences about constraints

Once again, we obtain a diffeomorphism constraint and a Hamiltonian one, but those are significantly modified with respect to the EH formulation, by the change of variables and by the new formulation of the theory based on Gauge invariance. Indeed both F_{ab}^j and G^i are, respectively, the curvature associated to the connection and the Gauss constraint that appear in Yang-Mills $SU(2)$ theory. In particular the term G_i is actually a new constraint: it is not surprising at all since we defined tetrad to keep in mind the invariance under local gauge transformation, so this new constraints exhibit this invariance at the canonical level. Yet the action we defined was required to be Lorentz invariant, we could be misled to expect the group of local symmetry to be the Lorentz one. This unexpected anomaly arises because of the change of variables in (2.57). The Ashtekar-Barbero connection is an $SU(2)$ connection, not a Lorentz's one. The pair of conjugated variables we used to perform Legendre map is indeed given by (A, E) that transform respectively as a $SU(2)$ vector and an $\mathfrak{su}(2)$ -valued connection one-form, thus the Gauss constraint generates $SU(2)$ local symmetry. The key point of this result is that we are using $SU(2)$ as an auxiliary group to describe local symmetry; that brings us to describe Gravity as a local $SU(2)$ Yang-Mills theory, more suitable for quantization.

2.2.4 Canonical quantization

So far we have defined Ashtekar-Barbero connection and densitized triad that brought us to formulate gravity as a local $SU(2)$ gauge theory. We would like to proceed by applying the typical step of the canonical quantization, so:

- Promote canonical variables to operators and Poisson bracket to commutators;
- define wave functionals of connection variables, namely $\psi[A]$, a scalar product on the space of functionals, so realizing an Hilbert space;
- promote Gauss constraint to operator and select "physical" states imposing $\hat{G}_i \psi[A] = 0$;
- study dynamics on this Hilbert space, by applying the Hamiltonian operator on the space of physical states.

We can thus promote canonical Poisson bracket to commutators [6] :

$$\{A_i^a(x), E_j^b(y)\} = \gamma \delta_b^a \delta_i^j \delta(x, y) \implies [\hat{A}_i^a(x), \hat{E}_j^b(y)] = \gamma \delta_b^a \delta_i^j \delta(x, y) \quad (2.60)$$

and define the wave functional such that \hat{A} and \hat{E} act respectively multiplicatively and derivatively, namely:

$$\begin{aligned} \hat{A}_i^a \psi[A_k^b] &= A_i^a \psi[A_k^b] \\ \hat{E}_a^i \psi[A_k^b] &= -i\gamma \frac{\delta}{\delta A_a^i} \psi[A_k^b] \end{aligned} \quad (2.61)$$

In order to simplify the equations of constraints, Ashtekar proposed to use $\gamma = i$. This choice leads to a simplification of Hamiltonian constraint but, on the other hand, variables become complex and to recover GR one has to impose reality conditions. Since this approach is particularly difficult at quantum level, most of the recent works on LQG focus on γ real [29, 30].

2.2.5 Holonomy-flux algebra

Following the procedure usually adopted in local gauge theory, we have to regularize connections and electric fields by integrating them over the whole space with the same type of test functions. The different tensorial nature of A_a^i and E_i^a plays a key role.

In fact densitized triads are 2-forms, so it's natural to smear them on a surface:

$$E_i(S) = \int_S n_a E_i^a d^2\sigma \quad (2.62)$$

where $n_a = \epsilon_{abc} \frac{\partial x^b}{\partial \sigma_1} \frac{\partial x^c}{\partial \sigma_2}$ is the normal to the surface. This quantity belongs to $\mathfrak{su}(2)$. Concerning Ashtekar connections, they are 1-form so it is natural to smear them on a one-dimensional path. Indeed one can consider the fact that connections define a notion of parallel transport of fiber over the base manifold, thus we can associate to a given Lie algebra-valued connection 1-form $A = A_a^i \tau_i dx^a$ an element of the group $h_\gamma(A)$ called holonomy defined by

$$h_\gamma(A) = \mathcal{P}exp \left\{ \int_\gamma A \right\} \quad (2.63)$$

where

- $\gamma : [0, 1] \rightarrow \Sigma$ is a path in the spatial hypersurface parametrized by

$$s \in [0, 1] \quad \text{such that} \quad \int_\gamma A = \int_0^1 ds A_a^i(x(s)) \frac{dx^a(s)}{ds} \tau_i \quad (2.64)$$

- \mathcal{P} stands for the path ordered product:

$$\mathcal{P}exp \left\{ \int_\gamma A \right\} = Id_{SU(2)} + \sum_{n=1}^{\infty} \int_0^1 ds_1 \int_{s_1}^1 ds_2 \cdots \int_{s_{n-1}}^1 A(\gamma(s_1)) \cdots A(\gamma(s_n)) \quad (2.65)$$

The holonomy of a connection A along γ is the unique solution of the equations

$$\begin{cases} \frac{d}{ds} h_\gamma(A(\gamma(s))) = h_\gamma(A(\gamma(s))) A(\gamma(s)) \\ h_\gamma(A(\gamma(0))) = Id_{SU(2)} \end{cases} \quad (2.66)$$

Physically, a holonomy gives a measure of how data fail to be preserved when parallel transported along a closed path. Performing this change of variable

$A \rightarrow h_\gamma(A)$ we have no loss of information, so we can consider all the possible paths in the manifold and get the same information as specifying connection at each point.

We can list some of the key properties of the holonomies:

1. The definition of $h_\gamma(A)$ does not depend on the parametrization of the path.
2. Connections transform under gauge transformation $g \in SU(2)$ as

$$A \rightarrow A_g = g^{-1}dg + g^{-1}Ag \quad (2.67)$$

so h_γ transforms as

$$h_\gamma(A) \rightarrow h_\gamma(A_g) = g(\gamma(0)) h_\gamma(A) g^{-1}(\gamma(1)) \quad (2.68)$$

If we identify $\gamma(0)$ and $\gamma(1)$ as the **source** and the **target** of the path γ , say the initial and end point, we understand that if we act with a Gauge transformation on the bulk of the path, the holonomy will change only on the end points of γ .

3. The holonomy of a degenerate path (single point) is simply given by $Id_{SU(2)}$.
4. If we have two oriented path such that $\gamma_1(1) = \gamma_2(0)$, the holonomy

$$h_{\gamma_1 \circ \gamma_2}(A) = h_{\gamma_1}(A) h_{\gamma_2}(A) \quad (2.69)$$

5. Combining the two previous point we have:

$$h_\gamma^{-1}(A) = h_{\gamma^{-1}}(A) \quad (2.70)$$

6. If we act with a diffeomorphism $\phi \in Diff(M)$:

$$h_\gamma(\phi^* A) = h_{\phi \circ \gamma}(A) \quad (2.71)$$

We have regularized connections A and electric fields E through flux and holonomies, thus smearing the conjugated variables on paths and surfaces instead of all the space. It is possible to write the new algebra in terms of h_γ and $E_i(S)$. This is called the **holonomy-flux algebra**. This algebra becomes very simple if we assume S and γ only have one intersection [6]:

$$\begin{aligned} \{h_\gamma(A), h_{\gamma'}(A)\} &= 0 \\ \{E_i(S), E_j(S)\} &= -\epsilon_{ijk} E_k(S) \\ \{E_i(S), h_\gamma(A)\} &= \tau_i h_\gamma(A) \end{aligned} \quad (2.72)$$

We can easily notice a particular anomaly with respect to what we usually get in Poisson brackets: although the electric fields E_i play the role of conjugated

momenta, they do not commute. This leads us to consider only holonomies as configuration variables to avoid the difficulties that arise if we proceed with a non commutative flux algebra.

Since the metric is a dynamical object in the theory, we need to find a way to define a measure on the space of connections that is metric independent. In order to achieve this task, in the next section we will introduce the **cylindrical function** as functionals depending on the connection only through holonomies on a finite set of paths. This will bring us to define graphs and spin network states.

Before introducing the notion of spin network, it's useful to underline the role of $SU(2)$ in this approach: starting from a generalization of the Ponzano-Regge model, we will give a description of the geometry of Spin Network state in terms of simplicial complex, i.e. a triangulation of the manifold, where each face of the simplicial complex is labeled by a spin variable associated to an irreducible representation of $SU(2)$. In particular, being Σ a 3-dimensional manifold, tetrahedra will be the main protagonists along the path. This approach will be soon discussed in detail and will be particularly fascinating because geometrical quantities, such as areas and volumes, have a clear and well defined description in terms of quantum observables. Moreover we will be able to introduce graphs both as paths of connected holonomies and as the dual picture of connected tetrahedra.

2.3 Spin Network states

So far we have obtained a description of gravity in terms of $SU(2)$ holonomies $h_\gamma(A)$ associated to a path γ and of Ashtekar-Barbero connections A_a^i . These paths play a crucial role in the Dirac quantization procedure. Our aim is to construct the unconstrained kinematic Hilbert space \mathcal{H}_{kin} .

2.3.1 Cylindrical functions

Cylindrical functions are functionals on the space of connection that only depends on the connections through a finite set of parameters [6]. In particular it is straightforward to define such functions as depending on connections through holonomies evaluated on a finite set of paths γ_i embedded in Σ .

A **Graph** [22] $\Gamma \subset \Sigma$ is a finite collection of L oriented paths γ_l with $l = 1, \dots, L$ embedded in Σ that meet at most at their endpoints. Paths are usually referred to as *links* or *edge*, while intersection points are called *nodes* or *vertices*.

Since a $SU(2)$ holonomy lives on each link, we can define a smooth function $f : SU(2)^L \rightarrow \mathbb{C}$ of L holonomies evaluated on the links of the graph $f = f(h_{\gamma_1}(A), \dots, h_{\gamma_L}(A))$. We can define a **Cylindrical function** as the functional of connection associated to a given graph Γ and a given function f defined as above:

$$\psi_{(\Gamma, f)}[A] := f(h_1, \dots, h_L) \tag{2.73}$$

where we denoted $h_l = h_{\gamma_l}$. It is also possible to define the space of all cylindrical functions associated to a graph as:

$$Cyl_{\Gamma} = \{\psi_{\Gamma} : A \rightarrow \psi_{\Gamma}[A] \in \mathbb{C}\} \quad (2.74)$$

This space can be turned into an Hilbert space if we introduce a scalar product between function: :

$$\langle \psi_{(\Gamma, f)} | \psi_{(\Gamma, f')} \rangle = \int_{SU(2)} \prod_{l=1}^L dh_l \overline{f(h_1(A), \dots, h_L(A))} f'(h_1(A), \dots, h_L(A)) \quad (2.75)$$

Where dh_l are L copies of the Haar measure on $SU(2)$. Here we notice that the change of variable that led us to $SU(2)$ connections (instead of $SO(3, 1)$ ones) is essential in order to define this scalar product. Indeed Haar measure is a gauge invariant normalized measure, well defined on a compact Lie Group. Being $SU(2)$ compact we can unambiguously integrate and calculate scalar product between cylindrical functions.

We can briefly recall the main properties of Haar measure:

1. $dh = d(gh) = d(hg) = d(h^{-1}) \forall g \in SU(2)$
2. $\int_{SU(2)} dh = 1$

Moreover, we can underline that a scalar product so defined has the advantage to exhibit invariance under both gauge transformations and diffeomorphisms. Indeed the first one is guaranteed by the invariance of Haar measure under left and right translation; diffeomorphism invariance is a direct consequence of the fact that the integral does not depend on path γ and the holonomy of the pullback of A leads back to the holonomy of A on a transformed curve:

$$h_{\gamma}(\phi^* A) = h_{\phi \circ \gamma}(A) \quad (2.76)$$

So Cyl_{Γ} is identified with the Hilbert space H_{Γ} associated to a given graph Γ . We can thus construct the kinematic Hilbert space of Σ as the space associated to all the graph embedded in the hypersurface Σ

$$H_{kin} = \bigcup_{\Gamma \subset \Sigma} H_{\Gamma} \quad (2.77)$$

In fact we are considering a canonical quantization of General Relativity in the continuum, so we need to take into account of all the graph embedded in Σ with holonomies along all their edges and surfaces dual to each edge such that the latter are pierced by one and only one edge in a single point.

This new Hilbert space requires the scalar product to be defined also on cylindrical function associated to different graphs. This scalar product can be inherited from that on H_{Γ} by introducing the *cylindrical equivalence relation*: namely, we can define equivalence classes of graphs that can be considered as subgraphs of a bigger one.

$$[\Gamma] = \{\Gamma_1 \sim \Gamma_2 \text{ iff } \exists \Gamma \subset \Sigma : \Gamma \supset \Gamma_1 \Gamma_2\} \quad (2.78)$$

So the inner product can be extended as follows:

$$\langle \psi_{\Gamma_1, f_1} | \psi_{\Gamma_2, f_2} \rangle \equiv \langle \psi_{\Gamma, f_1} | \psi_{\Gamma, f_2} \rangle \quad (2.79)$$

In the sense that Γ contains both Γ_1 and Γ_2 and the functions f_i are trivially extended on $\Gamma \setminus \Gamma_i$ by setting them constant over the links that do not belong to their original graph.

With this setup, the unconstrained kinematic Hilbert space is thus:

$$H_{kin} = \frac{\bigcup_{\Gamma \subset \Sigma} H_{\Gamma}}{\sim} \quad (2.80)$$

The main result, due to Ashtekar and Lewandowski [31], is that is possible to identify this Hilbert space as:

$$H_{kin} = L^2[A, d\mu_{AL}] \quad (2.81)$$

that is an Hilbert space over gauge connections A and is endowed with a measure $d\mu_{AL}$ called Ashtekar-Lewandowski measure. This means we can see the inner product (2.79) as scalar product between cylindrical functional with respect to Ashtekar-Lewandowski measure:

$$\langle \psi_{\Gamma_1, f_1} | \psi_{\Gamma_2, f_2} \rangle = \int d\mu_{AL} \overline{\psi_{\Gamma_1, f_1}(A)} \psi_{\Gamma_2, f_2}(A) \quad (2.82)$$

So far we obtained an Hilbert space that does not require a background metric. We shall now focus on the representation of holonomy-flux algebra on this space. It is convenient to find an orthogonal basis on this space.

The **Peter Weyl theorem** states that a square-integrable function on a compact Lie group $f \in L^2[G, d\mu_{Haar}]$ can be decomposed into matrix elements of the unitary irreducible representations of the group.

In this case, for $g \in G = SU(2)$, one has

$$f(g) = \sum_j \hat{f}_{mn}^j D_{mn}^j(g) \quad (2.83)$$

where j is an half integer representing the *spin* of the representation and $m, n = -j, \dots, j$ are magnetic indices.

$D_{mn}^j(g)$ is the spin- j irreducible matrix representation of the group element g ; this matrices are called **Wigner matrices**.

Since $H_{\Gamma} = L^2[SU(2)^L, d\mu_{Haar}]$, where L is the number of link of the graph, we can apply the Peter Weyl theorem and decompose the cylindrical functions as follow,

$$\psi_{\Gamma, f}[A] = \sum_{\{j\}, \{m\}, \{n\}} \hat{f}_{m_1 \dots m_L n_1 \dots n_L}^{j_1 \dots j_L} D_{m_1 n_1}^{j_1}(h_1[A]) \dots D_{m_L n_L}^{j_L}(h_L[A]). \quad (2.84)$$

Thus an orthonormal basis on H_{Γ} is given by

$$\langle A | \Gamma, \vec{j} \vec{m} \vec{n} \rangle = D_{m_1 n_1}^{j_1}(h_1[A]) \dots D_{m_L n_L}^{j_L}(h_L[A]) \quad (2.85)$$

where we have used a vectorial notation for $\vec{j}, \vec{m}, \vec{n}$ to denote the labels of the UIR of $SU(2)$ associated on each link of the graph.

2.3.2 Gauge-invariant Hilbert space

So far, we have defined an unconstrained kinematic Hilbert space of the graph, that is metric independent and endowed with a well defined scalar product.

The next step is solve quantum Gauss constraint and obtain $SU(2)$ gauge invariant states.

A generic gauge transformation of the connection is given by $A \rightarrow gAg^{-1} + g^{-1}dg$ where $g(x) \in SU(2)$ is a local gauge transformation. This translates into the requirement that holonomies transform as:

$$h_l \rightarrow h'_l = g(\gamma(0))h_l g^{-1}(\gamma(1)) \quad (2.86)$$

Where we can identify $\gamma(0)$ and $\gamma(1)$ as the *source* and *target* of the holonomy and, to shorten the notation, we can write $g(\gamma(0)) = g_{s(l)}$ and $g(\gamma(1)) = g_{t(l)}$. Thus a generic Wigner matrix will transform as

$$\begin{aligned} D_{m_l n_l}^{j_l}(h_l) &\rightarrow D_{m_l n_l}^{j_l}(h'_l) = D_{m_l n_l}^{j_l}(g_{s(l)} h_l g_{t(l)}^{-1}) \\ &= \sum_{\alpha_l, \beta_l = -j_l}^{j_l} D_{m_l \alpha_l}^{j_l}(g_{s(l)}) D_{\alpha_l \beta_l}^{j_l}(h_l) D_{\beta_l n_l}^{j_l}(g_{t(l)}^{-1}) \end{aligned} \quad (2.87)$$

By looking at (2.87) we notice that gauge transformations act only on sources and targets, namely the *nodes* of the graph. Thus imposing gauge-invariance on Hilbert space means to impose cylindrical function to be gauge invariant under $SU(2)$ action at every node:

$$f_0(h_1, \dots, h_L) = f_0(g_{s_1} h_1 g_{t_1}^{-1}, \dots, g_{s_L} h_L g_{t_L}^{-1}) \quad (2.88)$$

Given a cylindrical function $f \in H_\Gamma$ we can easily obtain a gauge invariant function through *group averaging*:

$$f_0(h_1, \dots, h_L) = \int_{SU(2)} \prod_n dg_n f(g_{s_1} h_1 g_{t_1}^{-1}, \dots, g_{s_L} h_L g_{t_L}^{-1}) \quad (2.89)$$

In the following paragraphs we will explicitly calculate how to impose gauge invariance on some simple example of graph that will be generalized and will constitute the building brick for each complex graph. The key point is to introduce (at each node) a projector onto the gauge invariant subspace of the Hilbert space, called **intertwiner**.

In order to introduce such tool, it is useful to recall that, through Peter-Weyl decomposition theorem, it is possible to decompose the Hilbert space associated to a graph into the tensor product of orthogonal subspaces that are basis of an irrep of $SU(2)$, say $H = \bigotimes_l V^{j_l}$. We will show that for a p -valent node, an intertwiner is an element of $Inv_{SU(2)}[V^{j_1} \otimes \dots \otimes V^{j_p}]$.

Wilson Line Wilson lines (and loops) arise in quantum field theory as gauge invariant operators. In particular Wilson loops are gauge invariant operators

associated to parallel transport of gauge variables along closed paths. The aim is to fully describe gauge theories in term of loops.

Let consider the formulation of gauge theories in terms of principal bundle: for each point of the spacetime M there exists a copy of the gauge group G , the fibre of the fibre bundle. Wilson lines allow us to compare points on fibres at different points on M . This is the same role of the connection in GR that makes possible to compare tangent vector of tangent space at different point. For principal bundle, this can be made by introducing a connection, that is equivalent to a gauge field. The unique solution of Wilson line equation, in term of the Lie-algebra valued gauge field A is given by:

$$W[x_1, x_2] = \mathcal{P}exp\left(i \int_{x_1}^{x_2} A_\mu dx^\mu\right) \quad (2.90)$$

Loops are defined as the trace of a closed Wilson line:

$$W[\gamma] = tr \left[\mathcal{P}exp\left(i \int_\gamma A_\mu dx^\mu\right) \right] \quad (2.91)$$

The set of holonomies forms a subgroup of the gauge group.

In our framework Wilson lines are exactly the holonomies, so a state of the Hilbert space corresponding to a single edge of the graph. We can label the matrix irrep of this state with γ, j, a and b , being a and b , mathematically speaking the magnetic indices of the representation or graphically speaking the source and the target of the link.

$$|W\rangle = |\gamma, j, a, b\rangle \quad (2.92)$$

The wave function associated to this state is:

$$\underline{\quad a \quad \quad \quad j \quad \quad \quad b \quad}$$

$$\psi_{\gamma, j, a, b}[h(A)] = \langle h | \gamma, j, a, b \rangle = \sqrt{2j+1} D_{ab}^j \left(h_\gamma(A) \right) \quad (2.93)$$

where $\sqrt{2j+1}$ is a coefficient that is necessary for the normalization of the state. Our aim is to glue together two Wilson line in a node, imposing gauge invariance through group averaging.

Consider two Wilson line states:

$$\langle h_1 | \gamma_1, j_1, a, b \rangle = \sqrt{2j_1+1} D_{ab}^{j_1}(h_1)$$

$$\langle h_2 | \gamma_2, j_2, b, c \rangle = \sqrt{2j_2+1} D_{bc}^{j_2}(h_2)$$



Since we have a single node we have to integrate over only one element of $SU(2)$, in particular we notice that the node b can be seen as the target of the holonomy h_1 and the source of the holonomy h_2 . Thus, our gauge invariant state will be:

$$\begin{aligned}
\psi_0 &= \sqrt{2j_1 + 1} \sqrt{2j_2 + 1} \int dg D_{ab}^{j_1}(h_1 g^{-1}) D_{bc}^{j_2}(g_1 h_2) = \\
&= \sqrt{2j_1 + 1} \sqrt{2j_2 + 1} \int dg D_{a\alpha}^{j_1}(h_1) D_{\alpha b}^{j_1}(g_1^{-1}) D_{b\beta}^{j_2}(g_1) D_{\beta c}^{j_2}(h_2) = \\
&= \sqrt{2j_1 + 1} \sqrt{2j_2 + 1} D_{a\alpha}^{j_1}(h_1) D_{\beta c}^{j_2}(h_2) \int dg D_{\alpha b}^{j_1}(g_1^{-1}) D_{b\beta}^{j_2}(g_1) = \\
&= \sqrt{2j_1 + 1} \sqrt{2j_2 + 1} D_{a\alpha}^{j_1}(h_1) D_{\beta c}^{j_2}(h_2) \frac{\delta_{j_1 j_2} \delta_{\alpha b} \delta_{b\beta}}{2j_1 + 1} \\
&= \sqrt{2j_1 + 1} D_{a\alpha}^{j_1}(h_1) D_{\beta c}^{j_1}(h_2) \frac{\delta_{\alpha\beta}}{\sqrt{2j_1 + 1}}
\end{aligned}$$

Where we have used the following properties of representations and Wigner matrices:

1. $D_{ab}^j(g^{-1}) = (D_{ab}^j(g))^{-1} = D_{ab}^j(g)^*$
2. $\int_{SU(2)} D_{ab}^j(g)^* D_{a'b'}^{j'}(g) = \frac{\delta_{jj'} \delta_{aa'} \delta_{bb'}}{2j+1}$

After the calculation we notice that it is possible to build a gauge invariant state made up of two Wilson line by multiplying the projector¹ $\frac{\delta_{\alpha\beta}}{\sqrt{2j+1}}$ in the vertex. Geometrically speaking, this is the same configuration of two angular momentum recoupling to give null total angular momentum, so in this simple case the only possibility is given by $j_1 = j_2$ and magnetic number of the first target and the second source to be equal.

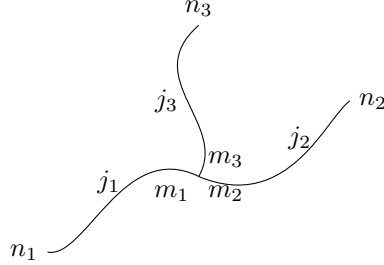
Moreover we notice that, since we imposed gauge invariance on a single node, performed through group averaging by integrating over a $g \in SU(2)$, the Hilbert space of the resulting state ψ_0 will no longer be $H = L_2(SU(2)^2)$ but

$H = L_2\left(\frac{SU(2)^2}{SU(2)}\right)$ since we have restricted the space from the one generated by product of Wigner matrices to the quotient set of the previous one with respect to the action of $SU(2)$.

In the following example we will show that this situation can be generalized for a graph with L links and N nodes.

¹It is possible to demonstrate that this object is a projector. This will be clear once we define intertwiners and their properties.

Trivalent node and Intertwiner The case of a trivalent node is way more interesting both at the conceptual level and at the computational level. We can



begin considering a generic state in $H = L_2(SU(2)^3)$ build up as product of three Wigner matrices with some generic coefficients:

$$\psi(h_1, h_2, h_3) = \sum_{\{j_i\}, \{m_i\}, \{n_i\}} f_{m_1 m_2 m_3 n_1 n_2 n_3}^{j_1 j_2 j_3} D_{m_1 n_1}^{j_1}(h_1) D_{m_2 n_2}^{j_2}(h_2) D_{m_3 n_3}^{j_3}(h_3) \quad (2.94)$$

To obtain a gauge invariant state, once again, we have to compute group averaging on the node. Since we have a single node we shall integrate over a single $g \in SU(2)$. It is possible to consider this node as source or target of the three links and the result will be the same.

$$\begin{aligned} \psi_0(h_1, h_2, h_3) &= \sum_{\{j_i\}, \{m_i\}, \{n_i\}} f_{m_1, \dots, n_3}^{j_1, \dots, j_3} \int dg D_{m_1 n_1}^{j_1}(gh_1) D_{m_2 n_2}^{j_2}(gh_2) D_{m_3 n_3}^{j_3}(gh_3) = \\ &= \sum_{\{j_i\}, \{m_i\}, \{n_i\}} f_{m_1, \dots, n_3}^{j_1, \dots, j_3} D_{\alpha_1 n_1}^{j_1}(h_1) D_{\alpha_2 n_2}^{j_2}(h_2) D_{\alpha_3 n_3}^{j_3}(h_3) \times \\ &\quad \times \int dg D_{m_1 \alpha_1}^{j_1}(g) D_{m_2 \alpha_2}^{j_2}(g) D_{m_3 \alpha_3}^{j_3}(g) \end{aligned} \quad (2.95)$$

The quantity $\int dg D_{m_1 \alpha_1}^{j_1}(g) D_{m_2 \alpha_2}^{j_2}(g) D_{m_3 \alpha_3}^{j_3}(g)$ projects the state on the gauge invariant subspace. It can be written in terms of *Wigner 3-j symbols*:

$$\int dg D_{m_1 \alpha_1}^{j_1}(g) D_{m_2 \alpha_2}^{j_2}(g) D_{m_3 \alpha_3}^{j_3}(g) = \begin{pmatrix} j_1 & j_2 & j_3 \\ m_1 & m_2 & m_3 \end{pmatrix} \overline{\begin{pmatrix} j_1 & j_2 & j_3 \\ \alpha_1 & \alpha_2 & \alpha_3 \end{pmatrix}} \quad (2.96)$$

where the 3-j symbols are normalized Clebsch-Gordan coefficients:

$$\begin{pmatrix} j_1 & j_2 & j_3 \\ m_1 & m_2 & m_3 \end{pmatrix} = \frac{(-1)^{j_1 - j_2 - m_3}}{2j_3 + 1} \langle j_1 m_1, j_2 m_2 | j_3 m_3 \rangle \quad (2.97)$$

Obviously the standard conditions for CB coefficients to no be null still hold:

1. $|m_i| \leq j_i$
2. $\sum_i m_i = 0$

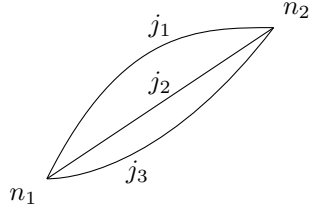
$$3. |j_1 - j_2| \leq j_3 \leq (j_1 + j_2)$$

So imposing gauge invariance requires the spin associated to the representations to satisfy CB conditions as if we are recoupling two angular momentum into a non-vanishing third one. We also understand that the previous case (two Wilson line) is a trivial case of the trivalent node where $j_3 = 0$. In fact it is possible to prove that (2.97) with $j_3 = m_3 = 0$ gives back the product of three δ as in the previous case. The gauge-invariant state can be written as:

$$\begin{aligned} \psi_0(h_1, h_2, h_3) &= \sum_{\{j_i\}, \{m_i\}, \{n_i\}} f_{m_1, \dots, n_3}^{j_1, \dots, j_3} \begin{pmatrix} j_1 & j_2 & j_3 \\ m_1 & m_2 & m_3 \end{pmatrix} \overline{\begin{pmatrix} j_1 & j_2 & j_3 \\ \alpha_1 & \alpha_2 & \alpha_3 \end{pmatrix}} \times \\ &\quad \times D_{\alpha_1 n_1}^{j_1}(h_1) D_{\alpha_2 n_2}^{j_2}(h_2) D_{\alpha_3 n_3}^{j_3}(h_3) = \\ &= \sum_{\{j_i\}, \{n_i\}} f_{n_1, n_2, n_3}^{j_1, \dots, j_3} t_{j_1, j_2, j_3}^{\alpha_1 \alpha_2 \alpha_3} D_{\alpha_1 n_1}^{j_1}(h_1) D_{\alpha_2 n_2}^{j_2}(h_2) D_{\alpha_3 n_3}^{j_3}(h_3) \quad (2.98) \end{aligned}$$

Where the 3j symbol with magnetic indices m has been absorbed in the coefficients that only depend on the degrees of freedom on the dangling legs of the graph. The second 3-j symbol is an invariant tensor in the space $\otimes_{l \in n} j_l$ of all the spins entering the node n . It is called **intertwiner** and plays the role of projecting the state onto its gauge invariant part. After the following example it will be shown that intertwiners project each node into the **singlet state**. This gauge invariant state belongs to $H = L_2\left(\frac{SU(2)^3}{SU(2)}\right)$.

Theta graph The theta graph is a closed graph composed of three links and two nodes. We can write the cylindrical function in term of the orthonormal



basis. To impose gauge invariance this time we need to integrate over two element since we have a source and a target for each link:

$$\begin{aligned} \psi_0(h_1, h_2, h_3) &= \sum_{\{j_i\}, \{m_i\}, \{n_i\}} f_{m_1, \dots, n_3}^{j_1, \dots, j_3} \times \\ &\quad \times \int dg_1 dg_2 D_{m_1 n_1}^{j_1}(g_1 h_1 g_2^{-1}) D_{m_2 n_2}^{j_2}(g_1 h_2 g_2^{-1}) D_{m_3 n_3}^{j_3}(g_1 h_3 g_2^{-1}) = \\ &= \sum_{\{j_i\}, \{m_i\}, \{n_i\}} f_{m_1, \dots, n_3}^{j_1, \dots, j_3} D_{\alpha_1 \beta_1}^{j_1}(h_1) D_{\alpha_2 \beta_2}^{j_2}(h_2) D_{\alpha_3 \beta_3}^{j_3}(h_3) \times \\ &\quad \times \int dg_1 dg_2 D_{m_1 \alpha_1}^{j_1}(g_1) D_{m_2 \alpha_2}^{j_2}(g_1) D_{m_3 \alpha_3}^{j_3}(g_1) D_{\beta_1 n_1}^{j_1}(g_2^{-1}) D_{\beta_2 n_2}^{j_2}(g_2^{-1}) D_{\beta_3 n_3}^{j_3}(g_2^{-1}) \quad (2.99) \end{aligned}$$

Using the properties of Haar measure the last integral can be written in terms of product of 3-j symbols:

$$\begin{aligned} \psi_0(h_1, h_2, h_3) = & \sum_{\{j_i\}, \{m_i\}, \{n_i\}} f_{m_1, \dots, n_3}^{j_1, \dots, j_3} D_{\alpha_1 \beta_1}^{j_1}(h_1) D_{\alpha_2 \beta_2}^{j_2}(h_2) D_{\alpha_3 \beta_3}^{j_3}(h_3) \times \\ & \times \begin{pmatrix} j_1 & j_2 & j_3 \\ m_1 & m_2 & m_3 \end{pmatrix} \overline{\begin{pmatrix} j_1 & j_2 & j_3 \\ \alpha_1 & \alpha_2 & \alpha_3 \end{pmatrix}} \begin{pmatrix} j_1 & j_2 & j_3 \\ \beta_1 & \beta_2 & \beta_3 \end{pmatrix} \overline{\begin{pmatrix} j_1 & j_2 & j_3 \\ n_1 & n_2 & n_3 \end{pmatrix}} \end{aligned} \quad (2.100)$$

Absorbing the first and the last 3-j in the coefficients we get the final gauge invariant state:

$$\psi_0(h_1, h_2, h_3) = \sum_{\{j_i\}} f_{j_1, j_2, j_3}^{j_1, j_2, j_3} D_{\alpha_1 \beta_1}^{j_1}(h_1) D_{\alpha_2 \beta_2}^{j_2}(h_2) D_{\alpha_3 \beta_3}^{j_3}(h_3) \iota_{j_1 j_2 j_3}^{\alpha_1 \alpha_2 \alpha_3} \iota_{j_1 j_2 j_3}^{\beta_1 \beta_2 \beta_3} \quad (2.101)$$

This wave function is a gauge invariant state with respect to two separate action of $SU(2)$ on the Hilbert space, namely:

$$\psi_0 \in L_2 \left(\frac{SU(2)^3}{SU(2)^2} \right). \quad (2.102)$$

We can finally generalize the results obtained in the previous example for a graph of L links and N nodes: *imposing $SU(2)$ gauge invariance on a graph reduces the Hilbert space to*

$$H_{kin}^0 = L_2 \left(\frac{SU(2)^L}{SU(2)^N}, d\mu_{Haar} \right) \quad (2.103)$$

Group averaging corresponds to inserting on each vertex v the quantity

$$\iota_v = \int dg \prod_{l \in v} D^{j_l}(g). \quad (2.104)$$

It is possible to show [6] that this object is a left and right invariant projector. Indeed it projects our state into its gauge invariant part.

The integrand in (2.104) is an element of the tensor product of base spaces of $SU(2)$ irrep:

$$\prod_l D^{j_l}(g) \in \bigotimes_l V^{(j_l)} \quad (2.105)$$

This tensor product space can be decomposed into:

$$\bigotimes_l V^{(j_l)} = \bigoplus_i V^{j_i} \quad (2.106)$$

So ι projects on the gauge invariant part of (2.106), namely the first term of the sum, or the **singlet space** $V^{(0)}$:

$$\iota_v : \bigotimes_l V^{(j_l)} \rightarrow V^{(0)} \quad (2.107)$$

Being this object a projector, it can be decomposed in terms of the basis $\{i_\alpha\}$ and the basis of its dual $\{i_\alpha^*\}$ as:

$$\iota_v = \sum_{\alpha=1}^{\dim V^{(0)}} i_\alpha i_\alpha^* \quad (2.108)$$

This invariant projectors are called **intertwiners**. Let's focus on the case of 3-valent and 4-valent intertwiner. About the former we know that the CG condition

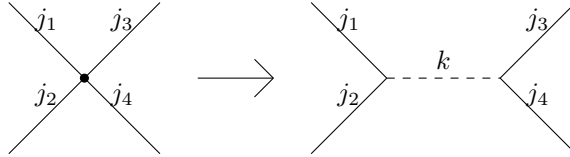
$$|j_1 - j_2| \leq j_3 \leq j_1 + j_2 \quad (2.109)$$

must hold. As explicitly calculated in Appendix A of [22]

$$\dim V^{(0)} = \dim \left(\text{Inv}_{SU(2)} \left[V^{j_1} \otimes V^{j_2} \otimes V^{j_3} \right] \right) = 1 \quad (2.110)$$

So for a 3-valent intertwiner there is one and only one intertwiner, given by the 3-j symbol.

However for a n-valent node ($n > 3$), $V^{(0)}$ will have larger dimension, and the construction of the intertwiner is still possible in term of 3-valent intertwiner, decomposing the node into 3-valent ones glued through virtual link, also labelled by a spin variable k . The case $n = 4$ is pretty easy to imagine and to derive:



Since triangular inequality must hold in both nodes we get:

$$\max\{|j_1 - j_2|, |j_3 - j_4|\} \leq k \leq \min\{(j_1 + j_2), (j_3 + j_4)\} \quad (2.111)$$

Thus it is clear that a 4-valent intertwiner is constructed by contracting two 3-valent intertwiner over the virtual spin k as follows:

$$\iota_{j_1 j_2 j_3 j_4} = \iota_{j_1 j_2}^k \iota_{k j_3 j_4} \quad (2.112)$$

Intertwiners will play a crucial role in the further discussions about quantum correlations in spin network. This is quite obvious if we think that the condition for which the space $V^{(0)}$ exists is that the Clebsch-Gordan conditions are satisfied. Moreover, in the next chapter we will show that gauge invariant state (obtained through intertwiner) are **maximally entangled** states: in fact gluing spin network with the gauge invariance requirement will be responsible for the appearance of entanglement in open spin networks. Although it's important to underline that the *maximum* entanglement holds only for base states and not necessarily for spin network that are superposition of base states.

2.3.3 A Spin Network basis for Quantum Geometry States

Intertwiners only act on the vertices of the graph. The action of ι_v on H_{kin} gives back gauge invariant states built contracting a Wigner matrix (irreducible spin- j representation of the holonomy h on the link) for each link of the graph with an intertwiner for each vertex of the graph. For a generic graph, a quantum geometry state is written as

$$\begin{aligned} \iota_v \in Inv\left[\bigotimes_{l \in v} V^{(j_l)}\right]: \\ \psi_0(\Gamma, j_l, \iota_v)[h_l] = \bigotimes_l D^{j_l}(h_l) \bigotimes_v \iota_v \end{aligned} \quad (2.113)$$

A **Spin Network** is a triplet $(\Gamma, \vec{j}, \vec{\iota})$ where Γ is the graph embedded in Σ , \vec{j} is a short hand notation for the L spins that label the links and similarly $\vec{\iota}$ are the N intertwiners associated to the nodes. The cylindrical function (2.113) is actually the wave function of a spin network state labeled by the quantum number associated to the *basis* $|\Gamma, \vec{j}, \vec{\iota}\rangle$:

$$\langle A | \Gamma, \vec{j}, \vec{\iota} \rangle = \psi_0(\Gamma, j_l, \iota_v)[h_l(A)] = \bigotimes_l D^{j_l}(h_l(A)) \bigotimes_v \iota_v, \quad (2.114)$$

where Wigner matrices and intertwiners are contracted according to the connectivity of the graph. The main result of this construction is that Spin Network states form a complete orthonormal **basis** for H_{kin} of a graph, in the sense that

$$\langle \Gamma, \vec{j}, \vec{\iota} | \Gamma', \vec{j}', \vec{\iota}' \rangle = \delta_{\Gamma\Gamma'} \delta_{\vec{j}\vec{j}'} \delta_{\vec{\iota}\vec{\iota}'} \quad (2.115)$$

and that $SU(2)$ gauge invariance is guaranteed by implementing in each node an intertwiner. As cited before the kinematic space can be obtained as direct sum over all the H spaces of the graphs embedded in Σ , namely

$$H_{kin} = \bigoplus_{\Gamma \subset \Sigma} H_{\Gamma}^0 \quad (2.116)$$

The physical interpretation of such states as **quantum geometry states** can be formulated by defining on this space observables related to geometric quantities.

In particular one can easily define an Area operator A of a surface in terms of triads.

The main results are:

- Areas are quantized and the spectrum is well known;
- eigenvalues of A are discrete and the minimal value is proportional to $l_{Planck}^2 = \hbar G_N$;
- Area operator acts diagonally on the link of a spin network

A similar discussion can be made for the Volume operator with the main differences that the minimal value of eigenvalue is proportional to l_{Planck}^3 and that this operator act on the intertwiners rather than on the links. We refer to [6] and [22] for a more detailed discussion on how these operators are built and diagonalized.

2.3.4 Spin Networks Dual to Simplicial Complexes

Further comprehension of how a spin network can clearly be identified as quantum geometry state, in the next section we will study the duality between spin network and simplicial complexes. In particular, we will understand that a spin network state associated to a 4-valent node can be seen as the state of a quantum tetrahedron.

So far the quantum states that appeared in the theory are the SN states built on a graph where each link is labelled by the spin of a certain irreducible representation of $SU(2)$ and each node is labelled by a quantum number of intertwiner, which is related to the $SU(2)$ gauge invariant subspace of the tensor product of the Hilbert spaces of the links meeting at the node. We have cited that those states diagonalize geometric operators such as Area and Volume operators. In this sense SN states are eigenstates of geometric observables. We also noticed that link states are area states and intertwiner are volume states.

It's well known that $SU(2)$ is the rotation group in Quantum Mechanics. So there is a link between quantum angular momentum and geometric observables. This link has been studied in many works with different approaches and different interpretations of the role of the spin.

In 1968, Ponzano and Regge [23] presented a quantum gravity model in 3 dimension, using some properties of invariant quantities obtained from $SU(2)$ representations. The main goal of the PR model is to define a partition function for a 3-dimensional simplicial complex on a 3d triangulated manifold: spins label the edges of the triangulation and are interpreted as the lengths of the edges. In fact, the 3-j symbol (2.97) are non zero only if the triangular inequality is satisfied. Then the product of two 3-j symbols is null unless the values of the representations' spins can represent the lengths of the edges of a **tetrahedron** which is the building block of a 3d triangulated manifold.

Barbieri [24] was among the first to understand that spin network states can be regarded as quantum geometric tetrahedra in three dimensions, leading to the idea that quantum gravity may be about studying discrete geometric structure, i.e. simplicial complexes.

We will follow the analysis proposed by Baez and Barret in [25], where, unlike the Ponzano-Regge (PR) model, spins do not label the lengths of the edges but the areas of the faces of a tetrahedron.

2.3.5 Quantum triangle in 3d gravity

Following the PR model, we can label the edges of a 3d triangulated manifold through irreducible representation of $SO(3)$ with spin j . Thus we associate to the spins j_1, j_2 and j_3 the length of the edges of a triangle. A quantum state of geometry of a triangle will be a state of the Hilbert space

$$\psi \in \bigotimes_{i=1}^3 V^{(j_i)} \quad (2.117)$$

such that the closure condition $\sum_i j_i = 0$ is satisfied. The quantum version of the closure condition translates into the requirement that the state be invariant under the action of $SO(3)$. If the j_i satisfy the triangular inequality there will be a unique invariant element called vertex. We can see graphically that it can be interpreted as a node of a 3-valent graph

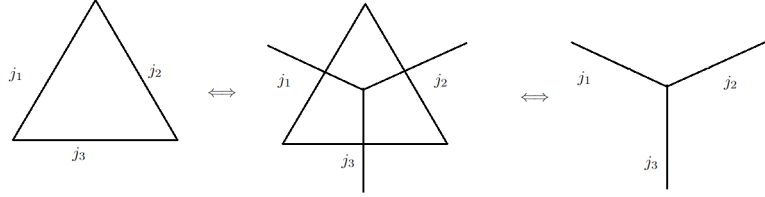


Figure 2.2: A 3-valent node as dual object to a quantum triangle.

So the geometry of the triangle is totally encoded in the length of its edges. The uniqueness of the vertex is due to the fact that the dimension of the space of this vertex is 0, and is explained in details in [25]. This is coherent with the previous example of 3-valent node: we had a unique intertwiner given by the 3-j symbols and the singlet space in $d = 3$ had dimension 0.

2.3.6 Classical tetrahedra

The main focus on the study of tetrahedra was to extend the Ponzano-Regge model in the case of 4-d gravity. In [32], Barret and Crane proposed a topological state sum model based on the triangulation of a 4-d manifold. The idea was to describe the geometry associated to a simplex in terms of the spin covering group $SU(2) \times SU(2)$ of the original symmetry group $SO(4)$. The description that arises is carried on in terms of *bivectors* in \mathbb{R}^4 , representing the vectorial areas of each face of the simplex. Performing a suitable quantization of this structure, spins come up to represent the *areas* of the faces of the simplex. Although this model completely encodes the geometry of tetrahedra in \mathbb{R}^4 , in order to obtain a description in terms of objects that are dual to the previous structure of spin network we need to restrict this result to \mathbb{R}^3 : this is obvious if we consider the fact that spin network states, defined in (2.114), emerge as gauge invariant states which include both information on holonomies and fluxes. Since the latter are defined by smearing the algebra of Ashtekar connections and densitized triads on the spatial manifold Σ , the natural ambient on which spin networks are well defined is a 3-d manifold. So, differently from Barret work [32], we would like to describe the geometry of a 3d manifold in terms of quantum states of tetrahedra.

This is a simple task thanks to Baez and Barret [25] that noticed that in the 4-d case, there are also extra constraints implying that all four faces lie in a common hyperplane. When these are satisfied we are essentially back in the 3-dimensional situation. The geometry of a classical tetrahedron is fully given by

three vectors e_1, e_2, e_3 $\mathfrak{3}$ which are the edge vectors for the three edges pointing out from a common vertex. As previously cited, this can be translated into a description in terms of bivectors associated to the each triangular face:

$$\begin{aligned} E_1 &= e_3 \wedge e_2 \\ E_2 &= e_1 \wedge e_3 \\ E_3 &= e_2 \wedge e_1 \\ E_4 &= -E_1 - E_2 - E_3 \end{aligned} \tag{2.118}$$

where \wedge is the usual wedge product, corresponding to cross product in \mathbb{R}^{33} , and the last equation implements the closure condition.

By identifying these bivector with normal areas of the faces and the wedge product with the usual cross product it is also possible to define:

$$-E_1 \cdot (E_2 \times E_3) = V^2 > 0 \tag{2.119}$$

where V is 6 times the volume of a non degenerate tetrahedron. Moreover we notice that all the previous definition can be computed in the same way also if the edges e_i are defined up to sign, i.e. the tetrahedron identified by $(-e_1, -e_2, -e_3)$ has the same structure but a different orientation in the space.

Since each bivector is an element of $\mathfrak{so}(3)^*$ we can start taking the following space:

$$(\mathfrak{so}(3)^*)^4 = \mathfrak{so}(3)^* \times \mathfrak{so}(3)^* \times \mathfrak{so}(3)^* \times \mathfrak{so}(3)^* \tag{2.120}$$

and impose the closure constraint thus obtaining a submanifold:

$$\mathcal{C} = \left\{ E_1 + E_2 + E_3 + E_4 = 0 \right\} \subset (\mathfrak{so}(3)^*)^4 \tag{2.121}$$

We note that this closure constraint generates the action of $SO(3)$ on $(\mathfrak{so}(3)^*)^4$ [25], so the reduced space will be obtained by quozienting the space \mathcal{C} with respect to this action.

In order to quantize this space we could follow two similar paths:

1. quantize $(\mathfrak{so}(3)^*)^4$ and then imposing constraints at quantum level;
2. quantize the constrained classical reduced space.

Since the second procedure is cumbersome due to geometric issues [22], we will follow the first and simpler path in order to obtain quantum states.

Geometric quantization takes product into tensor product, so

$$(\mathfrak{so}(3)^*)^4 \rightarrow \mathcal{H} = H^{\otimes 4} \tag{2.122}$$

where [22] H can be decomposed into:

$$H = \bigoplus_i \mathcal{V}^i \tag{2.123}$$

³In fact in \mathbb{R}^3 the space of bivector $\Lambda^2 \mathbb{R}^3 \cong \mathbb{R}^3$

We can promote the bivectors to operators trivially expanding them to the tensor product (2.122) as follows:

$$\begin{aligned}
E_1 &\rightarrow \hat{E}_1 = \hat{E}_1 \otimes \mathbb{1} \otimes \mathbb{1} \otimes \mathbb{1} \\
E_2 &\rightarrow \hat{E}_2 = \mathbb{1} \otimes \hat{E}_2 \otimes \mathbb{1} \otimes \mathbb{1} \\
E_3 &\rightarrow \hat{E}_3 = \mathbb{1} \otimes \mathbb{1} \otimes \hat{E}_3 \otimes \mathbb{1} \\
E_4 &\rightarrow \hat{E}_4 = \mathbb{1} \otimes \mathbb{1} \otimes \mathbb{1} \otimes \hat{E}_4
\end{aligned} \tag{2.124}$$

thus we can impose the closure constraints at quantum level: given $|\psi\rangle \in \mathcal{H}$

$$(\hat{E}_1 + \hat{E}_2 + \hat{E}_3 + \hat{E}_4)|\psi\rangle = 0. \tag{2.125}$$

Equation (2.125) imposes that the four triangles associated to vectorial areas E_i must close the boundary of a tetrahedron; this condition also corresponds to the request of invariance under rotation of the tetrahedron. So the states that naturally satisfy (2.125) are those who are $SU(2)$ invariant.

Thus the Hilbert space of a tetrahedron will be:

$$\mathcal{H}_T = \text{Inv}_{SU(2)} \left[H^{\otimes 4} \right] = \bigoplus_{j_1, j_2, j_3, j_4} \text{Inv}_{SU(2)} \left[\bigotimes_{l=1}^4 \mathcal{V}^{j_l} \right] \tag{2.126}$$

We soon recognize the same Hilbert space of an Intertwiner of a 4-valent node. In the previous case, this Hilbert space was associated to the Gauge invariant request under $SU(2)$ action at the node where 4 links of the graph met, forming a node described by a state in the gauge invariant subspace of the tensor product of the Hilbert space that were a base of the representation of link associated to holonomies.

Since we obtained the same identical result it is natural to consider spin network as a dual picture to a triangulation of a 3-manifold into tetrahedra, where, similarly to the case of the PR model, we associate a spin variable to the area of each face of the tetrahedron.

This result is also compatible to the point of view of many other works such as [33] and [34] where geometric observables related to tetrahedra (or spin network) are discrete, quantized and come up to be related to the value j that is the spin associated to the links forming the graph.

2.4 Summary

We can finally sum up the main goals of the previous sections:

1. Starting from Einstein-Hilbert action we managed to restrict GR to a 3-d spatial manifold Σ embedded in the spacetime.
2. The description in terms of Ashtekar-Barbero connections and densitized triads allowed us to switch from a $SO(1, 3)$ gauge theory to a $SU(2)$ Yang-Mills theory on lattice, more suitable to a quantization procedure.

Following Dirac procedure, we built the kinematic Hilbert space imposing Gauge invariance on the node of the lattice.

3. Using the definition of holonomy and intertwiner we got to introduce **spin Network states** as quantum gauge invariant state on a graph with a certain connectivity. Those states are build up contracting holonomies (labelled by a spin variable) and intertwiner (projector on gauge invariant subspace). It is also possible to introduce a scalar product between spin network, and expand this typical structure to the Hilbert space given by the union of all the graph embedded in Σ .
4. Duality between spin network and simplicial complexes gives us a deeper understanding of Spin network as **quantum geometry states**. In particular we shall focus on 4-valent graph, dual to a tetrahedra with a given classical geometry in the triangulation of space manifold Σ .
5. To convince us even more about the geometric nature of SN states, references were made to the possibility to define geometric operators, such as Area and Volume, such that SN states are actually eigenstates of these operators and the eigenvalues corresponds to the geometrical properties of the tetrahedron of which each node is dual.

Chapter 3

Entanglement Entropy for Spin Network states

In this Chapter, we review the notion of entanglement by focusing on Von Neumann entropy and its Rényi generalizations with applications to simple spin-network states.

After a short review on density matrix formulation of quantum mechanics, we introduce the concept of reduced state associate with a multipartite system. We first introduce the notion of Von Neumann (VN) entropy, as the quantum version of Shannon entropy in information theory. Through VN entropy, we can also define the entanglement entropy and the quantum mutual information for a bipartite system. Further we study the property of the Rényi entropy (of order k), as a generalization of the Von Neumann entropy.

We apply these notions to calculate correlations in quantum geometry states starting from the simple case of two Wilson lines glued together. The main goal of this calculation is to show first how entanglement is associated to topological connectivity of the spin network graph, where gluing edges corresponds to entangling the degrees of freedom at the free ends of the vertices, and secondly how the requirement of spin network states to be gauge invariant induces quantum correlations. We then characterise the difference of *ultra-local* gluing entanglement and non-local entanglement associated to the presence of quantum correlations among spin network vertices in the setting of two entangled tetrahedra. We notice that the ultra-local entanglement entropy contribution between two spin network vertices is proportional to the number of link crossing the surface that separate them: since links are area eigenstates, this shows that ultra-local entanglement entropy scales with area hence it gets a direct geometric characterisation and a holographic interpretation. Vertex entanglement is on the other hand associated to quantum correlations among quana of 3d space volume. The associated entropy contribution is generally not extensive leading to corrections to the area law.

3.1 Density operator

Quantum systems present different behavior from the classical one. This is well known for the case of single particle where properties like superposition and tunneling differ radically from the classical description of a 1-particle state. Quantum regime becomes even more fascinating if we study correlations emerging in a composite systems. **Entangled states** are states whose correlations cannot be described as classical probabilities. In order to study the properties of this type of state in the framework of spin network states, we start the review on the main tools of quantum information theory.

First of all we have to find a way to describe the physics of a quantum state, even if we have no complete knowledge of the state itself.

Suppose a quantum system be in one of the states $|\psi_i\rangle$ where $i = 1 \dots, n$ with a certain probability p_i . We define the *density operator* of the system as

$$\rho = \sum_i p_i |\psi_i\rangle \langle \psi_i|. \quad (3.1)$$

Density operator is also called *density matrix*. It is possible to show that (3.1) has enough information on the system to fully describe it's dynamics in quantum language, i.e. the postulates of quantum mechanics can be reformulated in terms of ρ . For example, the evolution under a unitary operator U translates into:

$$\rho' = \sum_i p_i |\psi'_i\rangle \langle \psi'_i| = \sum_i p_i U |\psi_i\rangle \langle \psi_i| U^\dagger = U \rho U^\dagger \quad (3.2)$$

If we have complete knowledge of a state, i.e. the state is a certain $|\psi\rangle$, the state is said to be **pure** and the density matrix associated is given by $\rho = |\psi\rangle \langle \psi|$. Otherwise, we can imagine that the system is prepared in a state ρ_i with a certain probability p_i , such that $\sum_i p_i = 1$. So the total density matrix can be written as:

$$\rho = \sum_i p_i \rho_i \quad (3.3)$$

The state ρ is said to be a **mixed states** or a **mixture**.

The class of density operators is characterized by the following properties:

$$\begin{aligned} \rho &\geq 0 \\ Tr(\rho) &= 1 \\ \rho &= \rho^\dagger \end{aligned} \quad (3.4)$$

Moreover, since we are interested in entanglement entropy of mixed quantum geometry states, we need a criterion to distinguish pure states and mixed states.

It is possible to prove that $Tr(\rho^2) \leq 1$, where equality holds if and only if ρ is a pure state. Therefore to verify if a state is a mixture we need to trace ρ^2 .

3.1.1 Composite system

So far the description in terms of density matrix is limited to the case of a state of a single Hilbert space, i.e. a single particle states. However most realistic situations that require this formalism are related to systems describing a large number of subsystem, such as many-body systems.

We call **composite** or **multipartite system** a system that can naturally be decomposed into two or more subsystem, each of which is a quantum state. The Hilbert space of a multipartite system is given by the tensor product of the Hilbert spaces of all the subsystem:

$$\mathcal{H} = \mathcal{H}_1 \otimes \dots \otimes \mathcal{H}_N \quad (3.5)$$

For simplicity we assume each space to be finite dimensional.

We can focus on the case of a *bipartite* system, to obtain results that will be easily generalized for the multipartite one:

$$\mathcal{H} = \mathcal{H}_A \otimes \mathcal{H}_B \quad (3.6)$$

Given a orthonormal **basis** for each system $\{|e_A\rangle\}$ and $\{|e_B\rangle\}$, the space \mathcal{H} will thus be spanned by $|e_A\rangle \otimes |e_B\rangle$. On this space we can define operators acting both on A and on B , $O_A \otimes O_B$ such that:

$$\begin{aligned} (O_A \otimes O_B)(O'_A \otimes O'_B) &= O_A O'_A \otimes O_B O'_B \\ (O_A \otimes O_B)^\dagger &= O_A^\dagger \otimes O_B^\dagger \\ \text{Tr}(O_A \otimes O_B) &= \text{Tr}(O_A)\text{Tr}(O_B) \end{aligned} \quad (3.7)$$

Since we are interested in studying local properties of subsystem, it is also useful to note that each operator acting only on one of the subsystems can be trivially expanded as acting on the multipartite system:

$$\begin{aligned} O_A &\rightarrow O_A \otimes \mathbb{1}_B \\ O_B &\rightarrow \mathbb{1}_A \otimes O_B \end{aligned} \quad (3.8)$$

Suppose now to deal with a composite system such that the state of each subsystem is pure. The total state is given by the tensor product:

$$|\psi\rangle = |\psi_A\rangle \otimes |\psi_B\rangle \quad (3.9)$$

If we perform a measure of a local observable on A , the state of the subsystem will be projected on the subspace of the eigenstate of O_A and the state in B is untouched by this operation. Then if we perform a measure on B the second measurement will not be modified by the previous one, i.e. the two results do not depend on each other. It is thus obvious that the two subsystem are uncorrelated.

Although this result may lead us to think that we have easily described a quantum multipartite system, we have to recall that the typical situation in quantum regime is to deal with **mixed states**.

A useful tool to deal with mixtures is the **reduced density operator**: it will allow us in short time to deeply understand how and why measurement outcomes on different subsystems will be now correlated.

Suppose we have a quantum system in the space (3.6) described by density operator ρ_{AB} . The reduced density operator relative to the system A is given by

$$\rho_A = Tr_B(\rho_{AB}) \quad (3.10)$$

where Tr_B is a map called **partial trace** over the system B , defined by

$$Tr_B(|e_{A1}\rangle\langle e_{A2}| \otimes |e_{B1}\rangle\langle e_{B2}|) = |e_{A1}\rangle\langle e_{A2}| Tr(|e_{B1}\rangle\langle e_{B2}|) \quad (3.11)$$

where the trace in the last term is the regular trace defined on the system B .

We can soon understand that ρ_A defined in (3.10) can be identified as a state that faithfully describe the state of the system A . In particular, it provides the correct measurement statistics for measurements made on system A . In fact if we consider a pure state in \mathcal{H} given by a superposition of state of the form $|\psi_A\rangle \otimes |\psi_B\rangle$, we can calculate the mean value of a local observable for the system A :

$$\begin{aligned} \langle O_A \rangle &= Tr[\rho(O_A \otimes \mathbb{1}_B)] = Tr[|\psi\rangle\langle\psi|(O_A \otimes \mathbb{1}_B)] = \\ &= Tr_A(Tr_B \rho O_A) = Tr_A(\rho_A O_A) \end{aligned} \quad (3.12)$$

This equation holds for each local operator in A . So the state in this subsystem is given by ρ_A . Obviously a similar argument is also valid for B :

$$\rho_B = Tr_A(\rho). \quad (3.13)$$

In [35] an explicit calculation underlines the very crucial point of reduced density operators: even if the state of a bipartite system is pure (we have complete knowledge of the state), the state of the subsystem is **mixed**, i.e. we apparently do not have maximal knowledge. This strange property, that the joint state of a system can be completely known, yet a subsystem be in mixed states, is another hallmark of quantum entanglement.

Moreover, even if the states in \mathcal{H}_A and \mathcal{H}_B can be written as the reduced density matrix, the total state of the system will not be given by the tensor product:

$$\rho \neq \rho_A \otimes \rho_B \quad (3.14)$$

In fact a measure on a subsystem induces a reduction of the state of the **entire system**. This means that a measurement on a subsystem will be correlated to previous measurement on the second subsystem.

3.1.2 Separable and entangled states

We have seen that, for a multipartite system, states differ depending on how measurements on subsystem are correlated. We can thus classify states in $\mathcal{H} = \mathcal{H}_A \otimes \mathcal{H}_B$ based on how local states arise from measurement.

1. A state is said to be **separable** if it can be written as tensor product of local states:

$$\begin{aligned} |\psi\rangle &= |\psi_A\rangle \otimes |\psi_B\rangle \\ |\psi_I\rangle &\in \mathcal{H}_I \quad I = A, B \end{aligned} \quad (3.15)$$

2. Otherwise, if local states $|\psi_I\rangle \in \mathcal{H}_I$ do not exist, the state is said to be **entangled**.

$$\nexists |\psi_I\rangle \in \mathcal{H}_I \text{ s.t. } |\psi\rangle = |\psi_A\rangle \otimes |\psi_B\rangle \quad (3.16)$$

In real situation, quantum systems cannot be separated by the environment, thus the state of a system has to be obtained by tracing out the environment. This lead us to deal with mixed states.

If we denote $\rho^{(I)}$, $I = A, B$ the density matrix associated to the subsystem A or B respectively, the state $\rho = \rho^{(A)} \otimes \rho^{(B)}$ has no correlations. If we define a state as convex combination of this type of state, we obtain a **separable mixed state**:

$$\rho = \sum_i p_i \rho_i^{(A)} \otimes \rho_i^{(B)} \quad (3.17)$$

such that $p_i \geq 0$ and $\sum_i p_i = 1$. measurements on this type of state will reveal correlations, in the sense that:

$$Tr[\rho(O_A \otimes O_B)] \neq Tr_A(\rho_A O_A) Tr_B(\rho_B O_B) \quad (3.18)$$

This correlations can be described in terms of p_i , i.e. the component of a vector of classical probability: thus we consider this correlation as classical correlation.

If there not exists local states $\rho_i^{(I)}$ such that the state of the total system can be written as (3.17), the state is said to be **mixed entangled state**, and the system will be characterized by correlations that can not be described in terms of classical probabilities.

Our aim is to apply all this definition to spin network states, in order to study different measure of quantum correlation between quanta of geometry. Besides an appropriate definition of entropy, we need a final fundamental tool to discriminate on sight separable states and entangled ones.

Schmidt decomposition Let $|\psi\rangle$ be a pure state of a composite system AB . There exists a set of orthonormal states $\left\{ |e_i^{(A)}\rangle \right\}, \left\{ |e_i^{(B)}\rangle \right\}$ of A and B respectively, such that[22][35]:

$$\begin{aligned} |\psi\rangle &= \sum_i \lambda_i |e_i^{(A)}\rangle \otimes |e_i^{(B)}\rangle \\ \lambda_i &\geq 0 \\ \sum_i \lambda_i^2 &= 1 \end{aligned} \quad (3.19)$$

The terms λ_i are called *Schmidt coefficients*. They are uniquely defined and the number of non-zero coefficients $|I|$ is called *Schmidt rank*.

A state is separable if its Schmidt rank is 1. Indeed if $|I| > 1$, $|\psi\rangle \neq |\psi_A\rangle \otimes |\psi_B\rangle$, thus the state is entangled.

Since Schmidt basis in(3.19) is composed by separable vector states, all the information on entanglement and correlations are encoded in the coefficients. The reduced density state of one of the subsystem in the Schmidt basis is given by[22]:

$$\begin{aligned}\rho_A &= Tr_B \left[|\psi\rangle \langle \psi| \right] = \sum_{i \in |I|} \lambda_i^2 \left| e_i^{(A)} \right\rangle \left\langle e_i^{(A)} \right| \\ \rho_B &= Tr_A \left[|\psi\rangle \langle \psi| \right] = \sum_{i \in |I|} \lambda_i^2 \left| e_i^{(B)} \right\rangle \left\langle e_i^{(B)} \right|\end{aligned}\tag{3.20}$$

Thus we see that the Schmidt basis is given in terms of eigenstates of reduced density matrix. Moreover, the two reduced states have the same non-vanishing spectrum, given by Schmidt coefficients.

We define a **maximally entangled state** a state with maximal Schmidt rank, such that all the coefficients are equal. The reduced density matrix of this state will be maximally mixed.

Through Schmidt decomposition, one can verify if a given quantum state is separable or entangled (i.e. Schmidt rank to be greater than 1). However, we need a *quantitative* measure of correlations, describing the amount of entropy associated to the lack of knowledge of a certain state.

In the next sections, we introduce two main measures of entanglement: the **Von Neumann entropy** and its **Rényi entropy** generalization. We will provide some examples of Von Neumann entropy for quantum states of geometry and define the setting of the Rényi derivation which will be used in Chapter 4 for the special class of random spin network states.

3.2 Von Neumann Entropy

In quantum statistical mechanics, Von Neumann entropy is the extension of the classical *Shannon Entropy*. Given a finite set (p_1, \dots, p_n) representing the weights of a classical discrete probability distribution, i.e. $\sum_i p_i = 1$ and $p_i \geq 0 \forall i$. We can quantify the amount of uncertainty on the outcome of an experiment, since each possible outcome will have probability p_i . The physical quantity that describes this uncertainty is called **Shannon Entropy**:

$$H(p_1, \dots, p_n) = - \sum_i p_i \log(p_i)\tag{3.21}$$

Shannon Entropy is also known as *Information entropy* and serves as the basis for many applications in information theory. Nevertheless it is strictly related

to *Gibbs Entropy* in statistical mechanics:

$$S = -k_B \sum_i p_i \log(p_i) \quad (3.22)$$

p_i being the probability of the i -th microstate taken from an **equilibrium** ensemble. Although (3.21) and (3.22) may look like the same formula, there is a subtle difference: while H can be calculated for any probability distribution, S only refers to thermodynamical systems. However this is a purely theoretical difference, since any probability distribution can be approximated arbitrarily closely by some thermodynamic system [36].

For a quantum system described in terms of ρ , Von Neumann entropy is defined as

$$S(\rho) = -\text{Tr}(\rho \log \rho) \quad (3.23)$$

Since $\rho = \sum_i p_i |\psi_i\rangle \langle \psi_i|$, by simple calculations it is possible to prove that

$$S(\rho) = -\sum_i p_i \log p_i \quad (3.24)$$

As

$$0 \leq p_i \leq 1 \quad \forall i \rightarrow \log p_i < 0 \quad (3.25)$$

we see that Von Neumann entropy is positive definite.

We can list some of the main properties of Von Neumann entropy:

1. $S(\rho) \geq 0$ where equality holds for pure state.
2. $\max\{S(\rho)\} = \log N$ where N is the dimension of the Hilbert space of the system. This equality holds for maximally mixed states.
3. Given any unitary operator U acting on \mathcal{H} , $S(\rho)$ is invariant under this transformation:

$$S(\rho) = S(U\rho U^\dagger) \quad (3.26)$$

4. **Subadditivity condition:** for bipartite system

$$S(\rho) \leq S(\rho_A) + S(\rho_B) \quad (3.27)$$

the equality holds for uncorrelated states, i.e. states that can be written as $\rho = \rho_A \otimes \rho_B$. This means that, tracing a subsystem we lose information about the correlations between the two subsystems, thus leading to increasing uncertainty on the state, that is increasing entropy.

5. **Strong subadditivity inequality:** for tripartite systems, there is a similar relation

$$S(\rho_{ABC}) + S(\rho_B) \leq S(\rho_{AB}) + S(\rho_{BC}) \quad (3.28)$$

this means that the subsystems B and C together have more correlations with A than just B by itself does.

If we focus on the case of a bipartite system, we notice that, if we perform Schmidt decomposition, the reduced states will have the same non negative entropy:

$$S(\rho_A) = S(\rho_B) = - \sum_i \lambda_i^2 \log \lambda_i^2 \quad (3.29)$$

This allows us to distinguish separable and entangled states as follows:

1. If

$$S(\rho_A) = S(\rho_B) = 0 \quad (3.30)$$

then ρ is separable;

2. If

$$S(\rho_A) = S(\rho_B) > 0 \quad (3.31)$$

then ρ is entangled;

3. If

$$S(\rho_A) = S(\rho_B) = \log(N_A) \quad (3.32)$$

(entropy of each subsystem is the **max**) the state is maximally entangled.

The quantity $S(\rho_A) = S(\rho_B)$ quantifies the entanglement between the two subsystem. It is called **Entanglement entropy** between A and B .

$$\mathcal{E}(A : B) = S(\rho_A) = S(\rho_B) \quad (3.33)$$

In order to take into account the quantity of information lost after tracing out a subsystem, we can define the **Quantum Mutual Information** as:

$$I(A : B) = S(\rho_A) + S(\rho_B) - S(\rho) \geq 0 \quad (3.34)$$

$I(A : B)$ measures the amount of information that A has on the system B . It vanishes for pure states.

3.3 Rényi Entropy

In 1960, [37] Rényi introduced **classical Rényi entropy** as a generalization of Shannon entropy, depending on a parameter $0 \leq q \leq \infty$:

$$S_q = \frac{1}{1-q} \log \sum_i p_i^q \quad (3.35)$$

In order to not divide by 0, we could be led to think that the case $q = 1$ is not allowed. Instead, thanks to L'Hôpital's rule, it is quite easy to prove that

$$\lim_{q \rightarrow 1} S_q = - \sum_i p_i \log(p_i) \quad (3.36)$$

Thus we can identify S_1 with the Shannon entropy.

Rényi entropy has a natural role in physics: it is in fact related to the concept of **free energy**. Baez [38] proved that such relation exists if we interpret the parameter q as a ratio of temperature.

If we consider a state of thermal equilibrium for some Hamiltonian at some chosen temperature T_0 with partition function defined as

$$Z(T) = \sum_i e^{-\frac{E_i}{T}} \quad (3.37)$$

and suppose we suddenly change to temperature to T_1 ; then the free energy

$$\mathcal{F}(T_1) = -T \log(Z(T_1)) \quad (3.38)$$

i.e. the maximum amount of work the system can do as it moves to equilibrium at the new temperature, is related to Rényi entropy as follows:

$$\mathcal{F}(T_1) = -(T_1 - T_0) S_{\frac{T_0}{T_1}} \quad (3.39)$$

where $\frac{T_0}{T_1} = q$. Relation (3.39) will still hold in quantum regime, although it will not be discussed here. We refer to Baez article for a more deep discussion and a detailed way to derive this equation.

Just as Von Neumann entropy, also Rényi entropy need the density matrix formulation of quantum mechanics to be well defined for quantum state.

Given a density matrix ρ with a certain spectrum $(\lambda_1, \dots, \lambda_n)$, we can define **quantum Rényi entropy** to be

$$S_k(\rho) = \frac{1}{1-k} \log \text{Tr}(\rho^k) = \frac{1}{1-k} \log \left(\sum_i \lambda_i^k \right) \quad (3.40)$$

Once again $0 \leq k \leq \infty$. Moreover we notice three particular cases:

1. $k = 0$: $S_0(\rho) = \log(\text{rank}(\rho))$
2. $k = 1$, : $S_1 = -\text{Tr}(\rho \log \rho)$
3. $k = \infty$: $S_\infty = \log(\lambda_1)$

The second case is just the Von Neumann entropy. The values $k = 0, \infty$ instead are quantities that appear frequently in quantum information theory.

Following [39], we can recall some of the main properties of Rényi entropy, that hold for each k :

1. If $k \leq l$ then $S_l \leq S_k$;
2. It follow from the first and from the definition of S_0 the fact that:

$$0 \leq S_k \leq \log(\text{rank}(\rho)) \quad (3.41)$$

3. S_k is minimized only by pure states;

4. S_k $k \neq 0$ is maximized only if $\lambda_i = \frac{1}{n} \forall i$

Also Rényi entropy obey a weak form of subadditivity. We remind that subadditivity for Von Neumann entropy reads as $S(\rho_{AB}) \leq S(\rho_A) + S(\rho_B)$, this form holds for S_k only if $k = 0, 1$.

It is possible to prove that, given a bipartite system described by density matrix ρ_{AB} , for each value of k :

$$S_k(\rho_A) - S_0(\rho_B) \leq S_k(\rho_{AB}) \leq S_k(\rho_A) + S_0(\rho_B) \quad (3.42)$$

The relation (3.42) is known as **Weak subadditivity**. The chain of disequality has been proven in [39].

3.3.1 Why Rényi Entropy?

Although Rényi entropy is defined as a generalization of Von Neumann entropy, there are several advantages over the latter. First of all, it contains richer physical information about the entanglement structure of a quantum state. In particular, the knowledge of Rényi entropies for all orders n allows one to determine the whole entanglement spectrum, i.e. the set of eigenvalues of ρ . Moreover Rényi Entropy has been deeply studied in many research fields, such as:

1. Numerical methods like quantum version of Monte Carlo method [40];
2. n-dimensional CFT [41];
3. Tensor network [42].
4. In quantum many-body systems it has been largely discussed [43] how the study of the second order Rényi entropy $S_2(A) = -\log \text{Tr}(\rho_A^2)$, namely the **purity** of the quantum state, is related to the expectation value of the parity of particle number. In this sense Rényi entropy is much easier to experimentally measure and numerically study.

Last but not least, it has been shown [10] that all Rényi entropies satisfy a similar area law in holographic theories: this property will be central in the our derivations in Chapter 5.

3.4 Entanglement of Spin Network States

Multipartite quantum systems exhibit correlation between subsystems. We have understood that such correlation can be identified through various methods and can also be quantified via entanglement entropy measurements. The next step is to study entanglement in quantum system corresponding to quantised geometry states realised via spin network states. We begin studying the simple case of two Wilson lines glued together with a bivalent intertwiner, then we will study the case of two 4-valent nodes linked through a single leg. The main goal is to

verify that gluing edges corresponds to entangle the degrees of freedom attached to their free ends.

Following the procedure of [22, 8, 9], we are going to build a bipartite system, find the Schmidt decomposition in the spin network basis and compute the Von Neumann entropy.

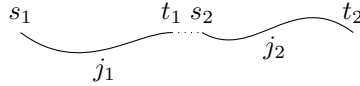
3.4.1 Entangled Wilson lines

In the previous chapter we derived the form of a spin network state (2.114). Let's keep a step back and consider two non gauge invariant basis states:

$$|\Gamma, \vec{j}, \vec{m}\rangle \quad (3.43)$$

Where Γ is the graph, \vec{j} is the collection of spin numbers we use to label irreducible $SU(2)$ representations for each link, and \vec{m} is a collection of vectors, each one belonging to the associated spin j_i representation space $\mathcal{V}^{(j_i)} \cong \mathbb{C}^{2j_i+1}$ [8]. Let us consider the states of two Wilson lines as in (2.92). We call γ_1 and γ_2 the unique paths of each graph, j_1 and j_2 the spin of the representations defining Wigner matrices, and s_i (t_i) the source (the target) of the i -th line. For simplicity, we start with the case of single basis state to emphasize the correspondence between imposing gauge invariance and inducing quantum correlations.

$$\begin{aligned} |\gamma_1, j_1, s_1, t_1\rangle &\rightarrow \psi_{\gamma_1 j_1 s_1 t_1}(h[A]) = \langle h | \gamma_1, j_1, s_1, t_1 \rangle = \sqrt{2j_1+1} D_{s_1 t_1}^{j_1}(h_{\gamma_1}[A]) \\ |\gamma_2, j_2, s_2, t_2\rangle &\rightarrow \psi_{\gamma_2 j_2 s_2 t_2}(h[A]) = \langle h | \gamma_2, j_2, s_2, t_2 \rangle = \sqrt{2j_2+1} D_{s_2 t_2}^{j_2}(h_{\gamma_2}[A]) \end{aligned} \quad (3.44)$$



The factor $\sqrt{2j+1}$ is necessary in order to normalize Wigner matrices. Via group averaging we can glue the two line into a gauge invariant state. This means to glue the two paths. The total wavefunction will be:

$$\begin{aligned} \psi_{\gamma_1 \circ \gamma_2} &= \sqrt{2j_1+1} \sqrt{2j_2+1} \int dg D_{s_1 t_1}^{j_1}(h_1 g^{-1}) D_{s_2 t_2}^{j_2}(g h_2) = \\ &= \sqrt{2j_1+1} \sqrt{2j_2+1} D_{s_1 \alpha_1}^{j_1}(h_1) D_{\alpha_2 t_2}^{j_2}(h_2) \int dg D_{\alpha_1 t_1}^{j_1}(g^{-1}) D_{s_2 \alpha_2}^{j_2}(g) \end{aligned} \quad (3.45)$$

Using wigner matrices properties [13]:

$$\begin{aligned} D_{\alpha_1 t_1}^{j_1}(g^{-1}) &= D_{t_1 \alpha_1}^{j_1}(g)^* \\ \int dg D_{t_1 \alpha_1}^{j_1}(g)^* D_{s_2 \alpha_2}^{j_2}(g) &= \frac{1}{\sqrt{2j_1+1}} \delta_{j_1 j_2} \delta_{t_1 s_2} \delta_{\alpha_1 \alpha_2} \end{aligned} \quad (3.46)$$

We get a familiar form for the composite state:

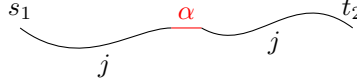
$$\psi_{\gamma_j s_1 t_2} = \sqrt{2j+1} \sum_{\alpha=1}^{2j+1} D_{s_1 \alpha}^j(h_1) D_{\alpha t_2}^j(h_2) \quad (3.47)$$

We can rewrite (3.47) in terms of the original cylindrical functions. This allows us to naturally obtain a Schmidt decomposition:

$$\begin{aligned} \psi_{\gamma_j s_1 t_2} &= \frac{1}{\sqrt{2j+1}} \sum_{\alpha=1}^{2j+1} \psi_{\gamma_1 j s_1 \alpha}(h[A]) \psi_{\gamma_2 j \alpha t_2}(h[A]) = \\ &= \frac{1}{\sqrt{2j+1}} \sum_{\alpha=1}^{2j+1} \langle h | \left(|\gamma_1, j, s_1, \alpha\rangle \otimes |\gamma_2, j, \alpha, t_2\rangle \right) \end{aligned} \quad (3.48)$$

This means that the state of $\mathcal{H}_\gamma \subseteq \mathcal{H}_{\gamma_1} \otimes \mathcal{H}_{\gamma_2}$ can be written as:

$$|\gamma, j, s_1, t_2\rangle = \frac{1}{\sqrt{2j+1}} \sum_{\alpha=1}^{2j+1} \left(|\gamma_1, j, s_1, \alpha\rangle \otimes |\gamma_2, j, \alpha, t_2\rangle \right) \quad (3.49)$$



We inserted an Intertwiner in α that according to (3.46) can be written as the identity realization in the gauge invariant subspace:

$$t_\alpha = \frac{(-1)^{j+\alpha}}{\sqrt{2j+1}} \sum_{\alpha=1}^{2j+1} |j, \alpha\rangle \langle j, \alpha| \quad (3.50)$$

Moreover we can easily compute entanglement entropy for the state (3.49):

1. Schmidt rank for both subsystem is $|I| = 2j + 1$;
2. Schmidt coefficients are all equal:

$$\lambda_i = \frac{(-1)^{j+\alpha}}{\sqrt{2j+1}} \quad \forall i \in |I| \quad (3.51)$$

Then, we have

$$\begin{aligned} \mathcal{E}(\gamma_1 : \gamma_2) &= S(\rho_1) = S(\rho_2) = - \sum_{i \in |I|} \lambda_i^2 \log \lambda_i^2 \\ &= -(2j+1) \frac{1}{2j+1} \log \left(\frac{1}{2j+1} \right) \\ &= \log(2j+1) = \log(\dim(V^{(j)})) \end{aligned} \quad (3.52)$$

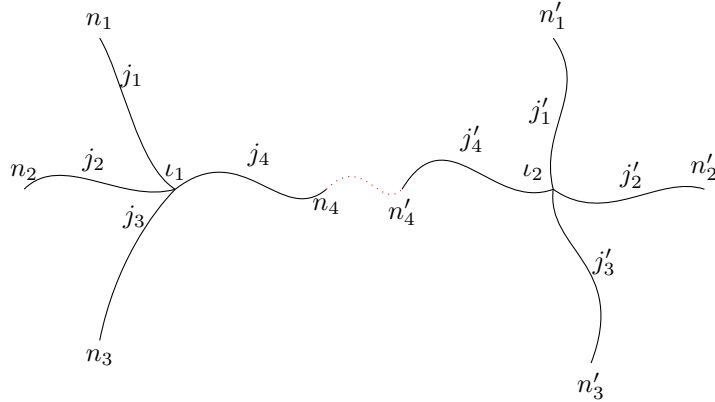
According to (3.32), since entanglement entropy is max, the state is **maximally entangled**. Thus we can say that *the requirement of spin network states to be gauge invariant induces quantum correlations that can be quantified through entanglement entropy*.

In particular, for basis states we have maximally entangled states; for general states with certain modes (according to Peter-Weyl decomposition theorem for Cylindrical functions) the resulting gauge invariant state will still be entangled, but not necessarily maximally entangled.

3.4.2 Entangling tetrahedra via links

We are going to consider two types of entanglement: the first one is the entanglement induced by the gluing among the links of the graph, that is related to the connectivity (i.e. topology) of the graph; the second one the entanglement between quanta of Volume (i.e. intertwiner), that is possibly related to the geometry rather than to the topology [44].

Now we can consider a more complex graph, constructed gluing two 4-valent nodes through only one of their dangling legs:



This system can be seen as dual to two tetrahedra sharing a face (triangle). We can consider the composite system obtained imposing gauge invariance on the links labelled by j_4 and j'_4 . The states of the single systems are:

$$\begin{aligned} \psi_1 &= \prod_{l=1}^4 \left(\sqrt{2j_l + 1} \right) D_{m_1 n_1}^{j_1}(h_1) D_{m_2 n_2}^{j_2}(h_2) D_{m_3 n_3}^{j_3}(h_3) D_{m_4 n_4}^{j_4}(h_4) \iota_{(1)}^{m_1 m_2 m_3 m_4} \\ \psi_2 &= \prod_{l=1}^4 \left(\sqrt{2j'_l + 1} \right) D_{m'_1 n'_1}^{j'_1}(h'_1) D_{m'_2 n'_2}^{j'_2}(h'_2) D_{m'_3 n'_3}^{j'_3}(h'_3) D_{m'_4 n'_4}^{j'_4}(h'_4) \iota_{(2)}^{m'_1 m'_2 m'_3 m'_4} \end{aligned} \quad (3.53)$$

To obtain gauge invariant state, we act with group averaging as usual:

$$\begin{aligned} \psi &= \prod_{l=1}^4 \left(\sqrt{2j_l + 1} \sqrt{2j'_l + 1} \right) \prod_{i=1}^3 D_{m_i n_i}^{j_i}(h_i) \prod_{j=1}^3 D_{m'_j n'_j}^{j'_j}(h'_j) \iota_{(1)}^{m_1 m_2 m_3 m_4} \iota_{(2)}^{m'_1 m'_2 m'_3 m'_4} \times \\ &\quad \times \int dg D_{m_4 n_4}^{j_4}(h_4 g^{-1}) D_{m'_4 n'_4}^{j'_4}(h'_4 g^{-1}) \end{aligned} \quad (3.54)$$

Using representations' properties and Haar measure invariance, the last integral can be written as:

$$D_{m_4 \alpha}^{j_4}(h_4) D_{m'_4 \alpha}^{j'_4}(h'_4) \int dg D_{\alpha n_4}^{j_4}(g) D_{\alpha n'_4}^{j'_4}(g) \quad (3.55)$$

Using the properties [13]

$$\begin{aligned} \int dg D_{\alpha n_4}^{j_4}(g) D_{\alpha n'_4}^{j'_4}(g) &= \frac{1}{2j_4 + 1} \delta_{j_4 j'_4} \delta_{\alpha, -\alpha'} \delta_{n_4, -n'_4} (-1)^{\alpha' - n'_4} \\ \iota_{m_1 m_2 m_3 m_4} &= (-1)^{j+m_4} \iota_{m_1 m_2 m_3, -m_4} \end{aligned} \quad (3.56)$$

Denoting $j_4 = j'_4 = j$, it is finally possible to prove [22] that:

$$\psi = \sum_{\alpha=1}^{2j+1} \frac{(-1)^{j+\alpha}}{\sqrt{2j+1}} \psi_{j_1, j_2, j_3, j, n_1, n_2, n_3, \alpha, \iota_{(1)}} \psi_{j'_1, j'_2, j'_3, j, n'_1, n'_2, n'_3, -\alpha, \iota_{(2)}} \quad (3.57)$$

Thus linking the nodes is equivalent to projecting the state on the following state of $\mathcal{V}^j \otimes \mathcal{V}^j$:

$$|l\rangle = \sum_{\alpha=1}^{2j+1} \frac{(-1)^{j+\alpha}}{\sqrt{2j+1}} |j, \alpha\rangle |j, -\alpha\rangle \quad (3.58)$$

We will soon prove that the link states $|l\rangle$ are maximally entangled and they will play a crucial role in the definition of **Projected Entangled-Pair States (PEPS)**.

Returning to the equation (3.57), with a similar computation of the case of the two Wilson lines, we can derive the Schmidt decomposition for the state of the composite system:

$$|\psi\rangle = \sum_{\alpha=1}^{2j+1} \frac{(-1)^{j+\alpha}}{\sqrt{2j+1}} |j_1, j_2, j_3, j, n_1, n_2, n_3, \alpha, \iota_{(1)}\rangle \otimes |j'_1, j'_2, j'_3, j, n'_1, n'_2, n'_3, -\alpha, \iota_{(2)}\rangle \quad (3.59)$$

Once again Schmidt rank is

$$|I| = 2j + 1 \quad (3.60)$$

and related coefficients are

$$\lambda_i = \frac{(-1)^{j+\alpha}}{\sqrt{2j+1}} \quad (3.61)$$

Thus we can easily compute Von Neumann entropy between the two tetrahedra as:

$$\mathcal{E}(\mathcal{T}_1 : \mathcal{T}_2) = S(\rho_1) = S(\rho_2) = \sum_{i=1}^{2j+1} \lambda_i \log \lambda_i = \log(2j+1) \quad (3.62)$$

The contribution to entanglement entropy is given by the dimension of the Hilbert space that is the basis of the j -representation associated to the link (or the shared area in the dual picture).

A similar example, the *dipole graph* Γ_2 [22] carries the same result: in this particular graph two nodes are linked through all their degrees of freedom, i.e. dangling legs. Computing entanglement entropy one found that:

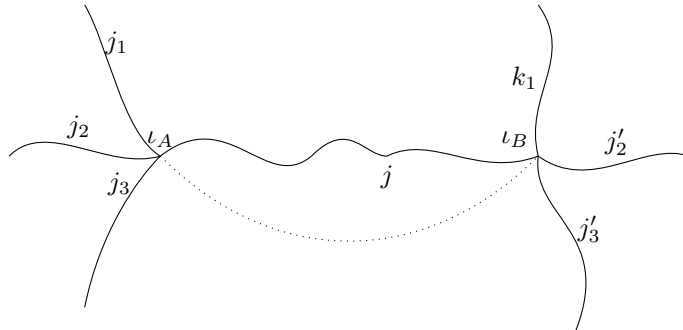
$$\mathcal{E}(\mathcal{T}_1 : \mathcal{T}_2) = \sum_{l=1}^4 \log(2j_l + 1) \quad (3.63)$$

This is a fascinating and clarifying result, since it becomes evident that each link shared by both subsystem carries a contribution to quantum correlation. So once again gauge invariance is strongly related to quantum correlation arising in the spin network framework.

3.4.3 Entangling tetrahedra via intertwiners

So far we investigated on the entanglement due to the connectivity of the graph, i.e. the entanglement between the spin states living on the external legs of the graph. Since intertwiners can be thought of mathematically as spin labels on virtual links, we can also consider the entanglement between the two intertwiners [44].

Consider two neighboring vertices of a spin network A and B linked by a single link labeled with a fixed spin j . We call $j_1 \dots j_3$ and $k_1 \dots k_3$ respectively the spins of the external legs of A and B.



Consider the Hilbert spaces of the intertwiners attached to the two vertices:

$$\begin{aligned}\mathcal{H}_A^0 &= \text{Inv}_{SU(2)} [\mathcal{V}^{j_1} \otimes \mathcal{V}^{j_2} \otimes \mathcal{V}^{j_3} \otimes \mathcal{V}^j \otimes] \\ \mathcal{H}_B^0 &= \text{Inv}_{SU(2)} [\mathcal{V}^{k_1} \otimes \mathcal{V}^{k_2} \otimes \mathcal{V}^{k_3} \otimes \mathcal{V}^j \otimes]\end{aligned}\quad (3.64)$$

Consider now a pure state $|\psi\rangle \in \mathcal{H}_{AB}^0 = \mathcal{H}_A^0 \otimes \mathcal{H}_B^0$. We can calculate the entanglement between A and B via the Von Neumann entropy of the reduced density matrices:

$$\mathcal{E}(A : B) = -\text{Tr}(\rho_A \log \rho_A) = -\text{Tr}(\rho_B \log \rho_B) \quad (3.65)$$

According to the properties of Von Neumann entropy, such entanglement entropy is bounded by the dimension of the intertwiner spaces:

$$\mathcal{E}(A : B) \leq \min(\log \dim(\mathcal{H}_A^0), \log \dim(\mathcal{H}_B^0)) \quad (3.66)$$

Considering also the connectivity entanglement given by the only internal link, it is possible to compare the different nature of such correlations [44] which we can summarize as follows:

1. For a pure basis state of \mathcal{H}_{AB}^0 , the intertwiner entanglement vanishes while the entanglement contribution associated to the connectivity of the graph (i.e. to the links) does not.
2. For an arbitrary pure state given by a superposition of states in \mathcal{H}_{AB}^0 neither intertwiner entanglement nor connectivity entanglement do vanish

So we can quantify the total entanglement of the two states of spin network as the finite sum of two contributions: the first one due to the connectivity of the graph, given by the sum of terms with the form $\log d_j$ (being d_j the Hilbert space dimension of the link gluing the two vertices); the second contribution is an additional term due to the intertwiners' correlation.

3.5 Discussion on Entropy-Area scaling

According to the results of the previous section, entanglement entropy for bipartite spin network states can be computed with standard methods as formerly shown [8][9][22]. We are now ready to ask ourselves: **why are we interested in entanglement entropy of quantum geometry states?**

This answer is a crucial point of many works of the last decades. Indeed it is well known in literature that it exists a strong correlation between entropy and geometric quantities. First of all, the pioneering works leading this idea are due separately to Hawking and Bekenstein [45][46]. They first noticed and studied the link between classical entropy and the area of the event horizon of a black hole:

$$S_{BH} = \frac{A}{4L_{Plank}} \quad (3.67)$$

This is the **Bekenstein-Hawking entropy**, and deserves the glory that belongs to it: it is possibly the most noticeable clue that a quantum regime of gravity required more investigation. Moreover an other noticeable fact is that thermodynamical quantities were actually related to geometric ones. When (3.67) was first published, entanglement entropy was already known in quantum system. Nevertheless S_{BH} referred to a **classical thermodynamics regime**, not a quantum one. Spin network states allowed to extend this result to quantum gravity research, thus leading to **Ryu-Tagayanagi formula** that will be the main protagonist of the following chapter, when *holographic properties* of spin network will be studied.

We can complete this discussion bringing two final arguments about Entropy-Area correlations that should already be clear at this level:

1. Since spin networks can be interpreted as geometric states, each link, gluing two nodes, is equivalent to a shared face of a tetrahedron in the simplicial complex point of view. In particular SNS are eigenstates of the Area operator and, given a spin j labelling the link state, the area's spectrum of this surface is given by $\sqrt{j(j+1)}$ and thus it scales like j for large enough value of j . We also remember that the entropy of such maximally entangled states is given by

$$S(\rho) = \log(2j + 1) \tag{3.68}$$

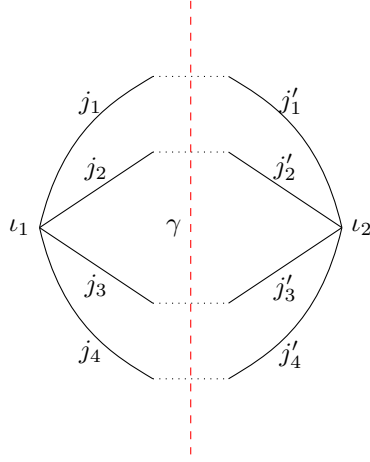
where $2j + 1$ is the dimension of the Hilbert space associated to the link, thus to the area of the shared surface. This dimension also scales like j for large values. So it seems reasonable to state that *large areas* \implies *bigger correlation*.

2. If we recall what has been said about the dipole graph entropy (3.63), assume that every j has the same value. We can thus write that result as:

$$\mathcal{E} = 4\log(D_j) \tag{3.69}$$

where $D_j = \dim \mathcal{V}^{(j)}$.

If we represent graphically the situation of the dipole graph:



We introduce the curve γ as the curve that separate and distinguish the two subsystem of which we are studying entanglement properties. We can notice that γ is pierced by 4 links. If we take a look at (3.69), 4 is exactly the number of contribution that appeared in entangled entropy. This is well know since each link brings contribution to correlation. Moreover (3.69) can be generalized for each number of links connecting two subsystem. We can interpret this number of intersection as the *area of the minimal surface separating the two subsystem, whose border is given by γ* . Thus if we denote with $|\gamma|$ the number of intersection between the graph and the curve, i.e. the number of links between the two subsystem, (3.69) can be generalized as follows:

$$\mathcal{E} = |\gamma| \log(D_j) \quad (3.70)$$

This situation is analogous to Ryu-Takayanagi formula emerging in the context of *AdS/CFT* duality. We refer to the next chapter for more detailed discussion on this topic; however it is worth to note that another area-entanglement correlation emerges from the study of spin network entanglement.

3. The role of intertwiner correlations introduced deviations from the area scaling behaviour. In facts we can understand such extra correlations as bulk correlations generally associated to **nonlocal** corrections.

3.6 Summary

We focused on the entanglement properties of spin network states:

1. The first step has been to recall how it is possible to describe quantum system, even if a given observer has no complete knowledge of the state. Thus we have been led to introduce **density operator** and a distinction between pure and mixed states.

2. This new tool allowed us to describe *multipartite system* and study a type of correlation that has no analogue in classical mechanics. We called this correlation **Entanglement**.
3. We introduced **Von Neumann entropy**, in order to quantify the amount of quantum correlations between two subsystem of a bipartite system, i.r. we introduce the concept of **Entanglement entropy** and **Quantum Mutual Information**.
4. We studied entanglement entropy for the simple cases of two Wilson line and two 4-valent nodes (entangled tetrahedra). We highlighted how gauge invariant state are naturally entangled: in particular base states are maximally entangled after the insertion of an intertwiner. Moreover we noticed that each link crossing the separation surface of the subsystems give a contribution to the Von Neumann entropy, equal to the logarithm of the dimension of the Hilbert space associated to the Wigner matrix of the link. Also we define an entanglement entropy contribution arising from quantum correlations among intertwiners in spin network states. Base states have vanishing entanglement; in the general case of a superposition of basis' states, both connectivity and intertwiner contributions are not null. In this framework entropy-area scaling is modified by the presence of quantum correlations between internal degrees of freedom of the spin network vertices.

These considerations allow us to qualitatively relate the entanglement properties of a spin network to two geometric aspects of the spin network basis states: local link correlations are associated to the topology of the quantum geometry state, reflected in the connectivity of the graph, while generally non-local entanglement among intertwiners defines correlations over volumes hence over actual geometric degrees of freedom. On top of such correlations, further geometric entanglement should be induced by the given choice of state expressed on the spin network basis [42, 43, 16, 3].

Chapter 4

Holographic properties of Random Spin Networks

Background independent quantisation of gravity requires discrete space-time structure to be responsible of continuum (macroscopical) geometry. In the previous sections we investigated discrete quantum geometry states described by spin network states, by focusing on how entanglement measures can reflect geometric properties of such states. In this chapter we seek a generalisation of the quantum spin network description within the formalism of Group Field Theory [11, 12, 16]. In this setting in particular:

- graphs are generic and not embedded; the role of holonomies is generalised in terms of group elements, in principle going beyond the $SU(2)$ case.
- in particular abstract graphs can be **open**, allowing for the study of boundary/bulk correlations and holography
- the bottom-up derivation of spin network states for quantum geometries of canonical quantisation is reversed. in a top-down approach: graphs are defined by the interaction of single vertex (group)fields interacting to create a quantum many-body system described by the spin network.

We review the Group Field Theory formalism [12], in which generalised spin networks states with boundary are defined in analogy with tensor network states. This allows us to investigate entanglement of quantum geometry states via tools of quantum many-body system [42, 43].

We specify the previous analysis to the study of entanglement entropy in terms of Rényi entropy [38] for a particular class of Spin Network states, i.e. *random* spin networks. This introduces a new statistical characterisation to the computation of the quantum correlations of a spin network state [3].

We deal with *open graphs*, characterised by an adjacency matrix, encoding all the information about its connectivity. In this setting, we distinguish two subregions of the graph: boundary and bulk. We call boundary the set of all the

dangling links (external degrees of freedom), while the bulk represents the set of internal degrees of freedom (contracted links and intertwiners). Via a bulk-to-boundary mapping [3], we study how quantum correlation between boundary subregions are affected by the bulk data, encoded in the state's coefficients after the contraction.

We are interested in entanglement induced by the combinatorial structure of the bulk, hence we consider Random Spin Network in which the information on the vertices is averaged out. This formalism allows us to perform random averaging as group integration, according to the Haar probability measure.

For such states, we review the key results in [16], where via Replica trick and performing ensemble averaging, the *typical* value of the Rényi second entropy of a bipartite boundary is computed via a mapping to the partition function of a Ising model, where after averaging:

1. the vertex density matrices at each node of the graph are replaced by the first two elements of the permutations group, identity and swap, which can be recast into a spin variable of value $+1$ or -1 ;
2. internal edges of the graph weights pairwise Ising interactions;
3. boundary dangling edges are dressed with “pinning fields” providing Ising model boundary conditions.

In these terms, the computation of typical Rényi entropy in the spin tensor network states can be mapped to the evaluation of partition functions of a classical statistical model, namely a generalized Ising models with boundary pinning fields.

Finally we will reproduce the celebrated **Ryu-Takayanagi formula**, arising in *AdS/CFT* contest, relating the entanglement entropy of a *boundary* region to the area of a minimal surface in the dual *bulk*, in the sense that we will divide a graph's degrees of freedom in internal d.o.f. (bulk, i.e. vertices and links) and external ones (boundary, i.e. open edges labelled by spin variables), thus realizing a correspondence between entanglement measure on the boundary and geometric observable in the bulk. This idea leads us, once again, to think to entanglement as the responsible of emerging space-time structures, thus interpreting quantum texture of space-time as being held together by the entanglement of its fundamental constituents.

4.1 GFT as Quantum Gravity model

GFT is the theory of a field defined on a group manifold; the excitations of the field, interpreted as quanta of space, are represented as fundamental simplices whose geometric properties are encoded in the group-theoretic variables of the field domain. Following [11] and [12] we can sum up the main result of this approach regarding the derivation of spin network states.

A Group Field Theory is the theory of a quantum field ϕ defined on d copies of a group G :

$$\phi : G^d \ni (g_1, \dots, g_d) \rightarrow \phi(g_1, \dots, g_d) \in \mathbb{C} \quad (4.1)$$

The GFT model suitable for quantum gravity requires $G = SU(2)$ and ϕ to satisfy a *closure condition*:

$$\phi(g_1, \dots, g_d) = \phi(hg_1, \dots, hg_d) \quad \forall h \in G \quad (4.2)$$

The excitations of this field [11] can be interpreted as $(d - 1)$ simplices, i.e. quanta of space, whose geometric informations are encoded in the group data g_1, \dots, g_d . The particular case $d = 4$ restores the tetrahedra picture and the dual spin network approach. In a vertex, each edge carries a group variable $g_i \in G$. Since we want a pure quantum description of a simplex, we need to require its structure to be gauge invariant under the action of the group: thus, for a single vertex state $\phi \in \mathcal{H}_v = L^2\left(\frac{G^d}{G}\right)$.

We can use Peter-Weyl decomposition theorem to write a single-vertex wavefunction in the spin network basis $\left\{ \left| \vec{j}, \vec{m}, \iota \right\rangle \right\}$, where \vec{j} are d spins labelling the irreducible representations of $SU(2)$, \vec{m} labels a basis in the corresponding representation space and ι is the intertwiner quantum number arising from the gauge-invariant recoupling of the edge spins.

$$|\iota\rangle \in \text{Inv}_{SU(2)} \left[\bigotimes_{i=1}^d \mathcal{V}^{j^i} \right] = \mathcal{I}^{\vec{j}} \quad (4.3)$$

So the state $|\phi\rangle$ can be decomposed as follows:

$$|\phi\rangle = \bigoplus_{\vec{j}} \sum_{\vec{m}, \iota} \phi_{\vec{m}, \iota}^{\vec{j}} \left| \vec{j}, \vec{m}, \iota \right\rangle \in \mathcal{H}_v = \bigoplus_{\vec{j}} \left[\mathcal{I}^{\vec{j}} \otimes \bigotimes_{i=1}^d \mathcal{V}^{j^i} \right] \quad (4.4)$$

Since the background independence of gravity requires the vertices to be indistinguishable, spin networks defined through GFT lives in a symmetric Fock space rather than a Hilbert space [12] [16]. However, for practical purposes related to quantum gravity formalism, we can use the first quantisation language, assuming that all physically quantities are symmetrized with respect to the vertex labels.

4.1.1 Tensor networks

In the following, we will briefly introduce the formalism of tensor networks [42] and will discuss how GFT states can be interpreted as generalized tensor network states [3].

Tensor Network A rank- n tensor is an object $T_{\mu_1 \dots \mu_n}$ where each leg μ_k can assume the values $\mu_k = 1, \dots, d_k$, d_k being the dimension of the Hilbert space \mathcal{H}_k associated to the k -th leg. Each tensor network can be matched one to one

to the wavefunction of a quantum state defined on the tensor product of the Hilbert spaces \mathcal{H}_k :

$$|T\rangle = \sum_{\mu_k} T_{\mu_1 \dots \mu_n} |\mu_1\rangle \otimes \dots \otimes |\mu_n\rangle \in \mathcal{H} = \bigotimes_{k=1}^n \mathcal{H}_k \quad (4.5)$$

Before connecting tensors in order to obtain a network, the collection of all tensors that represent a certain quantum state can be interpreted as a tensor product state associated to all the vertices, that is $\bigotimes_x |V_x\rangle$, where x labels the vertices. To each leg of a tensor we can associate a Hilbert space: there are 2 type of such space:

1. we denote by $\mathcal{H}_{x\partial}$ the Hilbert space (with dimension $d_{x\partial}$) of a dangling leg, starting from x and ending on the boundary ;
2. we denote by \mathcal{H}_{xy} the Hilbert space (with dimension d_{xy}) associated to a leg connecting the vertices x and y .

In fact, we can obtain a tensor network by connecting tensors, i.e. contracting a common leg (summing over a shared index). Moreover connecting two tensor with an internal link is the same to project the Hilbert space $\mathcal{H}_{xy} \otimes \mathcal{H}_{yx}$ onto its maximally entangled subspace. in particular the state associated to a link can be decomposed as follow:

$$|l_{xy}\rangle = \frac{1}{\sqrt{d_{xy}}} \sum_{\mu=1}^{d_{xy}} |\mu_{xy}\rangle \otimes |\mu_{yx}\rangle \quad (4.6)$$

Thus creating a tensor network means gluing vertex states, i.e. projecting on links of adjacent vertices (4.6):

$$|\psi\rangle = \left(\bigotimes_{\langle xy \rangle} |l_{xy}\rangle \right) \left(\bigotimes_x |V_x\rangle \right) \quad (4.7)$$

Tensor network with the form (4.7) are usually referred as Projected Entangled Pair States (**PEPS**).

This particular type of state recurs in the structure of GFT states: in fact if we want to glue two vertices together we have to entangle their degrees of freedom on the legs we are uniting. If we consider 2 vertices v and w and imagine to link them through their i -th edges, we have to project on the maximally entangled state:

$$|e_{vw}^i\rangle = \frac{1}{\sqrt{d_j}} \sum_n |jn\rangle \otimes |jn\rangle \in \mathcal{V}_v^{j^i=j} \otimes \mathcal{V}_w^{j^i=j} \quad (4.8)$$

In particular, in order to match the $SU(2)$ gauge invariance condition, we need to project in the singlet state corresponding to the bivalent intertwiner

described in (3.58), namely

$$|e_{vw}^i\rangle = \sum_n \frac{\sqrt{d_j}}{\sqrt{d_j}} (-1)^{j+n} |j, n\rangle |j, -n\rangle \quad (4.9)$$

that has exactly the same form of the general link (4.6). Thus we can say that *GFT states are generalized tensor network states* in the sense that these states are symmetric PEPS. Since the connectivity of the graph is expressed in terms of entangled structure, we refer to this states as **entanglement graphs**. Moreover, since connectivity plays a crucial role, we can use the adjacency matrix to encode all the information about the whole graph structure and thus formally distinguish between internal and external degrees of freedom, i.e. **bulk** and **boundary**.

4.1.2 Adjacency matrix, bulk and boundary degrees of freedom

Given a graph, with N vertices, we can encode all the information about the connectivity through a $N \times N$ matrix, called **adjacency matrix** [47]. Rows and columns of the matrix are labeled by the vertices of the graph, the elements being defined by:

1. $A_{vw} = 1$ if there exists at least one link between the two vertices;
2. $A_{vw} = 0$ if the two vertices are not linked.

Such information on connectivity can be expressed more in detail, if we include the information of which magnetic indices of the vertex states are contracted.

In order to include this information we shall promote each element of A to a $d \times d$ matrix where d is the valence of the network. So we have that $(A_{vw})_{ij} = A_{(v-1) \cdot d+i, (w-1) \cdot d+j}$ will be equal to 1 if the vertices v and w are linked through their i -th and j -th magnetic indices, 0 otherwise.

Thanks to this matrix we can encode all the connectivity information of each graph, in particular we can define two different set of link:

1. We denote by $L = \{e_{vw}^i \text{ s.t. } A_{(v-1) \cdot d+i, (w-1) \cdot d+i} = 1\}$ the set of all the internal links of the graph;
2. We denote by $\partial\gamma = \{e_v^i \text{ s.t. } A_{(v-1) \cdot d+i, (w-1) \cdot d+j} = 0 \ \forall w\}$ the boundary edges, i.e. dangling legs that are not connected to a vertex of the graph.

The set $E = L \cup \partial\gamma$ is the set of the edges of the graph.

Writing explicitly a generic quantum state defined on a graph γ [3], it is possible to show that the degrees of freedom of a graph state are:

1. Spins j_v^i (and magnetic number n_v^i) associated to the edges lying on the boundary $e_v^i \in \partial\gamma$;

2. Spins j_{vw}^i associated to the internal links of each vertex;
3. Intertwiner quantum number ι_v , associated to each vertex v , collectively indicated as $\dot{\gamma}$.

The first set identifies the **boundary** degrees of freedom, i.e. the external part of the graph. The two remaining sets constitute the **bulk** degrees of freedom, where in particular the first encodes the connectivity structure while the second represents the internal degrees of freedom associated to each vertex. From a geometric (simplicial) point of view, the bulk contains information on the volumes of tetrahedra (intertwiner) and on the areas of the connected faces of adjacent quanta of space (since spins j_{vw}^i encode information on such areas).

The tensor network formalism, can be used not only to define quantum states, but also to construct a **holographic map**, such that we can map bulk indices into boundary's ones.

4.1.3 Bulk and boundary subspaces

Each quantum state defined on a given graph, according to the previous discussions, lives in the Hilbert space [3]:

$$\mathcal{H}_\gamma = \bigoplus_J \left(\bigotimes_{v \in \dot{\gamma}} \mathcal{I}^{j^v} \otimes \bigotimes_{j \in \partial\gamma} \mathcal{V}^j \right) \quad (4.10)$$

Because of the sum over J , it is impossible to factorize this Hilbert space into $\mathcal{H}_{\dot{\gamma}}$ and $\mathcal{H}_{\partial\gamma}$. However such factorization is possible in each subspace with J fixed.

If we consider a *single* vertex Hilbert space:

$$\mathcal{H}_v = \bigoplus_{j_v} \mathcal{H}_v(j_v) = \bigoplus_{j_v} \left(\mathcal{I}^{j_v} \otimes \bigotimes_{i=1}^d \mathcal{V}^{j_v^i} \right) \quad (4.11)$$

each fixed-spin subspace $\mathcal{H}_v(j_v)$ can be naturally decomposed into tensor product of a space of intertwiner (bulk) and edges (boundary), thus we can factorize the basis vector onto bulk and boundary basis states:

$$\begin{aligned} \text{Bulk} \quad & \left| \vec{j}, \iota \right\rangle \in \mathcal{H}_{\dot{\gamma}} = \bigotimes_v \text{Inv}_{SU(2)} \left[\bigotimes_{l=1}^d \mathcal{V}^{j_v^l} \right] \\ \text{Boundary} \quad & \left| j^1 m^1 \right\rangle \otimes \dots \otimes \left| j^d m^d \right\rangle \in \mathcal{H}_{\partial\gamma} = \bigotimes_{l=1}^d \mathcal{V}^{j^l} \end{aligned} \quad (4.12)$$

Consider now a set of N vertices with individual wave functions f_v and spins \vec{j}_v composing a graph γ . A quantum state for the graph can be computed contracting the tensor product of all the vertex state $\bigotimes_v |f_v\rangle$ with an edge $|e_{vw}^i\rangle$

for each non vanishing element of the the adjacency matrix A , the link being a maximally entangled state (4.8). The state of the graph will be [3]:

$$\begin{aligned}
|\phi_\gamma\rangle &= \left(\bigotimes_{e_{vw}^i \in L} \langle e_{vw}^i | \right) \bigotimes_v |f_v\rangle = \\
&= \sum_{n_e \in \partial\gamma} \sum_{\iota_1, \dots, \iota_N} \left(\sum_{n_e \in L} \sum_p \prod_v (f_v)^{\vec{j}_v} \prod_{e_{vw}^i \in L} \delta_{m_v^i p_v^w} \delta_{m_w^i p_v^w} \right) \bigotimes_{e \in \partial\gamma} |j_e m_e\rangle \otimes \bigotimes_v | \vec{j}_v \iota_v \rangle
\end{aligned} \tag{4.13}$$

We can note that $\bigotimes_{e \in \partial\gamma} |j_e m_e\rangle$ is the basis element of the Hilbert space associated to the boundary, while $\bigotimes_v | \vec{j}_v \iota_v \rangle$ is the basis element of the Hilbert space associated to the bulk:

$$\begin{aligned}
\mathcal{H}_{\partial\gamma}(\partial J) &= \bigotimes_{e \in \partial\gamma} \mathcal{V}^{j_e} \\
\mathcal{H}_\gamma(J) &= \bigotimes_v \mathcal{I}^{j_v}
\end{aligned} \tag{4.14}$$

where J is the set of the spin attached to each vertex and ∂J is the set of spin of the boundary edges.

So we can decompose the Hilbert space of a fixed-spin graph as tensor product of bulk and boundary subspaces:

$$\mathcal{H}_\gamma(J) = \mathcal{H}_\gamma(J) \otimes \mathcal{H}_{\partial\gamma}(\partial J) \tag{4.15}$$

In the following, we will work in fixed-spin graph, in order to take advantage of being able to decompose the Hilbert space in the form (4.15).

This decomposition will be useful when we will consider the case of a *mixed bulk state*, described in terms of a certain density operator rather than a pure state $|\phi_{bulk}\rangle$.

4.1.4 Holographic map: from bulk to boundary

We will show that a spin network state naturally defines a map between bulk and boundary subspaces, according to the previous separation (4.15).

For simplicity, following [3], we can consider a graph state that is a PEPS constructed by some vertex wave function $\{f_v\}$ picked on edge spins j_v . We can define the total state $|\phi_\gamma\rangle \in \mathcal{H}_\gamma$. Moreover we can consider (in the j-fixed subspace), the bulk state, encoding information on intertwiner quantum number:

$$|\zeta\rangle = \sum_{\iota_1, \dots, \iota_N} \zeta_{\iota_1, \dots, \iota_N} \bigotimes_{v=1}^N | \vec{j}_v \iota_v \rangle \tag{4.16}$$

The corresponding boundary state, can be derived by contracting the total state $|\phi_\gamma\rangle$ with (4.16):

$$\begin{aligned}
|\phi_{\partial\gamma}(\zeta)\rangle &= \langle\zeta|\phi_\gamma\rangle = \\
&= \langle\zeta|\left(\bigotimes_{e_{vw}\in L} \langle e_{vw}^i|\bigotimes_v |f_v\rangle\right) = \\
&= \sum_{m_e\in\partial\gamma} (\phi_{\partial\gamma}(\zeta)_{m_e\in\partial\gamma}) \bigotimes_{e\in\partial\gamma} |j_e m_e\rangle
\end{aligned} \tag{4.17}$$

Where the coefficients are calculate by the contraction between $\zeta_{\iota_1,\dots,\iota_N}$ and the ones of $|\phi_\gamma\rangle$, according to the connectivity information encoded in the links.

Thus, given an entanglement graph described by a quantum state $|\phi_\gamma\rangle$ we can naturally define a map [3] that associates bulk state with the boundary state:

$$\mathcal{M}[\phi_\gamma] : \mathcal{H}_\gamma = \bigotimes_v \mathcal{I}^{j_v} \ni |\zeta\rangle \rightarrow \mathcal{M}[\phi_\gamma]|\zeta\rangle = \langle\zeta|\phi_\gamma\rangle = |\phi_{\partial\gamma}\rangle \in \mathcal{H}_{\partial\gamma} = \bigotimes_{e\in\partial\gamma} \mathcal{V}^{j_e} \tag{4.18}$$

We note that there exist a family of map of this form between the same bulk and boundary states, defined by all the possible states $|\phi_{\gamma_i}\rangle$ associated to graphs γ_i with the same bulk and boundary.

The previous discussions have been carried on with the assumption to work on the fixed spin subspaces of bulk and boundary, i.e. $\mathcal{H}_\gamma(J)$ and $\mathcal{H}_{\partial\gamma}(J)$. In the most general case, an entanglement graph will be given by an arbitrary spin superposition, that is performing the sum over J . To do so, link states and bulk states have to be modified, including the direct sum over J :

$$\begin{aligned}
|e_{vw}^i\rangle &= \bigoplus_J \sum_n \frac{(-1)^{j+n}}{\sqrt{d_j}} |jn\rangle |j-n\rangle \\
|\zeta\rangle &= \bigoplus_J \sum_{\iota_1,\dots,\iota_N} (\zeta_{\iota_1,\dots,\iota_N}^{(J)}) \bigotimes_v |j_{v\iota_v}\rangle
\end{aligned} \tag{4.19}$$

Thus it is possible to show [3], by direct calculation, that a map between bulk and boundary states still exists, but the input and output Hilbert space will be respectively

$$\mathcal{H}_\gamma = \bigoplus_J \mathcal{H}_\gamma(J), \quad \mathcal{H}_{\partial\gamma} = \bigoplus_J \mathcal{H}_{\partial\gamma}(J) \tag{4.20}$$

It is important to note that, although it is not possible to factorize the total Hilbert space without fixing the spins J , we can still read generic graph states as correspondences between bulk and boundary states.

The impossibility of factorizing the total Hilbert space depends on the fact that in the case of spin superposition, intertwiner degrees of freedom strictly depend on the incident spin. However it is possible to make bulk d.o.f. independent from the boundary one: to do so we have to fix the spin on the

boundary J_∂ ; by doing so the space \mathcal{H}_γ reduces to the direct sum of subspaces with certain value of J such that the boundary portion of J coincides with the fixed J_∂ .

In the following section, we will introduce **Rényi entropy** as a generalized Von Neumann entropy. In particular we will prove that the 2nd Rényi entropy is related to the partition function of a classical Ising model defined on the same graph as the tensor network. Moreover, the geometric parameters (the dimensions of the Hilbert spaces) of bulk and boundary will play the role of the temperature for the Ising model. Thus, within the limits of large dimensions, the Ryu-takayanagi formula emerges.

4.2 Rényi entropy from Ising free energy

Following [32] we can study the entanglement properties of the boundary of a spin network, in particular we will focus on how this entanglement is related to the combinatorial structure of the bulk and to the quantum correlations between intertwiner.

Since we are interested in entanglement induced by combinatorial structure of the bulk, it is useful to consider a particular class of quantum states, that is **Random Tensor Network** introduced in [42]. Differently from Hayden et al. work, tensor networks in our approach possess a natural geometrical interpretation, being dual to the triangulation of a space-time manifold.

Given a vertex state $|f_v\rangle$, we know that it is possible to build a network by gluing edges' degrees of freedom by projecting on the maximally entangled state (4.8), thus obtaining a **PEPS**.

To give a tensor network the "random" feature, we have to consider $|f_v\rangle$ as a unit vector chosen independently at random from its respective Hilbert space. To implement this randomness we can use the uniform probability measure, that is invariant under unitary transformation. Equivalently one can choose an arbitrary fiducial vector $|0_v\rangle$ and define:

$$|f_v\rangle = U_f |0_v\rangle \quad (4.21)$$

where U_f is a unitary operator. Thus we can perform the random average of an arbitrary function of this state as group integration, according to the Haar probability measure, that is well defined for Unitary operator:

$$\overline{g(|f_v\rangle)} = \int dU g(U |0_v\rangle) \quad \text{such that} \quad \int dU = 1 \quad (4.22)$$

Non trivial entanglement properties of Spin Network are induced by partial tracing a subsystem. The main advantage in using *random* spin network is that the average (4.22) can be carried out before taking the partial trace, since the latter is a linear operation.

Consider a spin network, which state is given by the tensor product of vertex

states contracted through PEPS:

$$|\tau_\gamma\rangle = \left(\bigotimes_{e \in L} \langle e_{vw}^i | \right) \otimes |f_v\rangle \quad (4.23)$$

where $|f_v\rangle = \sum_{j,m,\ell} f_{\vec{m},\vec{\ell}}^j |j\vec{m}\rangle \otimes |j\vec{\ell}\rangle$ and $|\tau_\gamma\rangle \in H_\gamma(J) = \bigotimes_{v=1}^N \mathcal{I}^{\vec{j}_v} \otimes \bigotimes_{e \in \partial\gamma} \mathcal{V}^{j_e^i}$. Consider now a *generic* bulk state $|\zeta\rangle \in \mathcal{H}_\gamma$ and its induced boundary state

$$|\tau_{\partial\gamma}(\zeta)\rangle = \langle \zeta | \tau_\gamma \rangle \quad (4.24)$$

Consider a region $A \subset \partial\gamma$ described by a density matrix $\rho_A = \text{Tr}_{\bar{A}}(\rho)$ where $\rho = |\tau_{\partial\gamma}\rangle \langle \tau_{\partial\gamma}|$ is the density matrix of the boundary state (4.24). Rényi second entropy of the density matrix ρ_A is thus given by:

$$S_2(\rho_A) = -\log \text{Tr}[\rho_A^2] \quad (4.25)$$

Rényi entropy (4.25) can be easily calculated using **replica trick**:

$$S_2(\rho_A) = -\log \text{Tr}[\rho_A^2] = -\log \left(\frac{\text{Tr}[(\rho \otimes \rho) S_A]}{\text{Tr}(\rho \otimes \rho)} \right) \quad (4.26)$$

Here we introduced the *Swap operator* S_A acting on the direct product $\rho \otimes \rho$ of two copies of the original system that swaps the states of the two copies in the region A, namely [42]:

$$S_A \left(|m_A\rangle_1 \otimes |n_{\bar{A}}\rangle_1 \otimes |m'_A\rangle_2 \otimes |n'_{\bar{A}}\rangle_2 \right) = \left(|m'_A\rangle_1 \otimes |n_{\bar{A}}\rangle_1 \otimes |m_A\rangle_2 \otimes |n'_{\bar{A}}\rangle_2 \right) \quad (4.27)$$

In order to shorten the notation in (4.26) we can put:

$$\begin{aligned} S_2(\rho_A) &= -\log \left(\frac{Z_1}{Z_0} \right) \\ Z_1 &= \text{Tr} \left[\rho^{\otimes 2} S_A \right] \\ Z_0 &= \text{Tr} \left[\rho^{\otimes 2} \right] \end{aligned} \quad (4.28)$$

Consider now the random character of vertex states $|f_v\rangle = U |0_v\rangle$, we can compute the average second Rényi entropy in the domain of large dimension, such that [16, 3]:

$$\overline{S_2(\rho_A)} = -\log \frac{\overline{Z_1}}{\overline{Z_0}} \quad (4.29)$$

with

$$\begin{aligned} \overline{Z_1} &= \text{Tr} \left[\rho_\zeta^{\otimes 2} \otimes \rho_L^{\otimes 2} \otimes \bigotimes_v \overline{\rho_v^{\otimes 2}} S_A \right] \\ \overline{Z_0} &= \text{Tr} \left[\rho_\zeta^{\otimes 2} \otimes \rho_L^{\otimes 2} \otimes \bigotimes_v \overline{\rho_v^{\otimes 2}} \right] \end{aligned} \quad (4.30)$$

where $\rho_\zeta = |\zeta\rangle\langle\zeta|$ is the bulk density matrix, $\rho_L = \bigotimes_{e \in L} |e\rangle\langle e|$ is the link density matrix and $\rho_v = |f_v\rangle\langle f_v|$ is the single vertex density matrix. The main result of this analysis [48] is that we can explicitly calculate the result of randomization on vertex state using Schur's Lemma:

$$\bigotimes_v \overline{\rho_v^{\otimes 2}} = \bigotimes_v \frac{\mathbb{1}_v + S_v}{D_v^2 + D_v} \quad (4.31)$$

The numerator is given by the sum of two operator (Identity and Swap) acting on each vertex v of the graph; the denominator is a numeric factor arising from Schur's Lemma that is proportional to the dimension D_v of the single vertex Hilbert space. For reasons that will be clear in the next chapter it is also convenient to notice that the numerator of (4.31) can be written as the sum of representation of the two element of the permutation group S_2 acting on the Hilbert space of the single vertex state:

$$\bigotimes_v \overline{\rho_v^{\otimes 2}} = \bigotimes_v \frac{\sum_{\sigma \in S_2} P(\sigma)}{D_v^2 + D_v} \quad (4.32)$$

However we can keep the calculation using (4.31) and write $\overline{Z_{1/0}}$ in the following way:

$$\overline{Z_{1/0}} = \prod_v \frac{1}{D_v^2 + D_v} \text{Tr} \left[\rho_\zeta^{\otimes 2} \otimes \rho_L^{\otimes 2} \otimes (\mathbb{1}_v + S_v) S_A / \mathbb{1} \right] \quad (4.33)$$

It is possible to show [3] that the quantities $Z_{1/0}$ are equivalent to partition functions of a classical Ising model defined on the graph.

The procedure to derive this result can be summed up in the following steps:

1. Randomization over vertex wavefunctions brings us to implement in each vertex v an Ising spin σ_v . Such spin can only assume value $+1$ or -1 .
2. Each edge e_v^i of the vertex carries a copy of the spin, in the sense that the Ising state of the vertex is *transmitted* to all its edges.
3. A set of virtual spins, called "**pinning fields**", carries the information about the region $A \subset \partial\gamma$: namely we attach a virtual spin $\mu_{e_v^i}$ to each dangling leg of the boundary $e_v^i \in \partial\gamma$. This spin take value -1 if $e_v^i \in A$ or $+1$ otherwise.
4. Ising spins and virtual spins on the same edge interact, and the strength of the interaction is proportional to $\log d_{j_v^i}$.
5. Ising spins σ_v and σ_w laying on linked vertices, interact and the strength of the interaction is proportional to $\log d_{j_{vw}^i}$.

It is also possible to write the partition function for this Ising model:

$$\overline{Z}[\mu] = \sum_{\vec{\sigma}} e^{-A[\mu](\sigma)} \quad (4.34)$$

when the action can be obtained by calculating all the traces in (4.33) (see Appendix A of [3] for details and entire calculation):

$$A[\mu](\sigma) = -\frac{1}{2} \sum_{e_{vw}^i \in L} (\sigma_v \sigma_w - 1) \log d_{j_{vw}^i} - \frac{1}{2} \sum_{e_v^i \in \partial\gamma} (\sigma_v \mu_{e_v^i} - 1) \log d_{j_v^i} + S_2(\rho_{\zeta\downarrow}) + k \quad (4.35)$$

where k is a constant term and $S_2(\rho_{\zeta\downarrow})$ is the 2nd Rényi entropy of the bulk state reduced to the region with $\sigma_v = -1$. By direct calculation it is possible to prove that the quantities (4.33) correspond to the partition function (4.34) evaluated with corresponding pinning field boundary condition. In particular

$$\begin{aligned} \bar{Z}_0 &= \bar{Z}(\mu_e = +1 \quad \forall e \in \partial\gamma) \\ \bar{Z}_1 &= \bar{Z}(\mu_e = -1 \quad \forall e \in \partial A, \quad \mu_e = +1 \quad \forall e \in \bar{A}) \end{aligned} \quad (4.36)$$

Remember now that Rényi entropy is given by:

$$\overline{S_2(\rho_A)} = -\log\left(\frac{\bar{Z}_1}{\bar{Z}_0}\right) = -\log \bar{Z}_1 + \log \bar{Z}_0 \quad (4.37)$$

In the previous section we introduced the Free energy \mathcal{F} as $\mathcal{F}(\vec{\mu}) = -\log Z(\vec{\mu})$, thus we can write Rényi second entropy as:

$$\overline{S_2(\rho_A)} = \mathcal{F}_1 - \mathcal{F}_0 \quad (4.38)$$

namely the free energy cost of flipping down the boundary pinning field in the region A .

4.3 Effects of bulk contribution and Ryu-Takayanagi formula

Now we will investigate how bulk entropy, namely physical correlations between intertwiners, lead to a correction term in the area scaling law. We will focus on the model of an *homogeneous spin network* that is associated to a graph with all spins variables along the link equal to each one other.

4.3.1 Homogeneous Spin Network

We can now study the correlation between bulk entropy $S_2(\rho_{\zeta\downarrow})$ in $A[\vec{\mu}]$ defined as:

$$A[\mu](\sigma) = -\frac{1}{2} \sum_{e_{vw}^i \in L} (\sigma_v \sigma_w - 1) \log d_{j_{vw}^i} - \frac{1}{2} \sum_{e_v^i \in \partial\gamma} (\sigma_v \mu_{e_v^i} - 1) \log d_{j_v^i} + S_2(\rho_{\zeta\downarrow}) + k \quad (4.39)$$

To do that we can consider the homogeneous case [16] in which all spins are equal to a certain value, namely

$$j_v^i = j_{vw}^i = J \quad \forall e_v^i, e_{vw}^i \quad (4.40)$$

We can thus introduce the parameter $\beta = \log d_J$, since all the dimensions in the action are equal. Indeed, in this particular regime, we can easily write the partition function in terms of an Hamiltonian

$$Z[\vec{\mu}] = \sum_{\vec{\sigma}} e^{-\beta \mathcal{H}[\vec{\mu}](\vec{\sigma})} \quad (4.41)$$

Where \mathcal{H} is given by

$$\mathcal{H}[\vec{\mu}](\vec{\sigma}) = \beta^{-1} A[\vec{\mu}](\vec{\sigma}) = -\frac{1}{2} \left[\sum_{e_{vw}^i} (\sigma_v \sigma_w - 1) + \sum_{e_v^i} (\sigma_v \mu_v - 1) \right] + \beta^{-1} S_2(\rho_{\zeta \downarrow}) + \text{cost} \quad (4.42)$$

Note that the Hamiltonian is given by a classical Ising model on γ plus an additional term related to the bulk entropy. In this framework β plays the role of the inverse of a temperature: since we started with a random state in the large d limit, we are actually interested in the low temperature regime. thus the partition function is dominated by the lowest energy configuration:

$$\mathcal{F} = -\log \bar{Z}[\vec{\mu}] \simeq \beta \min_{\vec{\sigma}} \mathcal{H}[\vec{\mu}](\vec{\sigma}) \quad (4.43)$$

Moreover since Rényi entropy is given by the difference of the values of the free energy of the two configurations, we can set the constant term equal to 0. By doing so $F_0 = 0$, i.e. the lowest energy configuration is the one where there is no interaction (all the spins point up). So Rényi entropy is given by \mathcal{F}_1 . We want to show how the presence of the bulk entropy becomes relevant.

4.3.2 Vanishing bulk entropy

To better understand the role of Bulk entropy, we can start considering the case of vanishing bulk entropy $S_2(\rho_{\zeta}) = 0$. In this case the Hamiltonian is given by:

$$\mathcal{H}_1(\vec{\sigma}) = -\frac{1}{2} \left[\sum_{e_{vw}^i} (\sigma_v \sigma_w - 1) + \sum_{e_v^i} (\sigma_v \mu_v - 1) \right] \quad (4.44)$$

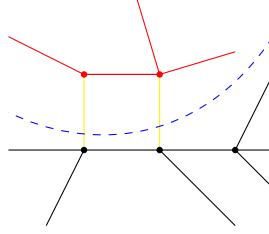
From this expression we can soon notice that each pair of linked vertices with antiparallel spins (i.e. $\sigma_v \sigma_w = -1$ carries a contribution of +1 to the energy and the same holds for the boundary pinning field. In this sense, \mathcal{H}_1 is equal to the size of the domain wall $\Sigma(\vec{\sigma})$ between the regions with spin up and spin down. The size of this domain wall is quantified by the number of link crossing it:

$$\mathcal{H}_1 = |\Sigma(\vec{\sigma})| \quad (4.45)$$

For example given a generic graph with a particular configuration of spin (tracking the boundary region A) we can visualize graphically the Hamiltonian of the configuration by counting the number of edges that link A to \bar{A} :

In the picture above, we used the following colours conventions:

1. red lines and dots represent edges and vertex of the region A ;



2. black lines and dots are graph elements belonging to \overline{A} ;
3. the blue dashed line is the domain wall between the two region in this particular configuration;
4. yellow lines are the links crossing the domain wall, which carry a contribution +1 to the Hamiltonian.

Finally, Rényi negativity can be computed as:

$$\overline{S_2(\rho_A)} \simeq \log d_j \min_{\vec{\sigma}} |\Sigma(\vec{\sigma})| \quad (4.46)$$

The equation (4.46) is a version of **Ryu-Takayanagi formula** [2, 1] for homogeneous random spin network. RT formula arises in *AdS/CFT* theory and relates the entanglement entropy of a boundary region to the area of a minimal surface in the dual bulk:

$$S_A = \frac{\text{Area of } \gamma_A}{4G_N} \quad (4.47)$$

In our result (4.46) $\log d_j$ is indeed proportional to the area of the surface dual to the link, while $\min_{\vec{\sigma}} |\Sigma(\vec{\sigma})|$ corresponds to the number of links (surfaces) that crosses the domain wall in the lowest energy configuration. In this sense we have a direct correspondence between Rényi second entropy and geometric observables (areas).

Geometrically, we can give a precise interpretation of what this formula means in the spin network case: the configuration associated to Z_0 all the spins point up; as the configuration switch to Z_1 the Ising spins next to A are induced to flip down thus realizing a spin down region that spreads into the bulk until $H_1(\vec{\sigma})$ is minimized. Moreover if the bulk entropy is not null but still negligible respect to H_1 , Rényi entropy continues to satisfy RT formula with a correction term to the area law:

$$\overline{S_2(\rho_A)} = \log d_j (\min_{\vec{\sigma}} |\Sigma(\vec{\sigma})|) + S_2(\rho_{\zeta\downarrow}) \quad (4.48)$$

in this case the minimization over $\vec{\sigma}$ can be performed independently from the bulk term: the spin down region spreads in the graph according to the minimization of \mathcal{H}_1 .

4.3.3 Bulk entropy effects

Consider now the case of large bulk entropy, i.e. the latter is comparable to the entanglement contribution of the Ising Hamiltonian \mathcal{H}_1 .

Consider the case of a bulk that is a random pure state, as studied by Hayden [42] in RTN, re-adapted in the spin network context [16]. Bulk entropy is thus given by:

$$S_2(\rho_\downarrow) = \log \frac{D_J^N + 1}{D_j^{|\sigma_\downarrow|} + D_J^{|\sigma_\uparrow|}} \quad (4.49)$$

where N is the number of vertices of γ , and $|\sigma_\downarrow|$ ($|\sigma_\uparrow|$) stands for the cardinality of the spin down (spin up) region. We can calculate the bulk contribution easily in the case of a 4-valent graph, since intertwiner's space dimension D_J is equal to edges' dimension d_j (in the homogeneous case). Following [16] we can thus consider

$$D_J = d_j = e^\beta \quad (4.50)$$

and evaluate the bulk entropy in the large β limit.

$$\frac{e^{\beta N} + 1}{e^{\beta|\sigma_\uparrow|} + e^{\beta|\sigma_\downarrow|}} \simeq \frac{e^{\beta N}}{e^{\beta|\sigma_\uparrow|}(1 + e^{\beta(|\sigma_\downarrow| - |\sigma_\uparrow|)})} \simeq e^{\beta(N - \max\{|\sigma_\downarrow|, |\sigma_\uparrow|\})} = e^{\beta \min\{|\sigma_\downarrow|, |\sigma_\uparrow|\}} \quad (4.51)$$

thus the bulk correction is given by

$$S_2(\rho_\downarrow) = \beta \min\{|\sigma_\downarrow|, |\sigma_\uparrow|\} \quad (4.52)$$

The Hamiltonian is given by the sum of the classical Ising Hamiltonian plus the additional term given by $\beta^{-1} S_2(\rho_\downarrow)$:

$$\mathcal{H}_1(\vec{\sigma}) = -\frac{1}{2} \left[\sum (\sigma_v \sigma_w - 1) + \sum (\sigma_v \mu_v - 1) \right] + \min\{|\sigma_\downarrow|, |\sigma_\uparrow|\} \quad (4.53)$$

In this case the procedure of minimization of \mathcal{H} strongly depends on the bulk entropy contribution: in particular the behaviour of the minimum domain wall depends on the number of vertices in each region of the graph.

An important consequence of the bulk entropy is **the lost of degeneracy of the minimum of \mathcal{H}_1** . An example of this result can be found in figure 3,4 and 5 of [16]: first consider a generic spin network and a boundary region $A \in \partial\gamma$. If the bulk state is a separable state, i.e. its entanglement contribution is null, there are two possible domain wall (Σ_a and Σ_b) such that the Hamiltonian \mathcal{H}_1 is minimum: $\mathcal{H}_a = \mathcal{H}_b = 5$.

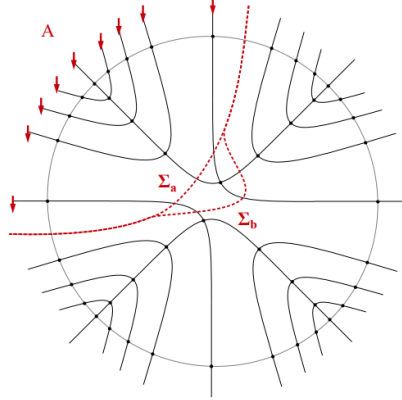


Figure 3 from *Bulk area law for boundary entanglement in spin network states: entropy corrections and horizon-like regions from volume correlations.*

Instead, if we insert a bulk state made up of a random pure state in a bulk disk Ω and a direct product state in $(\bar{\Omega} = \hat{\gamma} \setminus \Omega)$ namely:

$$|\zeta\rangle = |\zeta_\Omega\rangle \otimes \bigotimes_{v \in \bar{\Omega}} |\zeta_v\rangle \quad (4.54)$$

the degeneracy of the minimal energy surface is removed and the energetically favored configuration will be the one that enter "the least" in the bulk region (\mathcal{H}_a) .

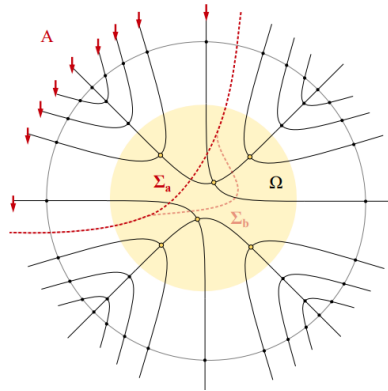


Figure 4 from *Bulk area law for boundary entanglement in spin network states: entropy corrections and horizon-like regions from volume correlations.*

By direct calculation $\mathcal{H}_a = 6$ and $\mathcal{H}_b = 7$. Moreover, increasing the dimension of the bulk disk, with more correlations, the domain wall gets pushed out of the bulk:

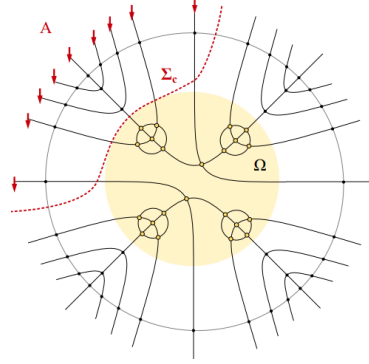


Figure 5 from *Bulk area law for boundary entanglement in spin network states: entropy corrections and horizon-like regions from volume correlations*

4.4 Summary

Concretely, the Rényi second entropy is computed as a minimal free energy of such a model, which ends up being equal to the number of links that cross the *minimal* surface in bulk that separate the two subsystems on the boundary. In this sense, the Rényi entropy is proportional to the area of that surface and one obtains an area law that is a version of Ryu-Takayanagi formula for entangled spin network.

Further, the presence of extra bulk entanglement reflects into a modification of the minimal surface hence in interesting deviation from the holographic area law. For instance, energetically favored configurations are the ones that enter the least in the bulk; if the correlation of the bulk are sufficiently large, the minimal surface gets pushed out thus creating a black hole-like region in the bulk.

Such a model is capable to describe the scaling of geometrical quantities such as areas, with entanglement entropy of a quantum states, described in terms of a generalised random spin network. A limits of this analysis is certainly given by the inability to derive such formulation for multipartite system of mixed states. Both of these situations represent a hot topic in the framework of quantum black holes [49, 14]. To use properly spin network formalism in this framework we must be able to quantify the entanglement entropy for a multipartite mixed state. In the next chapter we will introduce *Negativity* that will be a useful tool to generalize what has been derived in this chapter and adapt such ideas to mixed states of a multipartite spin network boundary.

Chapter 5

Negativity measures for Random Spin Networks

5.1 Rényi Negativity on random induced mixed states

Negativity [4] is a measure of entanglement that is well defined for both pure states and mixed states. We begin with a review of its definition and some results on its Rényi generalization on random mixed spin network states. We introduce Haar Random State that will allow us to study quantum correlation between two subregions of the boundary of a graph, described by a spin network state.

5.1.1 Negativity

Consider a bipartite Hilbert space $\mathcal{H} = \mathcal{H}_A \otimes \mathcal{H}_B$, whose states are given by a density matrix ρ_{AB} . We can fix an orthonormal basis $|i\rangle_A$ in \mathcal{H}_A and similarly $|j\rangle_B$ in \mathcal{H}_B . The **partial transpose** with respect to one of the subsystem, say B, is the density matrix with elements:

$$\rho_{i_A j_B, k_A l_B}^{T_B} = \rho_{i_A l_B, k_A j_B} \quad (5.1)$$

We can recall that the full transposition is an Hermitian and trace-preserving operation that lead to a new density matrix:

$$\rho^T = \rho^* \quad (5.2)$$

with the same eigenvalues of ρ . Hence the full transposition in a completely positive definite map.

Partial transpose is still Hermitian and trace-preserving map, therefore its eigenvalues are still real. Yet the map is not completely positive, i.e. ρ^T may have **negative eigenvalues**.

The fact that negative eigenvalues arise is related to the presence of quantum correlation in ρ . Checking if the partial transpose has negative eigenvalues is a test to distinguish quantum correlations from classical one.

Negativity is a measure that quantify the entanglement of a state according to the amount of negative eigenvalues of the partial transpose.

$$\mathcal{N}_{A:B} := \frac{\|\rho_{AB}^{T_B}\|_1 - 1}{2} \quad (5.3)$$

where $\|\bullet\|_1$ is the trace norm. Since $\rho_{AB}^{T_B}$ is Hermitian, its trace norm is the sum of absolute values of its eigenvalues, hence (5.3) can be rewritten as:

$$\mathcal{N}_{A:B} = \sum_{\lambda_i < 0} |\lambda_i| \quad (5.4)$$

The above quantity measures how negative the eigenvalues are.

We can easily prove that Negativity is related to quantum correlation. Indeed if we consider a separable state written as:

$$\rho = \sum_a p_a \rho_a^{(A)} \otimes \rho_a^{(B)} \quad (5.5)$$

with $p_a \geq 0$ and $\sum_a p_a = 1$. If such state is separable both $\rho^{(A)}$ and $\rho^{(B)}$ are density matrix. This implies that partial transpose acts trivially:

$$\rho^{T_B} = \sum_a p_a \rho_a^{(A)} \otimes (\rho_a^{(B)})^T \quad (5.6)$$

Since $\rho_a^{(B)T}$ is still a density matrix it will have no negative eigenvalues. This directly implies that $\mathcal{N}_{A:B} = 0$, i.e. **a necessary condition for a state to be unentangled is to have vanishing Negativity** [19].

It has also been proven by Peres [20] that the positivity of the partial transposition of the state is not a sufficient condition in general to distinguish unentangled states. Moreover we can notice that the previous result does not depend on the chosen basis for the Hilbert spaces and that it still holds if we interchange A and B.

A more suitable formulation [21] of entanglement in term of negative eigenvalues is given by *Logarithmic Negativity* (LN), defined as:

$$\mathcal{E}_{A:B} := \log \|\rho_{AB}^{T_B}\|_1 \quad (5.7)$$

This quantity exhibits monotonic behaviour under general positive partial transpose preserving operations, i.e. it is a monotone entanglement measure that will provide many simplifications in the calculations.

5.1.2 Rényi Negativity

In the previous chapter we have discussed on Von Neumann generalized entropy, called *Rényi entropy*:

$$S^{(k)}(\rho) = \frac{1}{1-k} \log \text{Tr}[\rho^k] \quad (5.8)$$

In a similar way [5] we can define Rényi generalization of Negativity measures:

$$N_k(\rho_{AB}) = \text{Tr}[(\rho_{AB}^{T_B})^k] \quad (5.9)$$

We refer to N_k as the k -th Rényi Negativity or as the *moment of order k* . Notice that, since $\rho_{AB}^{T_B}$ has negative eigenvalues, even and odd moments must be treated separately:

$$\begin{aligned} N_k^{(odd)}(\rho_{AB}) &= \sum_i \text{sgn}(\lambda_i) |\lambda_i|^k \\ N_k^{(even)}(\rho_{AB}) &= \sum_i |\lambda_i|^k \end{aligned} \quad (5.10)$$

Since LN only depends on the absolute values of eigenvalues, we can define it to be the $k \rightarrow 1$ limit of the logarithm of even momenta. Thus, if we set $k = 2n$, LN takes the form:

$$\mathcal{E}_{A:B} = \lim_{n \rightarrow \frac{1}{2}} \log N_{2n}^{(even)}(\rho_{AB}) \quad (5.11)$$

We can only consider the analytic continuation of even momenta since the logarithm of the odd ones vanishes in the limit $k \rightarrow 1$ since partial transpose is trace-preserving, i.e. $\text{Tr}(\rho_{AB}^{T_B}) = \text{Tr}(\rho_{AB}) = 1$. Since odd momenta are related to different measures of correlations, such as partially transposed entropy [5] and refined Rényi negativities [10], we will not deal with this quantities.

5.1.3 Haar Random State

Since we are interested in the study of negativity of mixed states, it is useful to introduce a particular class of random states that are suitable for dealing with *induced mixed states*.

Consider a multipartite system described by an Hilbert space that is tensor product of three Hilbert spaces [4] :

$$\mathcal{H} = \mathcal{H}_A \otimes \mathcal{H}_B \otimes \mathcal{H}_C \quad (5.12)$$

respectively endowed with an orthonormal basis $|i\rangle_A, |j\rangle_B$ and $|k\rangle_C$, such that $i = 1, \dots, d_A$, $j = 1, \dots, d_B$ and $k = 1, \dots, d_C$.

A **pure Haar Random state** is defined as:

$$|\psi\rangle = N \sum_{ijk} X_{ijk} |i\rangle_A |j\rangle_B |k\rangle_C \quad (5.13)$$

where X_{ijk} are complex gaussian i.i.d. matrix elements of the matrix X with unnormalized joint probability distribution given by:

$$\mathcal{P}(\{X_{ijk}\}) \propto \exp\left\{-d_A d_B d_C \text{Tr}(XX^\dagger)\right\} \quad (5.14)$$

In order to obtain an *induced random mixed state* we can trace out on of the subsystem, say C :

$$\rho = \frac{XX^\dagger}{\text{Tr}\{XX^\dagger\}} \quad (5.15)$$

The reduced density matrix on $\mathcal{H}_A \otimes \mathcal{H}_B$ is given by [50]:

$$\rho = \frac{XX^\dagger}{\text{Tr}\{XX^\dagger\}} \quad (5.16)$$

The unnormalized reduced density matrix XX^\dagger is called Wishart ensemble and it is a well known object in random matrix theory [18, 4].

This resulting density matrix will inherit the random character for the original pure state. Moreover it's a mixed state of which it is possible to calculate negativity. In particular we will study the residual quantum correlations between the two remaining system. In the spin network framework, the three Hilbert spaces are associated to different region of a given graph γ . In particular we will study quantum correlation between two specific regions (A and B) on the boundary $\partial\gamma$.

Instead of wildly going into the calculation of Rényi Negativity with this setup, we can anticipate a comfortable alternative path to describe Haar Random states. As we did in the previous section, we can consider a reference state $|0\rangle \in \mathcal{H}$ and act with an Unitary operator $U \in U(\dim\mathcal{H})$. In calculation of k -th negativity, using the replica trick, we will be interested in ensemble averaging over k copies of the Haar random states $\overline{(|\psi\rangle\langle\psi|)^{\otimes k}}$. In the next section we will bring strong arguments showing us that the unitary operator acting on the reference state has to be a unitary representation of the permutation group. Since it is a finite group, all the integrals, i.e. averaging, with respect to the Haar measure, are **finite sum**. In particular, the average over k copies of Haar random states are sum of permutation τ of the k copies [4]:

$$\overline{(|\psi\rangle\langle\psi|)^{\otimes k}} = \frac{\sum_{\tau \in S_k} g_\tau}{\sum_{\tau \in S_k} \text{Tr}\{g_\tau\}} \quad (5.17)$$

where g_τ is the matrix representation of the permutation $\tau \in S_k$ and the denominator ensures state has unit norm. The trace of a permutation is straightforward to calculate, being equal to the dimension of the Hilbert space to the number of **cycles** of the permutation. A deeper and more detailed discussion about the permutation approach will be given in the next sections. The main thing to focus on is that considering a mixed state, induced taking partial trace of a subsystem (consider a bipartite system for simplicity), we can easily compute the ensemble averaging over k copies of the reduced density matrix, since tracing and averaging are commuting operations:

$$\rho_A^{\otimes k} = \text{Tr}_B [\overline{(|\psi\rangle\langle\psi|)^{\otimes k}}] = \frac{\sum_{\tau \in S_k} g_{\tau_A} \text{Tr}[g_{\tau_B}]}{\sum_{\tau \in S_k} \text{Tr}[g_\tau]} \quad (5.18)$$

Where τ_I is a permutation acting only on the subsystem I . Thus the denominator can be written easily:

$$\sum_{\tau \in S_k} \text{Tr}[g_\tau] = \sum_{\tau \in S_k} (d_A d_B)^{C(\tau)} \quad (5.19)$$

In particular we will show that in the large dimension limit such denominator can be approximated to the leading order $(d_A d_B)^k$. It is easy to understand that in this limit, this averaging is completely equivalent to the Wishart ensemble result in (5.16).

To justify and rigorously prove what we have said so far about permutations, we will introduce the **diagrammatic approach** [4, 18] and some illuminating example in the calculation of the **purity** and third Rényi negativity in Random Tensor Network [17]. We will emphasize the visually distinguishable symmetries and the emergence of the permutation formula.

5.2 Diagrammatic approach

Consider a tensor network made up of a single tensor represented by a Haar pure state of a tripartite system [4].

$$|\psi\rangle = \sum_{ijk} X_{ijk} |i\rangle_A |j\rangle_B |k\rangle_C \quad (5.20)$$

Since our aim is to calculate Rényi negativities, we consider the multipartition of the system following the conventions that:

1. A is the part of the system that is left untouched;
2. B is the region that get partial transposed;
3. C is the subsystem we trace out in order to get a mixed state.

Diagrammatic approach has the advantage of skipping many calculation both of traces and of ensemble averaging.

Consider now the density matrix associated to the full state:

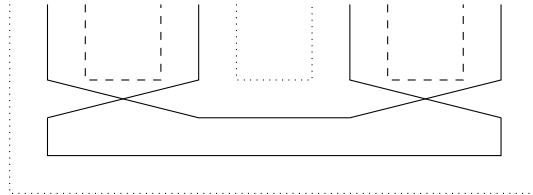
$$\rho = |\psi\rangle \langle \psi| \quad (5.21)$$

Each matrix element of the density matrix can be represented drawing a line for each index:

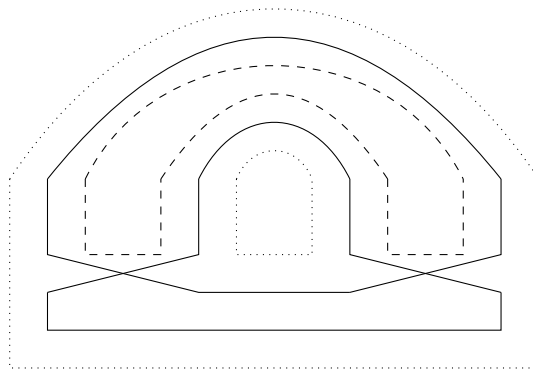
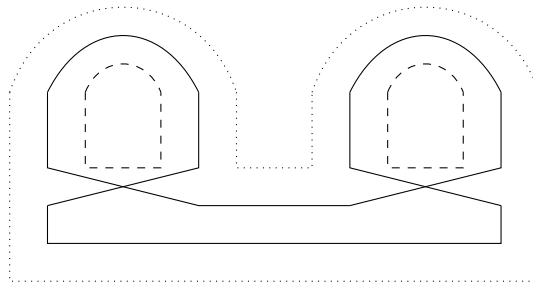
$$\rho_{ijk,lmn} = X_{ijk} X_{lmn}^* = \begin{array}{c} i \quad j \quad k \quad n \quad m \quad l \\ \vdots \quad | \quad \vdots \quad \vdots \quad | \quad \vdots \end{array} \quad (5.22)$$

Where we are using dotted lines for the system A, straight lines for B and dashed lines for C.

and its trace will be:



To calculate diagrammatically the ensemble averaging we have to work on the upper part of the drawing. Notice that each group of 3 three lines corresponds to the indices of a given ket (bra), i.e. it is the matrix element of X (X^\dagger), the random matrix of the Haar state (5.20). Averaging correspond to contract in each possible way X to X^\dagger . Since we are at second order, we have two copies of X to X^\dagger so there are only 2 possible way to do that:



Each of these diagrams will give a contribution to the second Rényi negativity that we have to sum up.

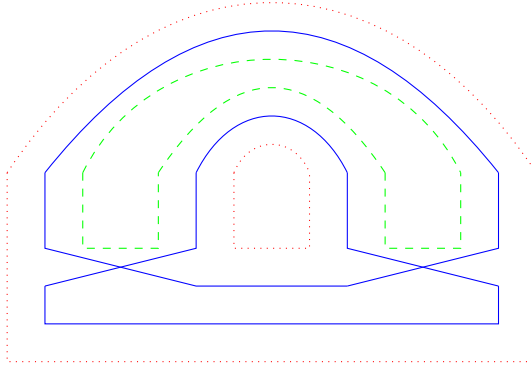
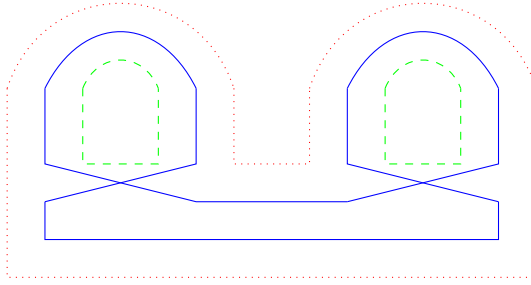
The two rules to obtain this contribution through diagrams are the following:

- A factor (variance) of $\frac{1}{\prod_I d_I}$ for each contraction in the upper part of the diagram.
- A factor d_I for each loop, for summing over the index of the random density matrix.

Note that we have chosen X_{ijk} to be a random variable with Gaussian distribution $P\{X_{ijk}\} = \text{Nexp}\{\frac{1}{d_A d_B d_C} X X^\dagger\}$ so that

$$\text{Var}(X) = \overline{X_{ijk} X_{lmn}^\dagger} = \frac{1}{d_A d_B d_C} \delta_{il} \delta_{jm} \delta_{kn} \quad (5.28)$$

and in the large d limit, fluctuations around this value are negligible. Thus if we refer to the two previous diagrams we can colour the lines of each subsystem to better identify loops:



The first contribution is $\frac{d_A d_B d_C^2}{d_A^2 d_B^2 d_C^2}$, the second one is $\frac{d_A d_B^2 d_C}{d_A^2 d_B^2 d_C^2}$. So the second Rényi negativity is:

$$N_2 = \langle \text{Tr}(\rho^{T_B})^2 \rangle = \frac{d_A d_B d_C^2}{d_A^2 d_B^2 d_C^2} + \frac{d_A^2 d_B^2 d_C}{d_A^2 d_B^2 d_C^2} = \frac{d_A d_B}{d_A d_B d_C} + \frac{d_C}{d_A d_B d_C} \quad (5.29)$$

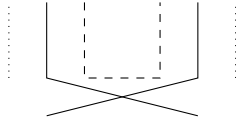
This is exactly the same result for the 2nd Rényi entropy in the large d limit [17]. This coincidence occurs because partial transpose is trace preserving but also has to obey the identity $\text{Tr}[(\rho^{TB})^2] = \text{Tr}[\rho^2]$, and this becomes very clear looking at diagrams.

Third Rényi Negativity The first non-trivial case we can approach through diagrams is 3rd Rényi Negativity

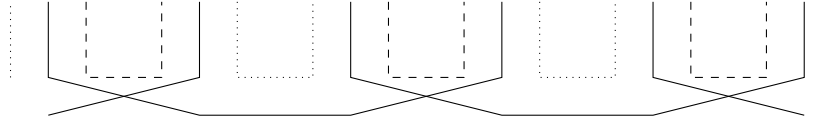
$$N_3 = \langle \text{Tr}(\rho^{TB})^3 \rangle \tag{5.30}$$

We can proceed as we did in the previous case.

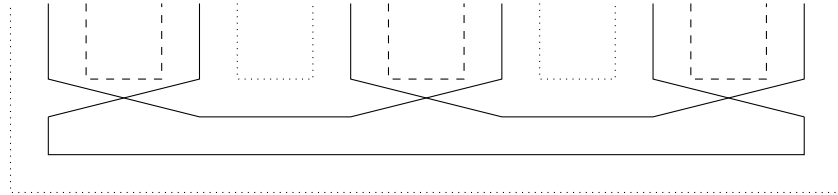
The partial transposed reduced density matrix is represented by:



ρ^3 is the multiplication of 3 copies of this diagramm:



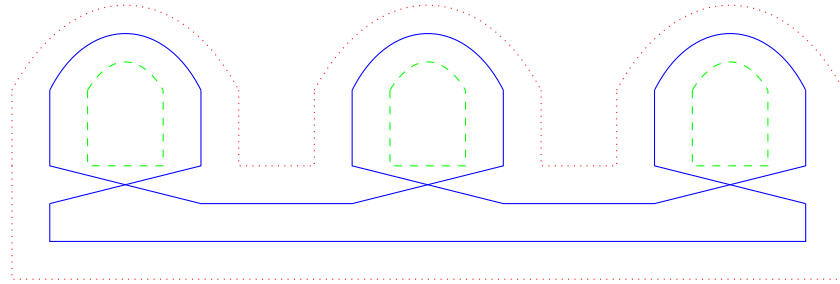
and its trace will be



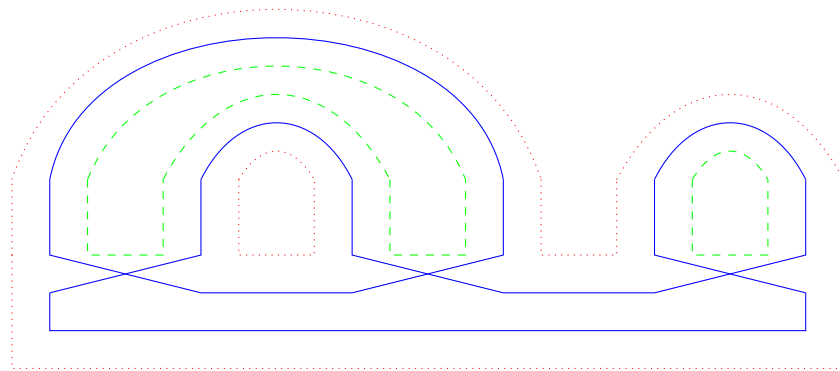
We have three copies of XX^\dagger , so there are $6 = 3!$ possible way to contract in ensemble averaging. In fact if we label each copy with a number 1, 2 or 3, we can close the line in the upper part of the diagram in the following ways:

1. $X_I \longrightarrow X_I^\dagger \quad I = 1, 2, 3$ (1 diagram);
2. $X_I \longrightarrow X_I^\dagger \quad X_J \longrightarrow X_K^\dagger \quad s.t. \quad J, K \neq I$ (3 diagrams);
3. $X_I \longrightarrow X_{I\pm 1}^\dagger$ (2 diagrams);

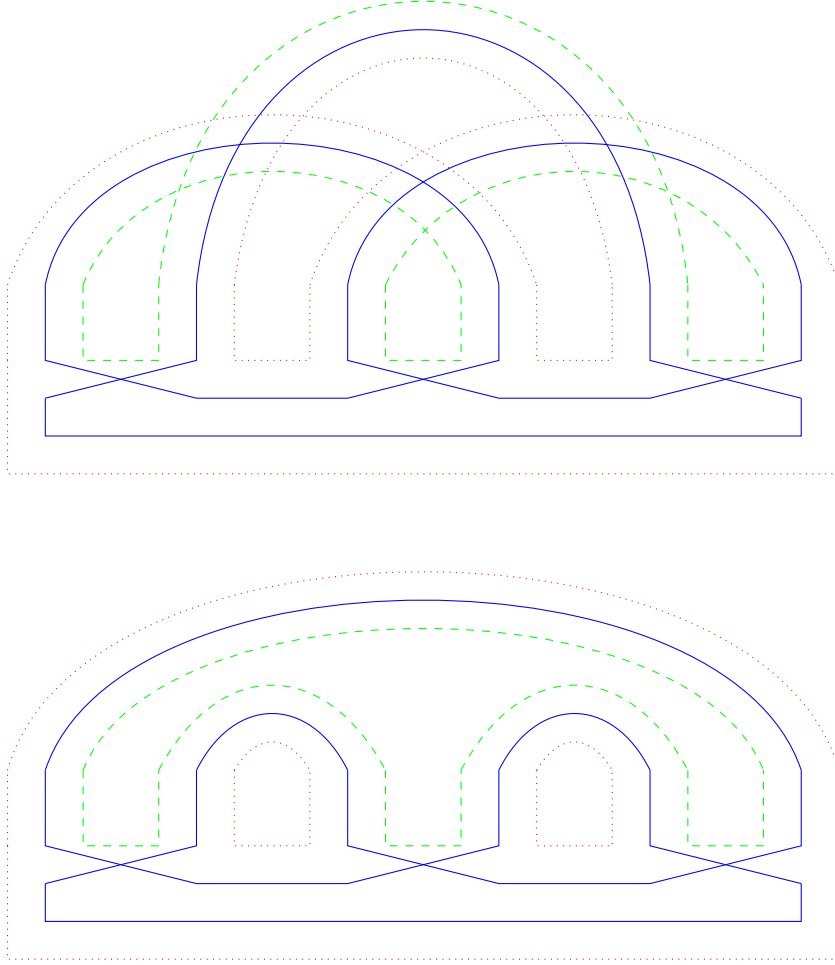
The diagram of the first case is:



The three cases with one X contracted with the X^\dagger of the same copy and the other two contracted with each other, are represented by diagrams of the form:



These 3 diagrams actually gives the same contributions so we can just count them three times.
The two remaining diagrams are the *cyclic* one and *anti cyclic* one.



We can calculate each contribution by counting the number of loop of each line and we get:

$$N_3 = \frac{d_A d_B d_C^3 + 3d_A^2 d_B^2 d_C^2 + d_A d_B^3 d_C + d_A^3 d_B}{d_A^3 d_B^3 d_C^3} = \frac{d_A^2 + d_B^2 + d_C^2 + 3d_A d_B d_C}{d_A^2 d_B^2 d_C^2} \quad (5.31)$$

Putting together the result of second and third Rényi negativities (5.29) and (5.31) we can notice two remarkable fact:

- $\langle \text{Tr}(\rho_{AB}^{T_B})^k \rangle$ is symmetric whit respect to the interchange $A \rightarrow B$; in fact given a partition (A and B) negativity, being defined as the sum of negative eigenvalues does not depend on what of the two subsystem we

partial transpose. This result confirms this fact.

- For $k = 2$ we have $2 = 2!$ terms caused by all the possible contraction in the ensemble averaging. For $k = 3$ we still have $6 = 3!$ terms.

At this point it should be clear that there is a strong correlation between entanglement in random tensor (spin) network and the permutation group S_n . In fact the number of diagrams (contributions to n -th Rényi negativity) is equal to the cardinality of the group S_n . In the following we will recap some properties, definitions and results about the permutation group, in order to obtain a statistical model "Ising-like" that generalizes the result on 2-nd Rényi entropy, in particular the action (4.39), for any order of negativity, in terms of the *Cayley metric* on permutation group. Instead of using spin variables attached to vertices we will use pinning fields (as seen in the previous chapter) given by group data (i.e. permutation) that spread into the graph and interact as spin did in the Hamiltonian (4.42).

5.3 Permutation approach

It seems evident that the permutation group is going to play a crucial role in the study of k -th Rényi negativity. We briefly recall some useful tools regarding this group. After that we will show how to interpret the results of diagrams through permutation.

5.3.1 Permutation Group

The Permutation group of order n is a finite group S_n which cardinality is $n!$. Each element $\sigma \in S_n$ is defined to be a bijection of a given set M to itself, i.e.

$$\sigma(i) = j \quad \forall i, j \in M \quad (5.32)$$

Notation There are different notations to represent a permutation. We will use two of them: the first one is *Cauchy's two lines notation* that is very practical in the calculation of the composition of two group element; the second one is the cyclic form, whose name itself suggest its strong usefulness in the calculation of cycles and Cayley's metric that we will define soon.

Cauchy's two lines notation consists in writing two rows. Say $\sigma \in S_n$ is a permutation acting on a given set of n element $\{x_1, \dots, x_n\}$. In the first row we list all the element of the set. In the second row we write the image under the permutation below each number:

$$\sigma = \begin{pmatrix} x_1 & x_2 & \dots & x_n \\ \sigma(x_1) & \sigma(x_2) & \dots & \sigma(x_n) \end{pmatrix} \quad (5.33)$$

For instance a particular permutation of the set $\{1, 2, 3, 4\}$ can be written as follows:

$$\sigma = \begin{pmatrix} 1 & 2 & 3 & 4 \\ 2 & 4 & 3 & 1 \end{pmatrix} \quad (5.34)$$

We can also write this permutation using *cyclic notation*: we write in round brackets the chains of number such that the second one is the image of the first one, the third element is the image of the second one and so on. For example the previous permutation is written as $(124)(3)$ where (3) is a trivial cycle because it is left unchanged by the permutation.

5.3.2 Geodesic on permutation group

Permutation group is equipped with a natural metric that will appear in the Ising model we will introduce in the following. Since our aim is to minimize the action of this model, we need to study geodesic on permutation group, in particular we focus on the class of permutations that are geodesic between the identity, the cyclic permutation and its inverse [5].

Consider a permutation $g \in S_k$, we can define the **length** of g as the minimum number of Swap to get g starting by the identity. For example in S_3 the permutations $(12)(3)$ and (123) have respectively length 1 and 2.

Similarly we can define the number of disjoint **cycles** of a permutation as $\chi(g) = \#(\text{cycles})$. The permutation $(12)(3)$ and (123) have respectively 2 and 1 cycles. By this example it is easy to understand that:

$$l(g) + \chi(g) = k \quad (5.35)$$

We can thus introduce a natural metric, given by:

$$d(g, h) = l(g^{-1}h) = k - \chi(g^{-1}h) \quad (5.36)$$

As cited before, we will be interested in studying the distance between 3 particular permutations of S_k :

$$\begin{aligned} \mathbb{1} &= (1)(2) \dots (k) \\ X &= (12 \dots k) \\ X^{-1} &= (k \dots 21) \end{aligned} \quad (5.37)$$

Since both lengths and cycles are easy to calculate for this permutations, we can easily resume the results on their distances:

$$d(\mathbb{1}, X) = k - 1 \quad d(\mathbb{1}, X^{-1}) = k - 1 \quad d(X, X^{-1}) = \begin{cases} k - 1 & k \text{ odd} \\ k - 2 & k \text{ even} \end{cases} \quad (5.38)$$

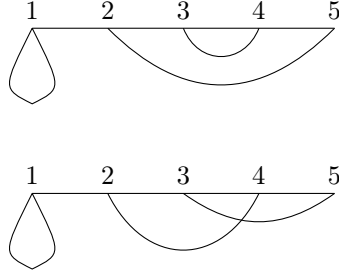
A set of permutation (g_1, g_2, \dots, g_n) is a **geodesic** on the permutation group if

$$d(g_1, g_2) + d(g_2, g_3) + \dots + d(g_{n-1}, g_n) = d(g_1, g_n) \quad (5.39)$$

The set of permutations that are on a geodesic between $\mathbb{1}$ and X , i.e. $d(\mathbb{1}, g) + d(g, X) = d(\mathbb{1}, X) = k - 1$, is known to be in bijection with the set of *Non-Crossing Partitions* of the set $[k] = \{1, 2, \dots, k\}$. A *NCP* is a set of non-empty pairwise disjoint subsets called "blocks", such that no two blocks cross each other: consider the following permutations in S_5

$$g = (1)(25)(34) \quad h = (1)(24)(35) \quad (5.40)$$

Those permutation can be diagrammatically drawn as: We can see that only



$(1)(25)(34)$ is a non crossing pairing. The number of NCP of S_k is given by the *Catalan number*:

$$C_k = |NC(k)| = \frac{\binom{2k}{k}}{k+1} \tag{5.41}$$

We will use this information to obtain the set of permutation that are simultaneously geodesic for the three distances (5.38). Namely we are looking for the permutations such that:

$$\begin{cases} d(\mathbb{1}, \tau) + d(\tau, X) = k - 1 \\ d(\mathbb{1}, \tau) + d(\tau, X^{-1}) = k - 1 \\ d(X, \tau) + d(\tau, X^{-1}) = \begin{cases} k - 1 & k \text{ odd} \\ k - 2 & k \text{ even} \end{cases} \end{cases} \tag{5.42}$$

These conditions are equivalent to:

$$\begin{aligned} d(\mathbb{1}, \tau) &= \left\lfloor \frac{k}{2} \right\rfloor \\ d(X, \tau) = d(X^{-1}, \tau) &= \left\lceil \frac{k}{2} \right\rceil - 1 \end{aligned} \tag{5.43}$$

where $\lfloor \frac{k}{2} \rfloor$ and $\lceil \frac{k}{2} \rceil$ represent respectively the approximation to the smaller and larger integer. Solving these conditions it is possible to prove that τ is on the geodesics only if it is a permutation corresponding to a non-crossing partition of the set $[k]$ containing only block of length 2 plus a single block of length 1 if k is odd. We call this set *Non Crossing Pairings* $NC_2(k)$ and its cardinality is denoted by a_k . For even k there exists a bijection $NC_2(k) \longleftrightarrow NC(\frac{k}{2})$, and for odd k we have $a_k = ka_{k-1}$. Thus we can calculate cardinality in the two different cases:

$$a_k = \begin{cases} kC_{\frac{k-1}{2}} & \text{odd} \\ C_{\frac{k}{2}} & \text{even} \end{cases} \tag{5.44}$$

whose limit for $k \rightarrow 1$ is given by:

$$\lim_{k \rightarrow 1} a_k = \begin{cases} 1 & \text{odd} \\ \frac{8}{3\pi} & \text{even} \end{cases} \tag{5.45}$$

This detailed discussion of permutations' properties provides a quick recap of all the mathematics we need to develop a statistical model for Rényi negativity. Indeed, recalling how we defined pure Haar Random states (5.13), we already said that there exists an alternative way to describe this class of states. Following the previous works on Random Spin Network [16, 3], we can consider a reference state $|0\rangle \in \mathcal{H}$ and consider all the state that can be obtained acting with a Unitary operator. As we show so far, Negativity exhibit a natural internal symmetry related to the permutation group. So it is natural to consider the Unitary operator acting on the reference state as a unitary representation of the group S_n . Since we are interested in ensemble averaging for induced mixed states, we can consider a preliminary example to see how permutations' properties arise in the calculation [18].

Consider a bipartite system:

$$\mathcal{H} = \mathcal{H}_A \otimes \mathcal{H}_B \quad (5.46)$$

described by a density matrix ρ . Tracing over B we have an induced mixed state. If we calculate the average over α copies of ρ_A , since trace and averaging are commuting operations, we get:

$$\overline{\rho_A^{\otimes \alpha}} = \text{Tr}_B \left[|\psi\rangle \langle \psi|^{\otimes \alpha} \right] \quad (5.47)$$

group averaging is given by the sum over all the possible permutations acting on α copies of the system, so:

$$\overline{\rho_A^{\otimes \alpha}} = \frac{\sum_{\tau \in S_\alpha} g_{\tau_A} \text{Tr} [g_{\tau_B}]}{\sum_{\tau \in S_\alpha} \text{Tr} [g_\tau]} \quad (5.48)$$

where τ_A and τ_B are permutation acting only on the subsystems A and B . The trace of a permutation is easy to calculate since it is equal to the dimension of the Hilbert space (d_A or d_B) to the number of the cycles $\chi(\tau)$. So the denominator becomes:

$$\sum_{\tau} \text{Tr} [g_\tau] = \sum_{\tau} (d_A d_B)^{\chi(\tau)} \quad (5.49)$$

This quantity can be summed exactly: the number of permutation of α element with k cycles is given by the well known Stirling number of first kind $\left[\begin{matrix} n \\ k \end{matrix} \right]$. Since we are interested in the regime of large dimensions, only the permutation that maximizes $\chi(\tau)$ will contribute at leading order. This permutation is the Identity, i.e. the only permutation of S_α with α cycles. Thus the denominator can be approximated to $(d_A d_B)^\alpha$.

5.4 Generalized Ising model for Rényi k-th Negativity

Consider a spin network state associated to a graph γ . For simplicity we consider the case of fixed spin. The three sets of degrees of freedom discussed in the previous chapters are:

1. boundary region $\partial\gamma$ given by the dangling legs of the graph;
2. bulk region, given by Intertwiner $\dot{\gamma}$ and internal links gluing vertices L .

To each vertex we associate a state belonging to a single vertex Hilbert space \mathcal{H}_v . So the state of the disconnected graph is given by the tensor product of all the vertex states described by:

$$|f_v\rangle = \sum_{\vec{m}, \iota} f_{\vec{m}, \iota}^{\vec{j}} |\vec{j}_v, \vec{m}, \iota\rangle \in \mathcal{H}_v = \mathcal{I}^{\vec{j}_v} \otimes \bigotimes_i V^{j_v^i} \quad (5.50)$$

The graph state is given by contracting with links that project the state into the maximally entangled state:

$$|\phi_\gamma\rangle = \left(\bigotimes_{e_{vw}^i \in L} \langle e_{vw}^i | \right) \bigotimes_v |f_v\rangle \quad (5.51)$$

where $|e_{vw}^i\rangle$ is a bivalent intertwiner that glue the vertices v and w through the i -th edge

$$|e_{vw}^i\rangle = \sum_m \frac{(-1)^{j+m}}{\sqrt{d_{j_{vw}^i}}} |j_{vw}^i, m\rangle |j_{vw}^i, -m\rangle \quad (5.52)$$

The density matrix associated to this state is given by

$$\rho = |\phi_\gamma\rangle \langle \phi_\gamma| = \text{Tr}_L \left\{ \rho_L \otimes \bigotimes_v |f_v\rangle \langle f_v| \right\} \quad (5.53)$$

where $\rho_L = \bigotimes_{e \in L} |e_{vw}^i\rangle \langle e_{vw}^i|$.

In order to calculate k -th Rényi Negativity, we can consider a tripartite system as in the previous example of diagrams. We will use the same notation, namely:

1. A is the part of the system that is left untouched;
2. B is the region that get partial transposed;
3. C is the subsystem we trace out in order to get a mixed state.

The average k -th Rényi negativity is given by:

$$\overline{N_k} = \text{Tr} \left[\overline{\left(\rho_{AB}^{T_B} \right)^k} \right] \quad (5.54)$$

Using replica trick, (5.54) can be rewritten as [5]:

$$\overline{N_k} = \frac{\overline{Z_k}}{\overline{Z_0}} \quad (5.55)$$

Where $\overline{Z_k}$ and $\overline{Z_0}$ are given by the following expressions:

$$\begin{aligned} \overline{Z_k} &= \text{Tr} \left[\rho_L^{\otimes k} \otimes \left(\bigotimes_v \overline{(|f_v\rangle \langle f_v|)^{\otimes k}} \right) \otimes P_A(X) \otimes P_B(X^{-1}) \otimes P_C(\mathbb{1}) \right] \\ \overline{Z_0} &= \text{Tr} \left[\rho_L^{\otimes k} \otimes \left(\bigotimes_v \overline{(|f_v\rangle \langle f_v|)^{\otimes k}} \right) \right] \end{aligned} \quad (5.56)$$

We denote by $P_I(\sigma)$ a unitary representation of the permutation σ acting on the subsystem I . That correspond to attach at each vertex of the graph an appropriate *pinning field* according to what subsystem the vertex belongs to. These pinning fields are respectively the cyclic, anticyclic and identity permutation for the system A, B and C . According to the previous discussion, the averaging over the vertex states can be computed as follows [18]:

$$\overline{(|f_v\rangle \langle f_v|)^{\otimes k}} = \frac{(D_v - 1)!}{(D_v + k - 1)!} \sum_{g_v \in S_k} P_v(g_v) \quad (5.57)$$

where $P_v(g_v)$ is the representation of the permutation g_v acting on the k copies of the vertex Hilbert space \mathcal{H}_v , whose dimension is D_v . In order to compute the effects of this permutation on the different degrees of freedom of the graph, we can factorize $P_v(g_v)$ into three different operators:

$$P_v(g_v) = P_{v,0}(g_v) \otimes \bigotimes_{e_{vw}^i \in L} P_{v,i}(g_v) \otimes \bigotimes_{e_{v\bar{v}}^i \in \partial\gamma} P_{v,i}(g_v) \quad (5.58)$$

where $P_{v,0}(g_v)$ acts on k copies of the Intertwiner space; $\bigotimes_{e_{vw}^i \in L} P_{v,i}(g_v)$ acts on k copies of the internal links; $\bigotimes_{e_{v\bar{v}}^i \in \partial\gamma} P_{v,i}(g_v)$ acts on the boundary semi-edges since \bar{v} represents (as in the previous sections) a virtual vertex which is connected with v with the boundary edge $e_{v\bar{v}}^i$.

We can focus on the expectation value of Z_k and, performing the average on the vertex states we obtain:

$$\overline{Z_k} = \text{Tr} \left[\rho_L^{\otimes k} \otimes \left(\bigotimes_v \sum_{g_v \in S_k} P_v(g_v) \right) \otimes P_A(X) \otimes P_B(X^{-1}) \otimes P_C(\mathbb{1}) \right] \quad (5.59)$$

This trace factorizes over the different degrees of freedom and it is given by a sum over all the configuration of elements g_v .

Link contribution Tracing over links:

$$\begin{aligned}
 \text{Tr}_L \left[\rho_L^{\otimes k} \otimes \bigotimes_v \sum_{g_v \in S_k} P_v(g_v) \right] &= \\
 \sum_{\{g_v\}} \text{Tr} \left[\frac{1}{d_{j_{vw}}^k} (|e_{vw}^i\rangle \langle e_{vw}^i|)^{\otimes k} \otimes (P_{v,i}(g_v) \otimes P_{w,i}(g_v)) \right] &= \\
 \sum_{\{g_v\}} \prod_{e_{vw}^i \in L} d_{j_{vw}}^{-k+\chi(g_v^{-1}g_w)} &= \\
 \sum_{\{g_v\}} \prod_{e_{vw}^i \in L} d_{j_{vw}}^{-d(g_v,g_w)} &
 \end{aligned} \tag{5.60}$$

Boundary contributions

$$\begin{aligned}
 \text{Tr}_{\partial A} \left[\bigotimes_{v \in A} \frac{1}{d_{j_v^i}^k} \sum_{g_v \in S_k} P_v(g_v) \otimes P_A(X) \right] &= \\
 \text{Tr}_{\partial A} \left[\bigotimes_{v \in A} \frac{1}{d_{j_v^i}^k} \sum_{g_v \in S_k} \bigotimes_{e_{v\bar{v}}^i \in \partial A} P_{v,i}(g_v) \otimes P_A(X) \right] &= \\
 \prod_{v \in A} \frac{1}{d_{j_v^i}^k} \sum_{g_v \in S_k} \prod_{e_{v\bar{v}}^i \in \partial A} \text{Tr}_{\partial A} [P_{v,i}(g_v) \otimes P_A(X)] &= \\
 \sum_{\{g_v\}} \prod_{v \in A} \prod_{e_{v\bar{v}}^i \in \partial A} d_{j_v^i}^{-k+\chi g_v^{-1}X} &= \\
 \sum_{\{g_v\}} \prod_{\partial A} d_{j_v^i}^{-d(g_v,X)} &
 \end{aligned} \tag{5.61}$$

Similarly, the terms related to ∂B and ∂C are given by:

$$\begin{aligned}
 \text{Tr}_{\partial B} \left[\bigotimes_{v \in B} \frac{1}{d_{j_v^i}^k} \sum_{g_v \in S_k} P_v(g_v) \otimes P_B(X^{-1}) \right] &= \\
 \sum_{\{g_v\}} \prod_{\partial B} d_{j_v^i}^{-d(g_v,X^{-1})} &
 \end{aligned} \tag{5.62}$$

$$\begin{aligned}
 \text{Tr}_{\partial C} \left[\bigotimes_{v \in C} \frac{1}{d_{j_v^i}^k} \sum_{g_v \in S_k} P_v(g_v) \otimes P_C(\mathbb{1}) \right] &= \\
 \sum_{\{g_v\}} \prod_{\partial C} d_{j_v^i}^{-d(g_v,\mathbb{1})} &
 \end{aligned} \tag{5.63}$$

Bulk contribution

$$\begin{aligned} \text{Tr}_{\dot{A}} \left[\bigotimes_v \sum_{g_v \in S_k} \frac{1}{D_{j_v}^k} P_{v,0}(g_v) P_A(X) \right] &= \\ \sum_{\{g_v\}} \prod_{\iota_v \in A} D_{j_v}^{-d(g_v, X, \mathbb{1})} &= \sum_{\{g_v\}} \prod_{\iota_v \in A} D_{j_v}^{-d(g_v, X^{-1})} \end{aligned} \quad (5.64)$$

$$\begin{aligned} \text{Tr}_{\dot{B}} \left[\bigotimes_v \sum_{g_v \in S_k} \frac{1}{D_{j_v}^k} P_{v,0}(g_v) P_B(X^{-1}) \right] &= \\ \sum_{\{g_v\}} \prod_{\iota_v \in B} D_{j_v}^{-d(g_v, X^{-1}, \mathbb{1})} &= \sum_{\{g_v\}} \prod_{\iota_v \in B} D_{j_v}^{-d(g_v, X)} \end{aligned} \quad (5.65)$$

$$\begin{aligned} \text{Tr}_{\dot{C}} \left[\bigotimes_v \sum_{g_v \in S_k} \frac{1}{D_{j_v}^k} P_{v,0}(g_v) P_C(\mathbb{1}) \right] &= \\ \sum_{\{g_v\}} \prod_{\iota_v \in C} D_{j_v}^{-d(g_v, \mathbb{1})} \end{aligned} \quad (5.66)$$

Putting together this results we can write \overline{Z}_k as follows:

$$\begin{aligned} \overline{Z}_k &= \left(\prod_v \frac{(D_v - 1)!}{(D_v + k - 1)!} \right) \sum_{\{g_v\}} \left\{ \left(\prod_{e_{vw}^i \in L} d_{j_{vw}^i}^{-d(g_v, g_w)} \right) \cdot \right. \\ &\quad \left(\prod_{e_{v\bar{v}}^i \in \partial A} d_{j_v^i}^{-d(g_v, X)} \right) \left(\prod_{e_{v\bar{v}}^i \in \partial B} d_{j_v^i}^{-d(g_v, X^{-1})} \right) \left(\prod_{e_{v\bar{v}}^i \in \partial C} d_{j_v^i}^{d(g_v, \mathbb{1})} \right) \cdot \\ &\quad \left. \cdot \left(\prod_{\iota_v \in \dot{A}} D_{j_v}^{-d(g_v, X^{-1})} \right) \left(\prod_{\iota_v \in \dot{B}} D_{j_v}^{-d(g_v, X)} \right) \left(\prod_{\iota_v \in \dot{C}} D_{j_v}^{-d(g_v, \mathbb{1})} \right) \right\} \end{aligned} \quad (5.67)$$

Following the procedure in [5], the result in (5.67) can be written as:

$$\overline{Z}_k = \sum_{\{g_v\}} e^{-A_k[\{g_v\}]} \quad (5.68)$$

where A_k is the action of a *generalized Ising Model*:

$$\begin{aligned} A_k[\{g_v\}] &= \sum_{e_{vw}^i \in L} d(g_v, g_w) \log d_{j_{vw}^i} + \sum_{e_{v\bar{v}}^i \in \partial A} d(g_v, X) \log d_{j_v^i} + \\ &+ \sum_{e_{v\bar{v}}^i \in \partial B} d(g_v, X^{-1}) \log d_{j_v^i} + \sum_{e_{v\bar{v}}^i \in \partial C} d(g_v, \mathbb{1}) \log d_{j_v^i} + \\ &+ \sum_{\iota_v \in \dot{A}} d(g_v, X, \mathbb{1}) \log D_{j_v} + \sum_{\iota_v \in \dot{B}} d(g_v, X^{-1}, \mathbb{1}) \log D_{j_v} + \\ &+ \sum_{\iota_v \in \dot{C} \cup \Omega} d(g_v, \mathbb{1}) \log D_{j_v} + \xi \end{aligned} \quad (5.69)$$

where ξ is a constant term.

The same procedure can be used to derive a similar expression for the denominator of (5.55):

$$\begin{aligned} \overline{Z}_0 &= \sum_{\{g_v\}} e^{-A_0[\{g_v\}]} \\ A_0[\{g_v\}] &= \sum_{e_{vw}^i \in L} d(g_v, g_w) \log d_{j_{vw}^i} + \sum_{e_{v\bar{v}}^i \in \partial\gamma} d(g_v, \mathbb{1}) \log d_{j_v^i} + \sum_{\iota_v \in \dot{\gamma}} d(g_v, \mathbb{1}) \log D_{j_v} + \xi \end{aligned} \quad (5.70)$$

The pinning fields X, X^{-1} and $\mathbb{1}$ are permutations attached to virtual vertices that interact via a two-body interaction with the *generalized spins* (i.e. permutations) on each vertex of the graph. The strength of these interactions is proportional to $\log d$, d being the dimension of the link, semi-link or Intertwiner space according to what term we are considering. Differently from [5], the partition function (5.69) contains new terms due to the internal degrees of freedom (Intertwiner), that characterize the spin network structure of the graph, interacting with boundary pinning fields. Since we are interested in the study of the entanglement structure for boundary states (Ryu-Takayanagi model) we have to insert a bulk state and repeat the same procedure with only boundary states.

Bulk entropy contribution As it has been shown in Cap. 3, given a graph γ with fixed spins j and a bulk state $|\tau\rangle$, the corresponding boundary state is given by the bulk-to-boundary map:

$$\mathcal{M}[\phi_\gamma] : \mathcal{H}_\gamma = \bigotimes_v \mathcal{I}^{j_v} \ni |\tau\rangle \rightarrow \mathcal{M}[\phi_\gamma]|\tau\rangle = \langle \tau | \phi_\gamma \rangle = |\phi_{\partial\gamma}\rangle \in \mathcal{H}_{\partial\gamma} = \bigotimes_{e \in \partial\gamma} \mathcal{V}^{j_e} \quad (5.71)$$

To study the effect of quantum correlations in the bulk on boundary entropy we can insert a particular bulk state:

$$|\tau\rangle = |\tau_\Omega\rangle \otimes \left(\bigotimes_{v \in \Omega} |\tau_v\rangle \right) \in \mathcal{H}_\gamma \quad (5.72)$$

Consider a region $\Omega \in \dot{\gamma}$ with a generic type and number of correlations between intertwiners encoded in the state $|\tau_\Omega\rangle$; its complementary region $\bar{\Omega}$ is contracted with a direct product state of intertwiner for each vertex (i.e. there is no correlations between them). After the mapping into $|\phi_{\partial\gamma}\rangle$ the three regions A,B and C are boundary regions, since there are no more free internal degrees of freedom. It is easy to show that non-correlated intertwiners give no contribution to the partition function. Indeed, consider $|\tau_v\rangle = \sum_\iota \tau_\iota^{(v)} |\vec{j}_v, \iota\rangle$ and its contraction with vertex states $|f_v\rangle$:

$$\langle f_v | \tau \rangle = \langle \tau_v | f_v \rangle = \sum_{\vec{m}} f(\tau)_{\vec{m}}^{\vec{j}} |\vec{j}_v, \vec{m}\rangle \quad (5.73)$$

5.4. GENERALIZED ISING MODEL FOR RÉNYI k -TH NEGATIVITY 99

where $f(\tau)_{\vec{m}}^j = \sum_L f_{\vec{m}_L}^j(\tau_L^{(v)})^*$ are the coefficients of the boundary states. Such states are random boundary states: we can compute typical values of Rényi Negativity:

$$\overline{N}_k = \text{Tr} \left[\overline{\left(\rho_{AB}^{T_B} \right)^k} \right] = \frac{\overline{Z}_k}{\overline{Z}_0} \quad (5.74)$$

The averaging over the random boundary states can be written in terms of permutations, as in the previous case:

$$\overline{(|f_v(\tau)\rangle \langle f_v(\tau)|)^{\otimes k}} = \frac{(D_v - 1)!}{(D_v + k - 1)!} \sum_{g_v \in S_k} P_v(g_v) \quad (5.75)$$

In order to obtain a *generalized Ising partition function*, we need to factorize the permutation like previously done (5.58). This time we can only factorize $P_v(g_v)$ into two different operator:

$$P_v(g_v) = \bigotimes_{e_{vw}^i \in L} P_{v,i}(g_v) \otimes \bigotimes_{e_{v\bar{v}}^i \in \partial\gamma} P_{v,i}(g_v) \quad (5.76)$$

the first term acts on k copies of the internal links; the second one acts on the boundary semi-edges. Compared to the previous case the term $P_{v,0}(g_v)$ does not appear, since we inserted a bulk state, i.e. contracted intertwiner degrees of freedom. Now we can show that the intertwiners that get contracted with a state $|\tau_v\rangle \in \bar{\Omega}$ do not contribute to Rényi negativity, while the remaining part $|\tau_\Omega\rangle$ gives a crucial contribution. We can write the partition functions as follows:

$$\begin{aligned} \overline{Z}_k &= \text{Tr} \left\{ \rho_{\tau_\Omega}^{\otimes k} \otimes \rho_L^{\otimes k} \otimes \left(\bigotimes_{v \in \Omega} \overline{(|f_v\rangle \langle f_v|)^{\otimes k}} \right) \otimes \left(\bigotimes_{v \in \bar{\Omega}} \overline{(|f_v(\tau)\rangle \langle f_v(\tau)|)^{\otimes k}} \right) \otimes \right. \\ &\quad \left. \otimes P_A(X) \otimes P_B(X^{-1}) \otimes P_C(\mathbb{1}) \right\} \quad (5.77) \end{aligned}$$

$$\overline{Z}_0 = \text{Tr} \left\{ \rho_{\tau_\Omega}^{\otimes k} \otimes \rho_L^{\otimes k} \otimes \left(\bigotimes_{v \in \Omega} \overline{(|f_v\rangle \langle f_v|)^{\otimes k}} \right) \otimes \left(\bigotimes_{v \in \bar{\Omega}} \overline{(|f_v(\tau)\rangle \langle f_v(\tau)|)^{\otimes k}} \right) \right\} \quad (5.78)$$

Using (5.75) and (5.76), these partition functions can be written in terms of permutations and, after the same calculations of the previous case, we can write down the action of the Ising model as follows:

$$Z_{k/0} = \sum_{\{g_v\}} e^{-A_{k/0}[\{g_v\}]} \quad (5.79)$$

$$\begin{aligned}
A_k[\{g_v\}] &= \sum_{e_{vw}^i \in L} d(g_v, g_w) \log d_{j_{vw}^i} + \sum_{e_{v\bar{v}}^i \in A} d(g_v, X) \log d_{j_v^i} + \\
&+ \sum_{e_{v\bar{v}}^i \in B} d(g_v, X^{-1}) \log d_{j_v^i} + \sum_{e_{v\bar{v}}^i \in C} d(g_v, \mathbb{1}) \log d_{j_v^i} + \\
&+ A(\Omega) + \xi
\end{aligned} \tag{5.80}$$

$$\begin{aligned}
A_0[\{g_v\}] &= \sum_{e_{vw}^i \in L} d(g_v, g_w) \log d_{j_{vw}^i} + \sum_{e_{v\bar{v}}^i \in \partial\gamma} d(g_v, \mathbb{1}) \log d_{j_v^i} + \\
&+ A(\Omega) + \xi
\end{aligned} \tag{5.81}$$

where

$$A(\Omega) = -\log \left[\text{Tr}_\Omega \left\{ \rho_\tau^{\otimes k} \left(\bigotimes_{v \in \Omega} P_{v,0}(g_v) \right) \right\} \right] \tag{5.82}$$

is a contribution related to the bulk entropy that depends on the correlation inserted in Ω , namely on the form of the state $|\tau_\Omega\rangle$.

In the following, we will consider only pair-wise correlations between couples of vertices in the bulk, so that the state can be written as a maximally entangled intertwiners state:

$$|\tau_\Omega\rangle = \bigotimes_{\langle v,w \rangle \in \Omega} D_{\vec{j}_{vw}}^{-\frac{1}{2}} \sum_{\iota} |\vec{j}_{vw}, \iota\rangle \otimes |\vec{j}_{vw}, \iota\rangle \tag{5.83}$$

With this setting, the bulk entropy contribution $A(\Omega)$ has the same structure of the link contribution:

$$A(\Omega) = \sum_{\langle vw \rangle \in \Omega} d(g_v, g_w) \log D_{\vec{j}_{vw}} \tag{5.84}$$

For each order of negativity, the denominator (5.81) can be easily computed in the large dimension limit, so we will focus our analysis on the minimization procedure of the k -th order action $A_k[\{g_v\}]$ for simple graphs, in particular we will focus on the effect of the bulk entropy.

5.4.1 Ising action of a homogeneous spin network

In order to investigate how an area law emerges from the statistical approach for Rényi negativity measures, we can consider an *homogeneous spin network state* with fixed spin, all of which are equal to a given value j . As considered in the previous chapter (4.40) we clearly obtain that all the dimensions of the Hilbert spaces are equal:

$$d_{j_{vw}^i} = d_{j_v^i} = D_{\vec{j}_{vw}} = d \tag{5.85}$$

5.4. GENERALIZED ISING MODEL FOR RÉNYI K -TH NEGATIVITY 101

We can introduce the *temperature parameter* $\beta = \log d$ and write the action A_k as:

$$A_k [\{g_v\}] = \beta \mathcal{H}_k [\{g_v\}] \quad (5.86)$$

where $\mathcal{H}_k [\{g_v\}]$ is the Ising-like Hamiltonian describing the two-body interaction between spin network vertices via Cayley distance on permutation group with pinning fields playing the role of boundary conditions. We will denote with $\mathcal{H}_k [\{g_v\}]$ and $\mathcal{H}_k^c [\{g_v\}]$ the Hamiltonians corresponding respectively to a tensor product bulk state (no correlations) and to a bulk state exhibiting link-wise correlation in the region Ω . With this notation:

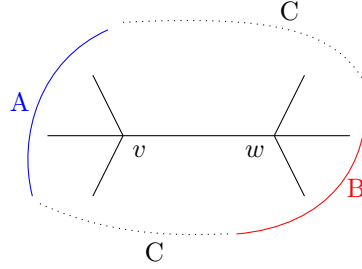
$$\mathcal{H}_k = \sum_{e_{vw}^i \in L} d(g_v, g_w) + \sum_{\partial A} d(g_v, X) + \sum_{\partial B} d(g_v, X^{-1}) + \sum_{\partial C} d(g_v, \mathbb{1}) \quad (5.87)$$

$$\mathcal{H}_k^c = \sum_{e_{vw}^i \in L} d(g_v, g_w) + \sum_{\partial A} d(g_v, X) + \sum_{\partial B} d(g_v, X^{-1}) + \sum_{\partial C} d(g_v, \mathbb{1}) + \sum_{\langle vw \rangle \in \Omega} d(g_v, g_w) \quad (5.88)$$

To study the effect of correlations and derive an entanglement-area law, similarly to [16] we will follow the following steps:

- Consider a graph γ composed by a given number of tetravalent vertices with a generic boundary tripartition A,B and C.
- We trace out the boundary degrees of freedom in C and calculate Rényi log negativity of the subsystem A.
- We are interested in the large dimension regime, so the relevant contribution from (5.79) are the one associated to the *spin configuration that minimize the action* (or the Hamiltonian). So we will numerically study the values of the Hamiltonians \mathcal{H}_k and \mathcal{H}_k^c .
- In particular, we will focus on the calculation of $\mathcal{H}_2, \mathcal{H}_3$ and \mathcal{H}_4 and relate the minimal values of such Hamiltonians to the values of the areas of the minimal surfaces that separate the subsystem in the graph.
- spin configurations will be studied according to the possibility of a vertex to belong to the domain of each subsystem A,B,C or to a intermediate internal domain, characterized by non-crossing pairings τ that satisfy the rules (5.43)

Two vertices graph Consider a graph γ composed by two tetravalent vertices v and w glued with a single link.



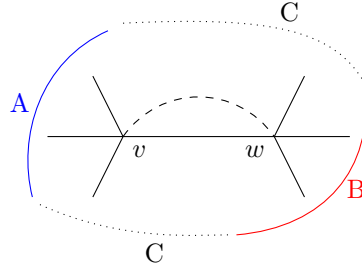
Looking at the graph above, we notice that the vertex v has two boundary legs in A and one in C and similarly w has two boundary legs in B and one in C; so the k -th Hamiltonian can be written as:

$$\mathcal{H}_k = d(g_v, g_w) + 2d(g_v, X) + 2d(g_w, X^{-1}) + d(g_v, \mathbb{1}) + d(g_w, \mathbb{1}) \quad (5.89)$$

Consider now the case of a correlated bulk insertion, with a link-wise correlation between intertwiners in v and w (5.84). The contribution of $A(\Omega)$ to the Hamiltonian will be given (in the homogeneous case) by an additional link contribution $d(g_v, g_w)$, so that the correlated k -th Hamiltonian can be written as:

$$\mathcal{H}_k^c = 2d(g_v, g_w) + 2d(g_v, X) + 2d(g_w, X^{-1}) + d(g_v, \mathbb{1}) + d(g_w, \mathbb{1}) \quad (5.90)$$

Moreover, such correlation can be drawn as an additional link between vertices, according to the link-wise nature of $|\tau_\Omega\rangle$ in (5.83).



We come out with the convention of representing correlations with dashed lines to make them distinguishable from the internal links.

k=2 The permutation group S_2 only has two element:

$$S_2 = \{\mathbb{1} = (1)(2), S = (12)\} \quad (5.91)$$

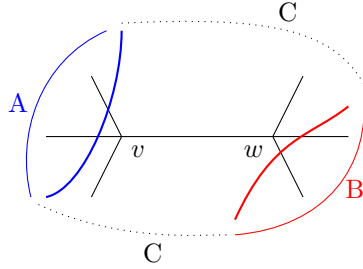
where S can be interpreted as a Swap operator. The cyclic and anticyclic permutation are equal since $X = S = S^{-1} = X^{-1} = (12)$. Moreover, the case $k = 2$ present the trivial situation in which the domain of the non-crossing

5.4. GENERALIZED ISING MODEL FOR RÉNYI K -TH NEGATIVITY 103

pairings corresponds to the domain of A and B since $X = X^{-1}$ is the only NCP. Motivated by this considerations, we can only consider three possible spin configurations. For each configuration we will calculate the value of \mathcal{H}_2 and draw the corresponding domain in the graph.

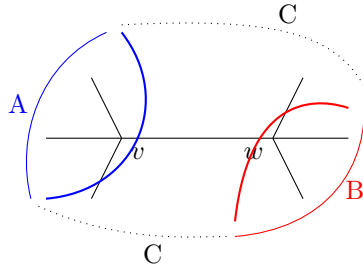
1. $g_v = \mathbb{1}, g_w = \mathbb{1} \rightarrow v, w \in C$ The non-correlated Hamiltonian (5.89) can thus be written as:

$$\begin{aligned} \mathcal{H}_2 &= d(\mathbb{1}, \mathbb{1}) + 2d(\mathbb{1}, X) + 2d(\mathbb{1}, X^{-1}) + d(\mathbb{1}, \mathbb{1}) + d(\mathbb{1}, \mathbb{1}) = \\ &= 2d(\mathbb{1}, X) + 2d(\mathbb{1}, X^{-1}) = \\ &= 2 + 2 = 4 \end{aligned}$$

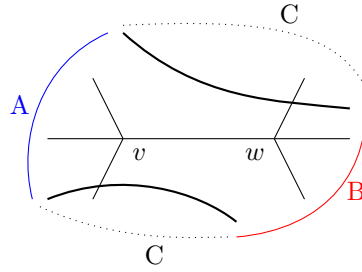


2. $g_v = X, g_w = X^{-1} \rightarrow v \in A, w \in B$

$$\begin{aligned} \mathcal{H}_2 &= d(X, X^{-1}) + 2d(X, X) + 2d(X^{-1}, X^{-1}) + d(X, \mathbb{1}) + d(X^{-1}, \mathbb{1}) = \\ &= d(X, \mathbb{1}) + d(X^{-1}, \mathbb{1}) = \\ &= 1 + 1 = 2 \end{aligned}$$

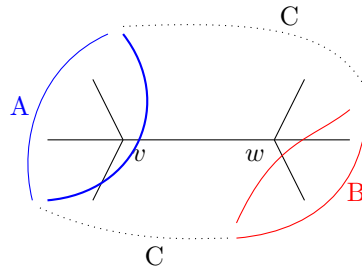


In this particular configuration, since we are working with S_2 and $X = X^{-1}$ the domains of A and B are labelled by the same permutation, so we can represent the domain walls as surfaces that separates the region AB from C, namely:



3. $g_v = X, g_w = \mathbb{1} \rightarrow v \in A, w \in C$

$$\begin{aligned} \mathcal{H}_2 &= d(X, \mathbb{1}) + 2d(X, X) + 2d(\mathbb{1}, X^{-1}) + d(X, \mathbb{1}) + d(\mathbb{1}, \mathbb{1}) = \\ &= d(X, \mathbb{1}) + 2d(\mathbb{1}, X^{-1}) + d(X, \mathbb{1}) = \\ &= 1 + 2 + 1 = 4 \end{aligned}$$

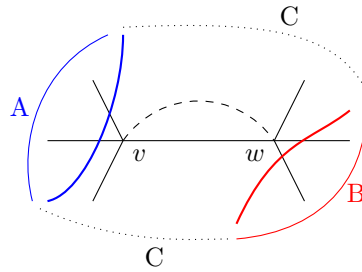


Note that the configuration $g_v = \mathbb{1}, g_w = X^{-1}$ is symmetric up to a reflection to the third case, so the Hamiltonian has the same value (4).

Now we can repeat the same analysis, including bulk correlation.

1. $g_v = \mathbb{1}, g_w = \mathbb{1} \rightarrow v, w \in C$

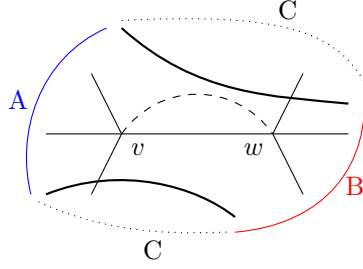
$$\begin{aligned} \mathcal{H}_2^c &= 2d(\mathbb{1}, \mathbb{1}) + 2d(\mathbb{1}, X) + 2d(\mathbb{1}, X^{-1}) + d(\mathbb{1}, \mathbb{1}) + d(\mathbb{1}, \mathbb{1}) = \\ &= 2d(\mathbb{1}, X) + 2d(\mathbb{1}, X^{-1}) = \\ &= 2 + 2 = 4 \end{aligned}$$



5.4. GENERALIZED ISING MODEL FOR RÉNYI k -TH NEGATIVITY 105

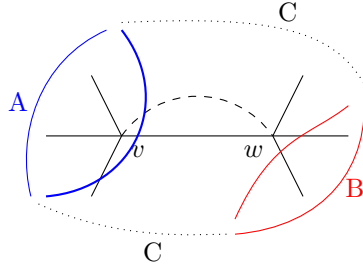
2. $g_v = X, g_w = X^{-1} \rightarrow v \in A, w \in B$

$$\begin{aligned} \mathcal{H}_2^c &= 2d(X, X^{-1}) + 2d(X, X) + 2d(X^{-1}, X^{-1}) + d(X, \mathbb{1}) + d(X^{-1}, \mathbb{1}) = \\ &= 2d(X, \mathbb{1}) + d(X^{-1}, \mathbb{1}) = \\ &= 1 + 1 = 2 \end{aligned}$$



3. $g_v = X, g_w = \mathbb{1} \rightarrow v \in A, w \in C$

$$\begin{aligned} \mathcal{H}_2^c &= 2d(X, \mathbb{1}) + 2d(X, X) + 2d(\mathbb{1}, X^{-1}) + d(X, \mathbb{1}) + d(\mathbb{1}, \mathbb{1}) = \\ &= 2d(X, \mathbb{1}) + 2d(\mathbb{1}, X^{-1}) + d(X, \mathbb{1}) = \\ &= 2 + 2 + 1 = 5 \end{aligned}$$



By looking at this partial results we can notice that in the lowest energy configuration (the second one), the domain wall does not enter the bulk region at all. Correlation seems to play a role in increasing the Hamiltonian value only in the third configuration, which is the only one with different permutations on the vertex. As previously said, this case seems to exhibit no particular results, because of the trivial features of S_2 , such as $X = X^{-1}$ and NCP given by only one permutation, whose domain is actually the same of the second configuration. More interesting results can be found investigating higher orders of negativity, since $X \neq X^{-1}$ if $k \neq 2$. Last we can observe that the value of the minimal Hamiltonian is equal to the number of links that cross the domain wall. For higher orders such equality is lost, but a proportionality still holds, thus allowing us to find a formula that directly relate the value of the Hamiltonian to the number of links crossing domain wall.

k=3 The permutation group S_3 has $3! = 6$ elements (identity, three swaps, cyclic and anticyclic):

$$S_3 = \{\mathbb{1} = (1)(2)(3), S_{12} = (12)(3), S_{13} = (13)(2), S_{23} = (1)(23), X = (123), X^{-1} = (321)\} \quad (5.92)$$

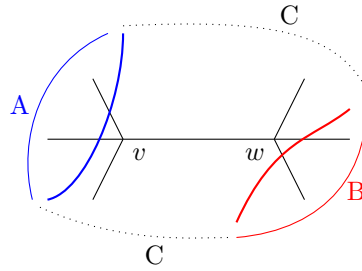
Cyclic and anticyclic permutations are now different. Using the relations (5.38) we can write some preliminary calculations on the distances:

$$d(\mathbb{1}, X) = k-1 = 2 \quad d(\mathbb{1}, X^{-1}) = k-1 = 2 \quad d(X, X^{-1}) = k-1 = 2 \quad (\text{odd } k) \quad (5.93)$$

Now we can compute the Hamiltonian for some more configuration, emerging from the six possible "spin" that can be attached to vertices. To lighten the notation, we will only write the non-vanishing terms of the Hamiltonian.

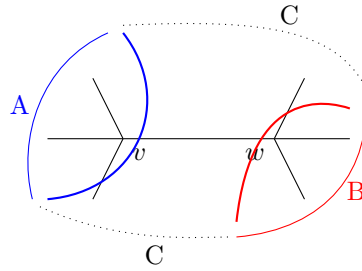
1. $g_v = g_w = \mathbb{1}, \rightarrow v, w \in C$

$$\mathcal{H}_3 = 2d(\mathbb{1}, X) + 2d(\mathbb{1}, X^{-1}) = 8 \quad (5.94)$$



2. $g_v = X, g_w = X^{-1} \rightarrow v \in A, w \in B$

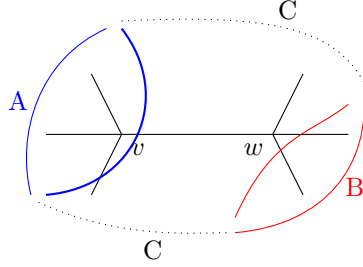
$$\mathcal{H}_3 = d(X, X^{-1}) + d(X, \mathbb{1}) + d(X^{-1}, \mathbb{1}) = 6 \quad (5.95)$$



This time the two domain remain separated since the two permutations are different.

3. $g_v = X, g_w = \mathbb{1} \rightarrow v \in A, w \in C$

$$\mathcal{H}_3 = d(X, \mathbb{1}) + 2d(\mathbb{1}, X^{-1}) + d(X, \mathbb{1}) = 8 \quad (5.96)$$



4. According to (5.43) we know that the set of permutations that are a geodesic for both $\mathbb{1}, X$ and X^{-1} is given by Non Crossing Pairings. As previously stated, NCP must *only* contain blocks of length two plus (possible) a *single* block of length one. In S_3 there are three NCP, given by the three Swap Operator S_{12}, S_{23} and S_{13} . We denote by τ a generic NCP, and, using the results in (5.43) we can calculate the value of the Hamiltonian of the configuration with Swap operators in the bulk vertices v and w . In fact:

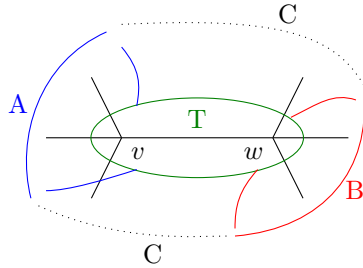
$$\begin{aligned} d(\mathbb{1}, \tau) &= 1 \\ d(X, \tau) &= d(X^{-1}, \tau) = 1 \end{aligned}$$

These permutations define a new intermediate domain in the bulk that we can call *transition domain* (T).

$$g_v = g_w = \tau \rightarrow v, w \in T$$

$$\mathcal{H}_3 = 2d(\tau, X) + 2d(\tau, X^{-1}) + 2d(\tau, \mathbb{1}) = 6 \quad (5.97)$$

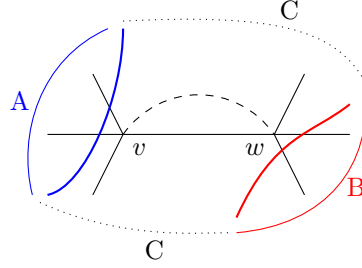
Such domain delimits the bulk region, preventing domain walls to enter the bulk:



Already at this level, differences with the previous case $k = 2$ can be noted. However to make them even more evident we can insert bulk correlations, repeat the analysis and sum up some concrete results.

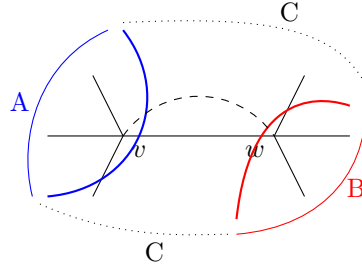
1. $g_v = g_w = \mathbb{1}, \rightarrow v, w \in C$

$$\mathcal{H}_3^c = 2d(\mathbb{1}, X) + 2d(\mathbb{1}, X^{-1}) = 8 \quad (5.98)$$



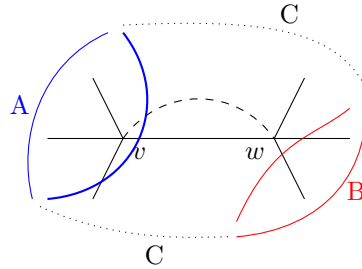
2. $g_v = X, g_w = X^{-1} \rightarrow v \in A, w \in B$

$$\mathcal{H}_3^c = 2d(X, X^{-1}) + d(X, \mathbb{1}) + d(X^{-1}, \mathbb{1}) = 8 \quad (5.99)$$



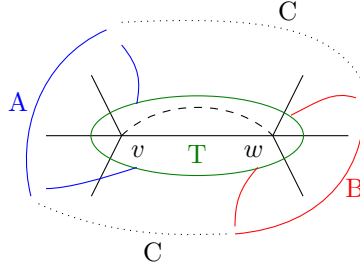
3. $g_v = X, g_w = \mathbb{1} \rightarrow v \in A, w \in C$

$$\mathcal{H}_3^c = 2d(X, \mathbb{1}) + 2d(\mathbb{1}, X^{-1}) + d(X, \mathbb{1}) = 10 \quad (5.100)$$



4. $g_v = g_w = \tau \rightarrow v, w \in T$

$$\mathcal{H}_3^c = 2d(\tau, X) + 2d(\tau, X^{-1}) + 2d(\tau, \mathbb{1}) = 6 \quad (5.101)$$



Now it is even more evident that the role of bulk correlation is to increase the value of the Hamiltonian in the configurations with different permutations on correlated vertices. Like it has been said in the case $k = 2$, such values depend on the number of link crossing the domain walls, that glue vertices in different domains. Because of the link-wise nature on the correlations we are considering, we also mentioned that those correlations can be drawn as additional links (the dashed ones). Hence it is clear that if we have the same permutation on two vertices, their interaction will give a contribution to the Hamiltonian that will vanish both in the link term as in the bulk term of (5.88). This results also stress a strong similarity with the discussions in [16], mentioned in the previous chapter (4.53): if the bulk entropy vanishes (i.e. there is no correlations between intertwiners) the minimal value of Hamiltonian is 6, and both configurations (2) and (4) have this value; in this sense we have a *degenerate minimum value* of \mathcal{H}_3 . However this degeneracy is lost if we insert bulk correlations: in fact, interpreting these correlations as links and *assuming the proportionality* between \mathcal{H} and the number of link crossing the domain walls, we can see that the second configuration has an higher energy cost because of the additional link, crossing both domain wall of A and B. Conversely, the transition domain T, is filled up by the same permutation on the two vertices, the domain wall is pushed out of the bulk region, the additional link does not cross any domain wall, hence the Hamiltonian is left untouched and becomes the *unique* minimum. Last we can discuss another detail that has been neglected on purpose in this analysis in view of the results already mentioned: if we consider the uncorrelated Hamiltonian, actually there are much more degenerate configurations with the same value of $\mathcal{H}_3 = 6$. In particular if we consider a transition domain including *only one vertex*, while the other one belongs to the domain of any other region and repeat the calculations, we can notice that the values of the Hamiltonian associated to all these configurations is still 6. However, since vertices belong to different domains, including correlations naturally eliminates all of these degeneracies. So all these configurations do not need to be discussed at all, since their behavior is the same of (2).

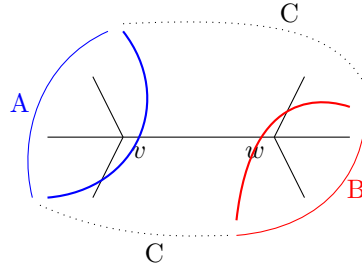
k=4 The permutation group S_4 has $4! = 24$ elements. We can focus on the set of permutations we are going to use in the calculation of \mathcal{H}_4 :

$$\begin{aligned} X &= (1234) & X^{-1} &= (4321) & \mathbb{1} &= (1)(2)(3)(4) \\ \tau &= (12)(34), (14)(23) \\ d(\mathbb{1}, X) &= d(\mathbb{1}, X^{-1}) = 4 - 1 = 3 \\ d(X, X^{-1}) &= 4 - 2 = 2 \\ d(\mathbb{1}, \tau) &= \left\lfloor \frac{4}{2} \right\rfloor = 2 \\ d(\tau, X) &= d(\tau, X^{-1}) = \left\lceil \frac{4}{2} \right\rceil - 1 = 1 \end{aligned}$$

In line with the results obtained so far, we can focus on the two degenerate minimal configurations:

1. $g_v = X, g_w = X^{-1} \rightarrow v \in A, w \in B$

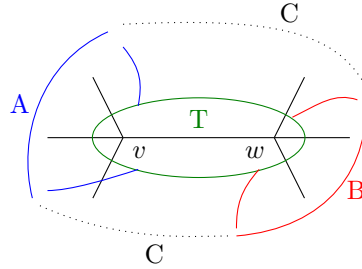
$$\mathcal{H}_4 = d(X, X^{-1}) + d(X, \mathbb{1}) + d(X^{-1}, \mathbb{1}) = 8 \quad (5.102)$$



2. The set of Non Crossing Pairings is made up by permutations with two blocks of length two. In S_4 there are two NCP, given by $S_{12}S_{34}$ and $S_{14}S_{23}$. Denoting by τ such permutations:

$$g_v = g_w = \tau \rightarrow v, w \in T$$

$$\mathcal{H}_4 = 2d(\tau, X) + 2d(\tau, X^{-1}) + 2d(\tau, \mathbb{1}) = 8 \quad (5.103)$$

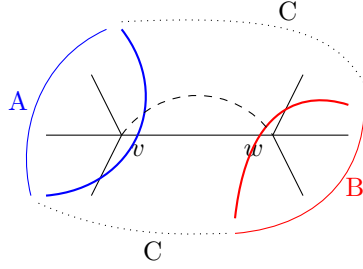


5.4. GENERALIZED ISING MODEL FOR RÉNYI k -TH NEGATIVITY 111

Considering again bulk correlations we have:

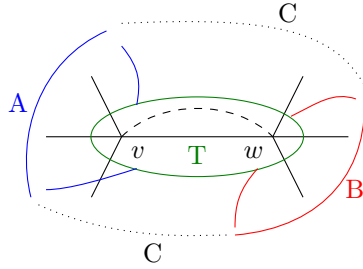
1. $g_v = X, g_w = X^{-1} \rightarrow v \in A, w \in B$

$$\mathcal{H}_4 = 2d(X, X^{-1}) + d(X, \mathbb{1}) + d(X^{-1}, \mathbb{1}) = 10 \quad (5.104)$$



2. $g_v = g_w = \tau \rightarrow v, w \in T$

$$\mathcal{H}_4 = 2d(\tau, X) + 2d(\tau, X^{-1}) + 2d(\tau, \mathbb{1}) = 8 \quad (5.105)$$



All the discussions about \mathcal{H}_3 still hold for \mathcal{H}_4 :

- bulk correlations increase the value of the Hamiltonian of the configuration with vertices in different domains;
- degeneracies of minimal Hamiltonian is removed by such correlations;
- the lowest energy configuration is characterized by a *transition domain* filling the bulk: in this configuration, the domain walls are pushed out of the bulk similarly to [16]. This configuration is associated to the largest contribution of the Ising action in the large dimension limit;

Looking at all the different values of the Hamiltonian, it is clear that it scales both with the number of links crossing the domain walls and with the order of H . In fact, the same configuration assumes larger and larger values of \mathcal{H}_k with increasing k . Moreover our results perfectly fit the formula (C.3) in [5],

referring to the lower bound of the energy for a given spin configuration of a random tensor network. We can thus write the same formula relating the values of the hamiltonian of our Ising model to the number of link crossing each domain wall, namely $|\gamma_A|$, $|\gamma_B|$ and $|\gamma_C|$:

$$\mathcal{H}_k = \begin{cases} \frac{k-1}{2} (|\gamma_A| + |\gamma_B| + |\gamma_C|) & \text{odd} \\ (\frac{k}{2} - 1) (|\gamma_A| + |\gamma_B|) + \frac{k}{2} |\gamma_C| & \text{even} \end{cases} \quad (5.106)$$

The action is thus given by:

$$A_k = \beta \mathcal{H}_k = \beta \begin{cases} \frac{k-1}{2} (|\gamma_A| + |\gamma_B| + |\gamma_C|) & \text{odd} \\ (\frac{k}{2} - 1) (|\gamma_A| + |\gamma_B|) + \frac{k}{2} |\gamma_C| & \text{even} \end{cases} \quad (5.107)$$

The partition function \overline{Z}_k is dominated by the lowest energy configuration term, which is unique if we have bulk correlations:

$$\overline{Z}_k = \sum_{\{g_v\}} e^{-\beta \mathcal{H}_k} = e^{-\beta \mathcal{H}_k^{(\min)}} \quad (5.108)$$

Recalling the negativity formula:

$$\overline{N}_k = \frac{\overline{Z}_k}{Z_0} \quad (5.109)$$

if we call \mathcal{H}_0 the hamiltonian of the denominator (i.e. the situation where all the permutation are switched with the identity (namely we trace out the whole boundary) we can write the average k -th Rényi negativity as follows:

$$\overline{N}_k = \frac{e^{-\beta \mathcal{H}_k^{(\min)}[g_v \in S_k]}}{\sum_{g_v \in S_k} e^{-\beta \mathcal{H}_0[g_v \in S_k]}} = \mathcal{P}_\beta(g_v) \quad (5.110)$$

where $P_\beta(g_v)$ is the *configuration probability* of a classical Ising model and is actually a Boltzman distribution with inverse temperature parameter $\beta = \log d$. We could say that the configuration with minimal hamiltonian is the one with higher probability in the statistical model. Since $\beta = \log d \gg 1$, the *temperature* associated $T = \frac{1}{K_B \beta} \ll 1$.

We can now calculate log negativity as

$$\log \overline{N}_k = \log \overline{Z}_k - \log \overline{Z}_0 \quad (5.111)$$

Looking at $\mathcal{H}_0 = \sum_L d(g_v, g_w) + \sum_{\partial\gamma} d(\mathbb{1}, g_v)$ we notice that its minimal value is 0, corresponding to the configuration with all vertex labeled by the identity permutation. So we have

$$\overline{Z}_0 = \sum_{\{g_v\}} e^{-\beta \mathcal{H}_0} \simeq e^0 = 1 \quad (5.112)$$

Therefore, the log Rényi negativity can be written as

$$\log \bar{N}_k = \log \bar{Z}_k = -\beta \mathcal{H}_k^{(\min)} \quad (5.113)$$

By using the definition of free energy for Ising model,

$$\mathcal{F} = -\frac{1}{\beta} \log Z \rightarrow \log \bar{Z}_k = -\beta \mathcal{F}_k \rightarrow \mathcal{F}_k = \mathcal{H}_k^{(\min)} \quad (5.114)$$

we can identify the free energy of the Ising model with the minimal value of the Hamiltonian, expressed in term of the geometric areas of the domain wall.

Eventually, we can derive a general expression for the log negativity of a tripartite boundary region of a spin network as the analytic continuation of logarithm of the even momenta. We get

$$\log \bar{N} = \lim_{k \rightarrow \frac{1}{2}} \log \bar{N}_{2k} = -\beta \lim_{k \rightarrow \frac{1}{2}} \mathcal{H}_{2k} = \beta \left[\frac{1}{2} (|\gamma_A| + |\gamma_B|) - \frac{1}{2} |\gamma_C| \right] \quad (5.115)$$

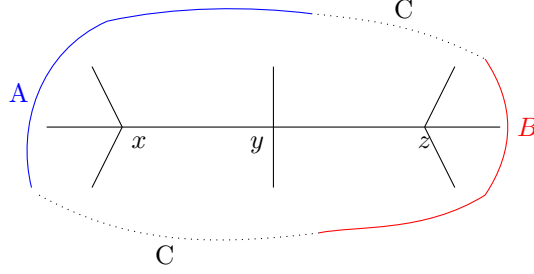
This is the main result of the Thesis. The entanglement entropy of a multipartite induced mixed state is quantified via log negativity and it scales with the areas of the domain walls spreading into the bulk region. In particular log negativity is affected by the bulk data, both by its combinatorial structure as by the quantum correlations between intertwiners. A similar result, has been recently pointed out in recent works [12, 16] regarding 2-nd Rényi entropy for a pure bipartite random spin network.

The same area scaling behavior has been obtained in the random tensor network framework [5], where the right-hand term of the (5.115) is the *quantum mutual information* $I_{A:B}$ of the two subsystems. In our case, in the domain of the third region $\gamma_C = (\gamma_A \cup \gamma_B)^c = \gamma_{AB}$ and we have the equality $\beta |\gamma_C| = S_{AB}$. By inserting quantum correlations among intertwiners we removed the degeneracies of $\mathcal{H}^{(\min)}$ and a new intermediate region (the *transition region* T) fill the bulk, thus fixing the domains of the three region. In particular γ_C can be seen as the complementary of the two remaining regions, and log negativity can be written as the mutual information between A and B. In this term, typical value of log negativity is given by

$$\log \bar{N}_{AB} = \frac{1}{2} [S_A + S_B - S_{AB}] \quad (5.116)$$

A further confirmation of such area scaling behavior can be seen studying a more complicated graph, with more vertices. In particular we will focus on a graph with three vertices and the effects of adding non-local correlations among intertwiners.

Three vertices graph Consider a graph γ composed by three tetravalent vertices x, y and z :

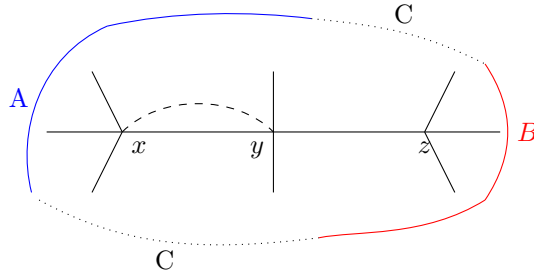


Beside the structural bulk correlation due to the two link xy and yz , we can insert bulk correlations between intertwiner. We will consider link-wise correlations, so that only one couple of intertwiners will be correlated. This simple case allows us to deal with the topic of *non-local* correlations. In fact we can insert a link-wise correlator among the intertwiner of two vertices that are not directly connected by a link, namely x and z . We will study the difference between local and non local correlations at different order of negativity, starting by the uncorrelated Hamiltonian

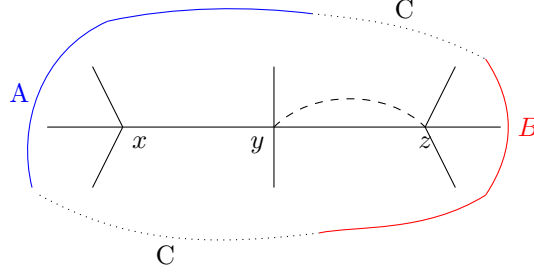
$$\begin{aligned} \mathcal{H}_k &= d(g_x, g_y) + d(g_y, g_z) + 2d(g_x, X) + d(g_y, X) \\ &+ d(g_x, \mathbb{1}) + d(g_y, \mathbb{1}) + d(g_z, \mathbb{1}) + 2d(g_z, X^{-1}) \end{aligned} \quad (5.117)$$

corresponding to the picture above. If we insert local correlations between adjacent pairs (xy and yz) the Hamiltonians become

$$\begin{aligned} \mathcal{H}_k^{(xy)} &= 2d(g_x, g_y) + d(g_y, g_z) + 2d(g_x, X) + d(g_y, X) \\ &+ d(g_x, \mathbb{1}) + d(g_y, \mathbb{1}) + d(g_z, \mathbb{1}) + 2d(g_z, X^{-1}) \end{aligned} \quad (5.118)$$

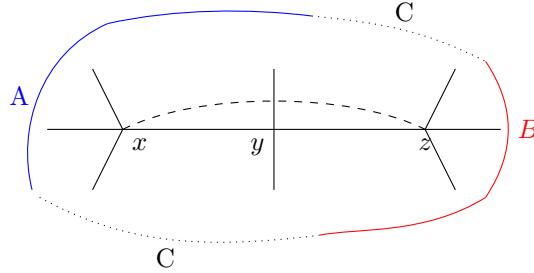


$$\begin{aligned} \mathcal{H}_k^{(yz)} &= d(g_x, g_y) + 2d(g_y, g_z) + 2d(g_x, X) + d(g_y, X) \\ &+ d(g_x, \mathbb{1}) + d(g_y, \mathbb{1}) + d(g_z, \mathbb{1}) + 2d(g_z, X^{-1}) \end{aligned} \quad (5.119)$$



Inserting bulk non-local correlations the Hamiltonian is modified by adding a new term $d(g_x, g_z)$ and graphically we can represent such correlation similarly to the previous ones.

$$\begin{aligned} \mathcal{H}_k^{(xz)} &= d(g_x, g_y) + d(g_y, g_z) + d(g_x, g_z) + 2d(g_x, X) + d(g_y, X) \\ &+ d(g_x, \mathbb{1}) + d(g_y, \mathbb{1}) + d(g_z, \mathbb{1}) + 2d(g_z, X^{-1}) \end{aligned} \quad (5.120)$$



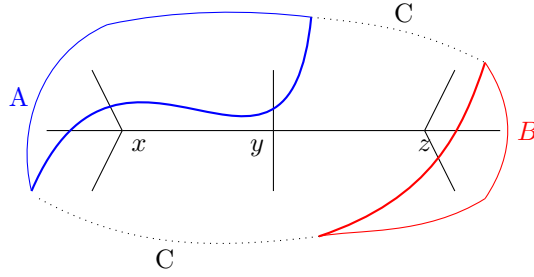
As we pointed out in the previous analysis, Rényi second negativity does not exhibit any relevant result, hence we will begin our investigation starting from the third order Hamiltonian.

Moreover, since we are dealing with a more complex graph, there are much more different spin configurations associated with all the possible ways in which domains can spread within the bulk. To simplify the analysis we will only discuss the relevant ones representing low energy configurations very close to the minimal value of the Hamiltonian and the degenerate configurations of the latter.

k=3 Using the relations on distances in (5.93) we can easily repeat the calculation for the following configurations:

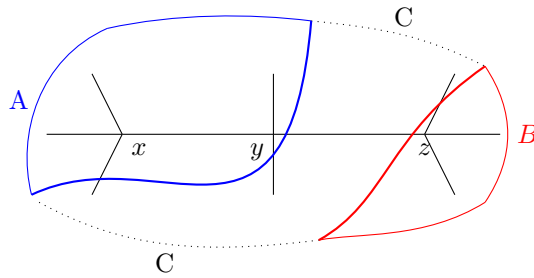
1. $g_x = g_y = g_z = \mathbb{1}, \rightarrow x, y, z \in C$

$$\mathcal{H}_3 = 2d(\mathbb{1}, X) + d(\mathbb{1}, X) + 2d(\mathbb{1}, X^{-1}) = 10 \quad (5.121)$$



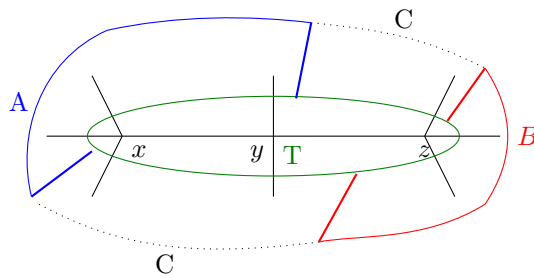
2. $g_x = g_y = X, g_z = X^{-1} \rightarrow x, y \in A, z \in B$

$$\mathcal{H}_3 = d(g_y, g_z) + d(\mathbb{1}, X) + d(\mathbb{1}, X) + d(\mathbb{1}, X^{-1}) = 8 \quad (5.122)$$



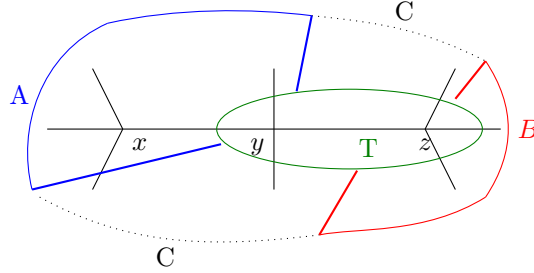
3. $g_x = g_y = g_z = \tau \rightarrow x, y, z \in T$

$$\mathcal{H}_3 = 2d(\tau, X) + d(\tau, X) + 3d(\mathbb{1}, \tau) + 2d(\tau, X^{-1}) = 8 \quad (5.123)$$



4. $g_x = X, g_y = g_z = \tau \rightarrow x \in A, y, z \in T$

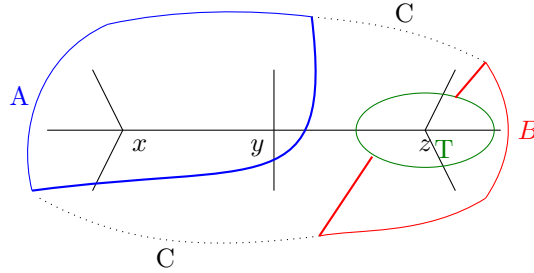
$$\mathcal{H}_3 = 2d(\tau, X) + d(\mathbb{1}, X) + 2d(\mathbb{1}, \tau) + 2d(\tau, X) = 8 \quad (5.124)$$



The configuration with x and y in T exhibit the same value of \mathcal{H}_3 .

5. $g_x = g_y = X, g_z = \tau \rightarrow x, y \in A, z \in T$

$$\begin{aligned} \mathcal{H}_3 &= d(\tau, X) + d(\tau, X^{-1}) + \\ &+ d(X, \tau) + d(\mathbb{1}, X) + d(\tau, X) + d(X^{-1}, \mathbb{1}) = 8 \end{aligned} \quad (5.125)$$



The configurations with x or y in T exhibit the same value of \mathcal{H}_3 .

Now we will see that *if we insert a bulk with local correlations between adjacent vertices (xy or yz) only some degenerations are removed*. In fact, consider the case with a bulk correlation between x and y : the Hamiltonian has an additional term that increases its value only if the vertices x and y belong to different domains, i.e. the distance between the permutations g_x and g_y is not vanishing.

The configurations (1), (2), (3) are left untouched, since the two spin variables in x and y are the same. The Hamiltonians of (4) and (5) must be discussed. As we pointed out (4) actually corresponds to three different degenerate configurations with $\mathcal{H}_3 = 8$: the ones with the transition region filling only a couple of vertices of the bulk, e.g. xy, yz and xz . The first of these configurations will have a vanishing contribution from the bulk link insertion, so one of these degeneracies will not be eliminated.

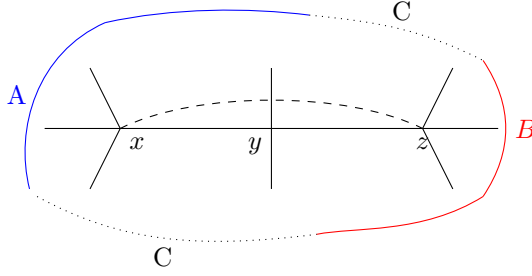
The same result holds for (5), since we have the three cases with the transition region only filling one vertex in the bulk; it is now clear that the configuration with $z \in T$ and $x, y \in A$ will still have $\mathcal{H}_3 = 8$.

Consider now the other possibility of local correlation, i.e. the couple yz . The Hamiltonians of the configurations (1) and (3) remain the same. The Hamiltonian of second one (2) becomes:

$$\mathcal{H}_3 = 8 + d(X, X^{-1}) = 10 \tag{5.126}$$

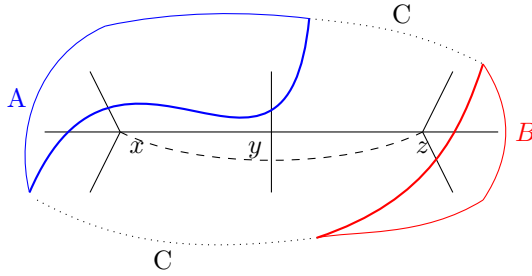
Similarly to the previous case, the degenerate configurations with pair of vertices in the transition regions are *partially* removed: xy and xz increase by 1 while $\mathcal{H}_3^{(yz)} = 8$.

The same result (degeneracy partially removed) goes for the configurations with the transition region filling only one vertex. We can only insert one type of *non-local correlation* in this graph, that is the xz one



We can study the effect of such correlation on the different configurations.

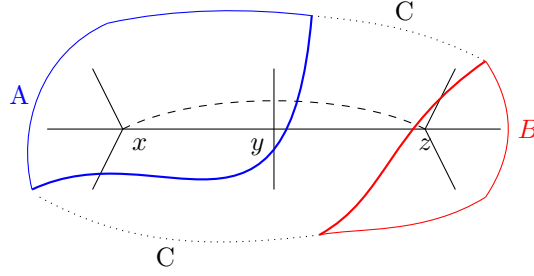
1. The first configuration is certainly not minimal one. Even if this correlation left in unchanged, $\mathcal{H}_3 = 10 > 8$.



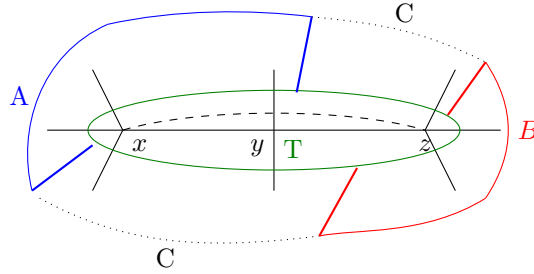
2. $g_x = g_y = X, g_z = X^{-1} \rightarrow x, y \in A, z \in B$

$$\begin{aligned} \mathcal{H}_3 &= d(g_y, g_z) + d(g_x, g_z) + \\ &+ d(\mathbb{1}, X) + d(\mathbb{1}, X) + d(\mathbb{1}, X^{-1}) = 10 \end{aligned} \tag{5.127}$$

5.4. GENERALIZED ISING MODEL FOR RÉNYI K-TH NEGATIVITY 119

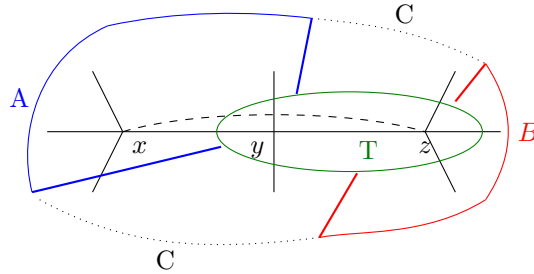


3. $g_x = g_y = g_z = \tau \rightarrow x, y, z \in T$
 $\mathcal{H}_3 = 2d(\tau, X) + d(\tau, X) + 3d(\mathbb{1}, \tau) + 2d(\tau, X^{-1}) = 8$ (5.128)

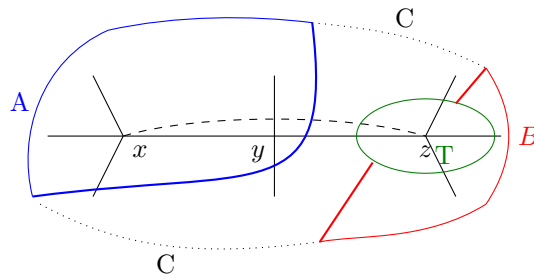


The configuration with the transition region filling the whole bulk remain unchanged.

4. $g_x = X, g_y = g_z = \tau \rightarrow x \in A, y, z \in T$
 $\mathcal{H}_3 = 2d(\tau, X) + d(\mathbb{1}, X) + 2d(\mathbb{1}, \tau) + 2d(\tau, X) + d(X, \tau) = 9$ (5.129)



5. $g_x = g_y = X, g_z = \tau \rightarrow x, y \in A, z \in T$
 $\mathcal{H}_3 = d(\tau, X) + d(\tau, X^{-1})$
 $+ d(X, \tau) + d(\mathbb{1}, X) + d(\tau, X)$
 $+ d(X^{-1}, \mathbb{1}) + d(X, \tau) = 9$ (5.130)



The lowest energy configuration is (3). Once again the dominant term is given by the configuration with the transition region filling the whole bulk and domain walls pushed out of the bulk.

The same analysis on fourth order Hamiltonian gives back exactly the same results: local correlations partially remove degeneracies of lowest energy configuration, while non-local correlation prevents the domain to enter the bulk, thus fixing a single area configuration as the minimal one.

Chapter 6

Discussion

Let us first spend a few words on the results of the previous chapter. The study of log negativity allowed us to formulate a description of entanglement-area correspondence in the framework of spin network states associated to quantum states of 3-d spatial geometry; we found a relation between log negativity and areas of the domain walls of the generalised Ising model built on a tripartite boundary of a spin network state, which gets modified by the insertion of a bulk realised in terms of Bell-like pairwise correlations between intertwiner states in the graph.

In particular, we have studied the case of a two-vertices and a three-vertices graph, with the aim of shedding light on the difference between local and non-local correlations. In both situations a transition domain T arises, preventing the domain wall to enter the bulk region. The configuration with such domain characterizes the minimal energy configurations of each order of the Ising model. For such configurations, we could identify the domain C as the complementary boundary region to the union of A and B , thereby identifying typical log negativity as the half the quantum mutual information between the two subsystem A and B .

Despite the expected behaviour of the results found, since all the degeneracies are eliminated and the calculation of log negativity is extremely simple in this situation, we have to take into account the fact that in a more complex graph, non-locality could have no more the same effect: indeed, by looking at such correlations as additional link (beside their different nature), the connectivity of the three-vertices graph we analysed is such that the additional link between vertices x and z spreads through all the graph, intersecting the domain walls of both A and B ; both if we consider a graph with more vertices or using a different tri-partition of the boundary, even non-local correlations could be not strong enough to push the domain walls out of the bulk, so that not all the degeneracy could be eliminated. In this sense, non-local correlations must be further investigated in graph with an arbitrary number of vertices in order to provide a deeper understanding of their role in the statistical method and their physical interpretation.

Actually the statistical analysis we conducted (leading to (5.115)) is still valid if we have degeneracies of the lowest energy configuration. Similarly to previous results in recent work [5], we obtain

$$\log \bar{N} = \lim_{k \rightarrow \frac{1}{2}} \log \overline{\mathcal{N}_{2k}} = \lim_{k \rightarrow \frac{1}{2}} [\mathcal{D}_k \beta \mathcal{H}_{2k}] = \mathcal{D} \beta \left[\frac{1}{2} (|\gamma_A| + |\gamma_B|) - \frac{1}{2} |\gamma_C| \right] \quad (6.1)$$

Where \mathcal{D}_k is the number of degenerate spins configurations for each order of negativity k . Such number should depend on both the negativity order and on the number of vertices and on the connectivity and on possible local or non-local correlations, so its $k \rightarrow \frac{1}{2}$ limit (that we denoted by \mathcal{D}) seems to be actually difficult to compute in the general case.

Some further considerations can be made on the thermodynamic aspects of our model. Even if we used a *statistical model*, the equation (5.110) (Boltzman distribution) suggest an *equilibrium condition* on the system; hence we are led to imagine that a (macroscopic) thermodynamic regime could emerge from this analysis.

Indeed, if we reconsider the partition function \overline{Z}_k within the homogeneous-spin assumption, we can think of the state as a system at equilibrium and calculate the internal energy of the system intended as a closed thermodynamic. We get

$$U = -\partial_\beta \log Z \rightarrow U_k = -\partial_\beta (-\beta \mathcal{H}_k^{(\min)}) = \mathcal{H}_k^{(\min)} \quad (6.2)$$

Looking at (5.114) we understand that, in this regime, the change of free energy of the system is equal to the change of its internal energy. This relation can also be obtained via Legendre transformation:

$$\mathcal{F} = U - TS \quad (6.3)$$

Since we are in the low temperature regime, we can consider the second term negligible and confirm the previous equality. Now we can use the first law of thermodynamics,

$$U = Q - L \quad (6.4)$$

and interpret Q as a form of *heat* that is transferred during the transformation when bodies with different temperature "interact". In the homogeneous case, since $\beta = \text{const}$ we can assume Q to be equal to 0 (heat effect could appear in the non-homogeneous case).

Nevertheless, we are improperly using terms such as energy and temperature, that rather refers to geometrical quantities associated to a portion of space-time, whose boundary areas spread inside the bulk. In our model, we have already seen that the concept of *Energy* is associated to the way the areas enter the bulk, while the dimensions of the Hilbert spaces of the graph edges components ($\beta = \log d$) play the role of a *Temperature* in the statistical model, thus encoding the thermal agitation of quantum *space atoms* via its structural (links and semilinks, i.e. areas) and internal (intertwiners, i.e. volumes) dimensions.

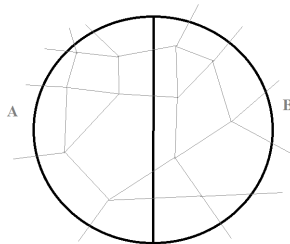


Figure 6.1: A-B bipartition of a (pure) boundary state of a quantum spin networks associated to a ball of 3-d space.

As we said before, in the analysis of homogeneous networks with *fixed areas*, which corresponds to a system with constant temperature, the internal energy of the system is thus only consisting of the *work term*

$$\frac{1}{\beta} \log \bar{N}_\beta = \left[\frac{1}{2} (|\gamma_A| + |\gamma_B|) - \frac{1}{2} |\gamma_C| \right] = -\mathcal{F}_\beta = -U_\beta = L_\beta \quad (6.5)$$

For an isothermal transformation such work term can be calculated as

$$L_\beta = nRT(\beta) \log \left(\frac{V_B}{V_A} \right) \quad (6.6)$$

Following the same procedure for switching from statistical mechanics to thermodynamics, all the above quantities need to be interpreted in a geometrical framework related to semi-classical regime of a quantum gravity theory. In this sense, we could imagine the hypothesis of an *isobaric transformation* such that

$$L_\beta = p\Delta V_\beta$$

particularly, since the work term is proportional to the area deformation, this argument could be read as a relation between volumes' transformation and areas' transformation with the pressure term being a proportionality coefficient that exhibit the *inertia* of space to change its volume after areas' deformations induced by connectivity and quantum correlations. These speculative deductions require further investigations and a more complete theory and phenomenology of gravitational field at quantum level.

Finally, we shall consider the study of the phase transition of the negativity for the AB reduced boundary state, as a function of the ratios between the dimensions of the different subsystems (i.e., one of the subsystems much larger than the remaining ones, along with the results in [17]. In particular, the entanglement can measure the capacity of the environment (e.g. the subsystem C) to thermalize the system (e.g. the AB reduced state), making it eventually separable. Such analysis is extremely interesting in relation to the possibility to model quantum black hole like regions of 3-d space in terms of spin networks.

In this framework, the *random character* of spin networks plays a key role in simulating the effects of the gravitational dynamics on a microscopical scale via a strongly interacting chaotic quantum system: recent developments suggest that scrambling of the quantum information and the emergence of thermalization as a result of dynamics in a closed quantum system are closely related. The typical situation that occurs in the study of quantum system requires to trace out the environment, thus taking into account the effects of loss of information from a system into the environment, since every system is loosely coupled with the energetic state of its surroundings. Such a phenomenon is known as *quantum decoherence* and the loss of information is quantified via entanglement between the system and environment.

A similar situation occurs in [44, 16, 3], where a bounded region of a 3-d slice of space is considered using spin network formalism. In these cases, it is possible to calculate the quantum correlations through the region using a bipartition of the associated boundary state, see Fig. 6.1.

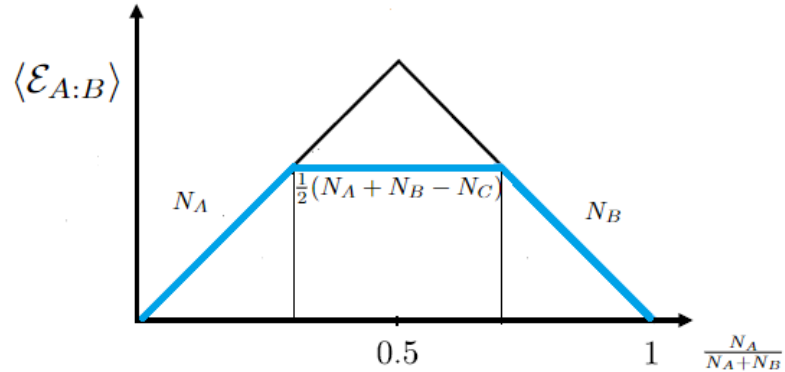
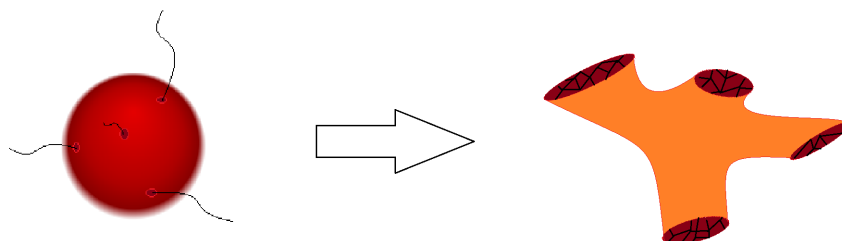


Figure 6.2: Page curve behaviour for a tripartite pure quantum system.

However, if we consider the correlations a system (S) has with its environment (eventually the rest of all the space in the whole universe) and we want to investigate the quantum correlations on two subregions A and B of S, we must trace out the environment, thus necessarily dealing with a mixed state for AB. Moving a step in this direction is the main contribution of our Thesis work with respect to the discussed literature. The ability of the environment to thermalize the system can be quantified via negativity measure for such tripartite mixed state. This analysis has to take into account the ratios between the dimensions of the three subsystems. In particular we can focus on the deformation of the *Page curve* relating the entanglement entropy between two subsystems to the dimensions of the two Hilbert spaces. The presence of a third region modifies this curve [17], so that there exist both an intermediate region in which

entanglement entropy is constant and a region in which entanglement entropy vanishes so that the state is separable in the regime of large dimension of the environment subsystem (see Fig. 6.2).

The study of this regimes could be a useful tool to develop a toy model for a quantum black hole if we consider additional degrees of freedom related to closure defects of spin network vertex states.



Last, these methods can be implemented in spinfoam model if we generalize all the previous discussions already to one higher dimension. Rather than considering a 3-d manifold associated to a spin-network, whose accessible degrees of freedom are external legs pointing out of the bulk region, we could deal with a 4-d model of space-time manifold considering external degrees of freedom given by spin network graph on the boundary subregions. Such approach could simulate the dynamical behaviour of geometry in presence of gravity in a 4-d manifold, allowing for a more precise study of the evolution of the quantum correlations in a concrete model of of quantum space time.

Bibliography

- [1] Veronika E Hubeny. “The AdS/CFT correspondence”. In: *Classical and Quantum Gravity* 32.12 (June 2015), p. 124010. DOI: 10.1088/0264-9381/32/12/124010. URL: <https://doi.org/10.1088/0264-9381/32/12/124010> (cit. on pp. 5, 74).
- [2] Shinsei Ryu and Tadashi Takayanagi. “Holographic derivation of entanglement entropy from AdS/CFT”. In: *Phys. Rev. Lett.* 96 (2006), p. 181602. DOI: 10.1103/PhysRevLett.96.181602. arXiv: hep-th/0603001 (cit. on pp. 5, 74).
- [3] Eugenia Colafranceschi, Goffredo Chirco, and Daniele Oriti. “Holographic maps from quantum gravity states as tensor networks”. In: *Phys. Rev. D* 105.6 (2022), p. 066005. DOI: 10.1103/PhysRevD.105.066005. arXiv: 2105.06454 [hep-th] (cit. on pp. 5, 59, 61–63, 65–68, 70–72, 93, 124).
- [4] Jonah Kudler-Flam, Vladimir Narovlansky, and Shinsei Ryu. “Negativity spectra in random tensor networks and holography”. In: *JHEP* 02 (2022), p. 076. DOI: 10.1007/JHEP02(2022)076. arXiv: 2109.02649 [hep-th] (cit. on pp. 5, 6, 79, 81–83).
- [5] Xi Dong, Xiao-Liang Qi, and Michael Walter. “Holographic entanglement negativity and replica symmetry breaking”. In: *JHEP* 06 (2021), p. 024. DOI: 10.1007/JHEP06(2021)024. arXiv: 2101.11029 [hep-th] (cit. on pp. 5, 6, 81, 91, 95, 97, 98, 111, 113, 122).
- [6] Pietro Doná and Simone Speziale. *Introductory lectures to loop quantum gravity*. 2010. DOI: 10.48550/ARXIV.1007.0402. URL: <https://arxiv.org/abs/1007.0402> (cit. on pp. 5, 9, 18, 21, 23, 24, 32, 34).
- [7] Carlo Rovelli and Francesca Vidotto. *Covariant Loop Quantum Gravity*. Cambridge University Press, 2014. DOI: <https://doi.org/10.1017/CB09781107706910> (cit. on pp. 5, 9, 12).
- [8] William Donnelly. “Entanglement entropy in loop quantum gravity”. In: *Phys. Rev. D* 77 (2008), p. 104006. DOI: 10.1103/PhysRevD.77.104006. arXiv: 0802.0880 [gr-qc] (cit. on pp. 5, 51, 56).

- [9] Fabio Anzà and Goffredo Chirco. “Typicality in spin-network states of quantum geometry”. In: *Phys. Rev. D* 94.8 (2016), p. 084047. DOI: 10.1103/PhysRevD.94.084047. arXiv: 1605.04946 [gr-qc] (cit. on pp. 5, 51, 56).
- [10] Xi Dong. “The Gravity Dual of Renyi Entropy”. In: *Nature Commun.* 7 (2016), p. 12472. DOI: 10.1038/ncomms12472. arXiv: 1601.06788 [hep-th] (cit. on pp. 5, 50, 81).
- [11] Goffredo Chirco, Daniele Oriti, and Mingyi Zhang. “Group field theory and tensor networks: towards a Ryu–Takayanagi formula in full quantum gravity”. In: *Class. Quant. Grav.* 35.11 (2018), p. 115011. DOI: 10.1088/1361-6382/aabf55. arXiv: 1701.01383 [gr-qc] (cit. on pp. 5, 61–63).
- [12] Eugenia Colafranceschi and Daniele Oriti. “Quantum gravity states, entanglement graphs and second-quantized tensor networks”. In: *JHEP* 07 (2021), p. 052. DOI: 10.1007/JHEP07(2021)052. arXiv: 2012.12622 [hep-th] (cit. on pp. 5, 61–63, 113).
- [13] Etera R. Livine and Daniel R. Terno. *Reconstructing Quantum Geometry from Quantum Information: Area Renormalisation, Coarse-Graining and Entanglement on Spin Networks*. 2006. DOI: 10.48550/ARXIV.GR-QC/0603008. URL: <https://arxiv.org/abs/gr-qc/0603008> (cit. on p. 5).
- [14] Qian Chen and Etera R. Livine. *Intertwiner Entanglement Excitation and Holonomy Operator*. 2022. DOI: 10.48550/ARXIV.2204.03093. URL: <https://arxiv.org/abs/2204.03093> (cit. on pp. 5, 77).
- [15] Edward Witten. “Anti-de Sitter space and holography”. In: *Adv. Theor. Math. Phys.* 2 (1998), pp. 253–291. DOI: 10.4310/ATMP.1998.v2.n2.a2. arXiv: hep-th/9802150 (cit. on p. 5).
- [16] Goffredo Chirco, Eugenia Colafranceschi, and Daniele Oriti. “Bulk area law for boundary entanglement in spin network states: Entropy corrections and horizon-like regions from volume correlations”. In: *Phys. Rev. D* 105.4 (2022), p. 046018. DOI: 10.1103/PhysRevD.105.046018. arXiv: 2110.15166 [hep-th] (cit. on pp. 5–7, 59, 61–63, 70, 72, 75, 93, 101, 109, 111, 113, 124).
- [17] Hassan Shapourian et al. “Entanglement Negativity Spectrum of Random Mixed States: A Diagrammatic Approach”. In: *PRX Quantum* 2.3 (2021), p. 030347. DOI: 10.1103/PRXQuantum.2.030347. arXiv: 2011.01277 [cond-mat.str-el] (cit. on pp. 5, 6, 83, 87, 123, 124).
- [18] Jonah Kudler-Flam, Vladimir Narovlansky, and Shinsei Ryu. “Distinguishing Random and Black Hole Microstates”. In: *PRX Quantum* 2.4 (2021), p. 040340. DOI: 10.1103/PRXQuantum.2.040340. arXiv: 2108.00011 [hep-th] (cit. on pp. 6, 82, 83, 93, 95).
- [19] Michal Horodecki, Pawel Horodecki, and Ryszard Horodecki. “On the necessary and sufficient conditions for separability of mixed quantum states”. In: *Phys. Lett. A* 223 (1996), p. 1. DOI: 10.1016/S0375-9601(96)00706-2. arXiv: quant-ph/9605038 (cit. on pp. 6, 80).

- [20] Asher Peres. “Separability criterion for density matrices”. In: *Phys. Rev. Lett.* 77 (1996), pp. 1413–1415. DOI: 10.1103/PhysRevLett.77.1413. arXiv: quant-ph/9604005 (cit. on pp. 6, 80).
- [21] M. B. Plenio. “Logarithmic Negativity: A Full Entanglement Monotone That is not Convex”. In: *Phys. Rev. Lett.* 95.9 (2005), p. 090503. DOI: 10.1103/PhysRevLett.95.090503. arXiv: quant-ph/0505071 (cit. on pp. 6, 80).
- [22] Fabio M. Mele. *Quantum Metric and Entanglement on Spin Networks*. 2017. DOI: 10.48550/ARXIV.1703.06415. URL: <https://arxiv.org/abs/1703.06415> (cit. on pp. 9, 24, 33, 34, 37, 45, 46, 51, 54–56).
- [23] Stefan Davids. “Semiclassical limits of extended Racah coefficients”. In: *Journal of Mathematical Physics* 41.2 (2000), pp. 924–943. DOI: 10.1063/1.533171. eprint: {<https://doi.org/10.1063/1.533171>}. URL: <https://doi.org/10.1063/1.533171> (cit. on pp. 9, 35).
- [24] A. Barbieri. “Quantum tetrahedra and simplicial spin networks”. In: *Nucl. Phys. B* 518 (1998), pp. 714–728. DOI: 10.1016/S0550-3213(98)00093-5. arXiv: gr-qc/9707010 (cit. on pp. 9, 35).
- [25] John C. Baez and John W. Barrett. “The Quantum tetrahedron in three-dimensions and four-dimensions”. In: *Adv. Theor. Math. Phys.* 3 (1999), pp. 815–850. DOI: 10.4310/ATMP.1999.v3.n4.a3. arXiv: gr-qc/9903060 (cit. on pp. 9, 35–37).
- [26] R. Arnowitt, S. Deser, and C. W. Misner. “Dynamical Structure and Definition of Energy in General Relativity”. In: *Phys. Rev.* 116 (5 Dec. 1959), pp. 1322–1330. DOI: 10.1103/PhysRev.116.1322. URL: <https://link.aps.org/doi/10.1103/PhysRev.116.1322> (cit. on p. 11).
- [27] R. Arnowitt, S. Deser, and C. W. Misner. “Canonical Variables for General Relativity”. In: *Phys. Rev.* 117 (6 Mar. 1960), pp. 1595–1602. DOI: 10.1103/PhysRev.117.1595. URL: <https://link.aps.org/doi/10.1103/PhysRev.117.1595> (cit. on p. 11).
- [28] P. A. M. Dirac. “The Theory of Gravitation in Hamiltonian Form”. In: *Proceedings of the Royal Society of London. Series A, Mathematical and Physical Sciences* 246.1246 (1958), pp. 333–343. ISSN: 00804630. URL: <http://www.jstor.org/stable/100497> (visited on 09/04/2022) (cit. on p. 11).
- [29] Olivier J. Veraguth and Charles H.-T. Wang. “Immirzi parameter without Immirzi ambiguity: Conformal loop quantization of scalar-tensor gravity”. In: *Physical Review D* 96.8 (Oct. 2017). DOI: 10.1103/physrevd.96.084011. URL: <https://doi.org/10.1103/physrevd.96.084011> (cit. on p. 22).
- [30] Mohammad H. Ansari. “Generic degeneracy and entropy in loop quantum gravity”. In: *Nuclear Physics B* 795.3 (June 2008), pp. 635–644. DOI: 10.1016/j.nuclphysb.2007.11.038. URL: <https://doi.org/10.1016/j.nuclphysb.2007.11.038> (cit. on p. 22).

- [31] Abhay Ashtekar et al. “Quantization of diffeomorphism invariant theories of connections with local degrees of freedom”. In: *J. Math. Phys.* 36 (1995), pp. 6456–6493. DOI: 10.1063/1.531252. arXiv: gr-qc/9504018 (cit. on p. 26).
- [32] John W. Barrett and Louis Crane. “Relativistic spin networks and quantum gravity”. In: *J. Math. Phys.* 39 (1998), pp. 3296–3302. DOI: 10.1063/1.532254. arXiv: gr-qc/9709028 (cit. on p. 36).
- [33] Abhay Ashtekar and Jerzy Lewandowski. “Quantum theory of geometry. 2. Volume operators”. In: *Adv. Theor. Math. Phys.* 1 (1998), pp. 388–429. DOI: 10.4310/ATMP.1997.v1.n2.a8. arXiv: gr-qc/9711031 (cit. on p. 38).
- [34] Carlo Rovelli and Lee Smolin. “Discreteness of area and volume in quantum gravity”. In: *Nucl. Phys. B* 442 (1995). [Erratum: Nucl.Phys.B 456, 753–754 (1995)], pp. 593–622. DOI: 10.1016/0550-3213(95)00150-Q. arXiv: gr-qc/9411005 (cit. on p. 38).
- [35] Michael A. Nielsen and Isaac L. Chuang. *Quantum Computation and Quantum Information: 10th Anniversary Edition*. Cambridge University Press, 2011. ISBN: 9781107002173. URL: <https://www.amazon.com/Quantum-Computation-Information-10th-Anniversary/dp/1107002176?SubscriptionId=AKIAI0BINVZYXZQZ2U3A&tag=chimbiori05-20&linkCode=xm2&camp=2025&creative=165953&creativeASIN=1107002176> (cit. on pp. 44, 45).
- [36] Wayne C. Myrvold. *On the Relation of the Laws of Thermodynamics to Statistical Mechanics*. July 2021. URL: <http://philsci-archive.pitt.edu/19361/> (cit. on p. 47).
- [37] Gavin E. Crooks. *On Measures of Entropy and Information*. 2015 (cit. on p. 48).
- [38] John C. Baez. “Rényi Entropy and Free Energy”. In: *Entropy* 24.5 (2022), p. 706. DOI: 10.3390/e24050706. arXiv: 1102.2098 [quant-ph] (cit. on pp. 49, 61).
- [39] Wim van Dam and Patrick Hayden. “Renyi-entropic bounds on quantum communication”. In: *arXiv e-prints*, quant-ph/0204093 (Apr. 2002), quant-ph/0204093. arXiv: quant-ph/0204093 [quant-ph] (cit. on pp. 49, 50).
- [40] Matthew B. Hastings et al. “Measuring Renyi Entanglement Entropy in Quantum Monte Carlo Simulations”. In: *Phys. Rev. Lett.* 104.15 (2010), p. 157201. DOI: 10.1103/PhysRevLett.104.157201. arXiv: 1001.2335 [cond-mat.str-el] (cit. on p. 50).
- [41] Thomas Faulkner. “The Entanglement Renyi Entropies of Disjoint Intervals in AdS/CFT”. In: (Mar. 2013). arXiv: 1303.7221 [hep-th] (cit. on p. 50).

- [42] Patrick Hayden et al. “Holographic duality from random tensor networks”. In: *JHEP* 11 (2016), p. 009. DOI: 10.1007/JHEP11(2016)009. arXiv: 1601.01694 [hep-th] (cit. on pp. 50, 59, 61, 63, 69, 70, 75).
- [43] Rajibul Islam et al. “Measuring entanglement entropy through the interference of quantum many-body twins”. In: (Sept. 2015). DOI: 10.1038/nature15750. arXiv: 1509.01160 [cond-mat.quant-gas] (cit. on pp. 50, 59, 61).
- [44] Etera R. Livine. “Intertwiner entanglement on spin networks”. In: *Physical Review D* 97.2 (Jan. 2018). DOI: 10.1103/physrevd.97.026009. URL: <https://doi.org/10.1103/physrevd.97.026009> (cit. on pp. 53, 55, 56, 124).
- [45] S. W. Hawking. “Particle Creation by Black Holes”. In: *Commun. Math. Phys.* 43 (1975). Ed. by G. W. Gibbons and S. W. Hawking. [Erratum: *Commun.Math.Phys.* 46, 206 (1976)], pp. 199–220. DOI: 10.1007/BF02345020 (cit. on p. 56).
- [46] Jacob D. Bekenstein. “Black Holes and Entropy”. In: *Jacob Bekenstein: The Conservative Revolutionary*. Ed. by Lars Brink et al. Singapur: World Scientific, 2020, pp. 307–320. DOI: 10.1142/9789811203961_0023 (cit. on p. 56).
- [47] JOHN W. ESSAM and MICHAEL E. FISHER. “Some Basic Definitions in Graph Theory”. In: *Rev. Mod. Phys.* 42 (1970), pp. 271–288. DOI: 10.1103/RevModPhys.42.271 (cit. on p. 65).
- [48] Aram W. Harrow. “The Church of the Symmetric Subspace”. In: *arXiv e-prints*, arXiv:1308.6595 (Aug. 2013), arXiv:1308.6595. arXiv: 1308.6595 [quant-ph] (cit. on p. 71).
- [49] Aranya Bhattacharya, Kevin T. Grosvenor, and Shibaji Roy. “Entanglement entropy and subregion complexity in thermal perturbations around pure AdS spacetime”. In: *Physical Review D* 100.12 (Dec. 2019). DOI: 10.1103/physrevd.100.126004. URL: <https://doi.org/10.1103/physrevd.100.126004> (cit. on p. 77).
- [50] Karol Zyczkowski and Hans-Jürgen Sommers. “Induced measures in the space of mixed quantum states”. In: *Journal of Physics A Mathematical General* 34.35 (Sept. 2001), pp. 7111–7125. DOI: 10.1088/0305-4470/34/35/335. arXiv: quant-ph/0012101 [quant-ph] (cit. on p. 82).